

UNIVERSITÄTSKLINIKUM HAMBURG-EPPENDORF

Universitäres Herz- und Gefäßzentrum, Klinik und Poliklinik für Gefäßmedizin

Prof. Dr. med. E. Sebastian Debus

Sphingosine 1-phosphate receptors and selected cell markers in aneurysmatic and dissected tissue from the human infrarenal abdominal aorta

Dissertation

zur Erlangung des Grades eines Doktors der Medizin
an der Medizinischen Fakultät der Universität Hamburg.

vorgelegt von:

Louisa Irma Grete Michaels
aus Otterndorf

Hamburg 2021

**Angenommen von der
Medizinischen Fakultät der Universität Hamburg am: 06.03.2023**

**Veröffentlicht mit Genehmigung der
Medizinischen Fakultät der Universität Hamburg.**

Prüfungsausschuss, der Vorsitzende: Prof. Dr. Viacheslav Nikolaev

Prüfungsausschuss, zweiter Gutachter: Prof. Dr. Axel Larena-Avellaneda

Für meine Familie

Table of contents

List of abbreviations	1
1 Objectives	3
2 Introduction	4
2.1 Anatomical and physiological aspects of the abdominal aorta	5
2.2 Abdominal aortic aneurysms.....	7
2.2.1 Pathophysiology of abdominal aortic aneurysms	8
2.3 Aortic dissection.....	10
2.3.1 Pathophysiology of aortic dissections	11
2.4 Atherosclerosis in the abdominal aorta.....	12
2.5 The Sphingosine 1-phosphate (S1P)/S1P receptor system	14
2.5.1 Sphingosine 1-phosphate receptor 1	16
2.5.2 Sphingosine 1-phosphate receptor 2	17
2.5.3 Sphingosine 1-phosphate receptor 3	18
2.6 Vascular genes NOS3 and SIRT1	19
2.6.1 Endothelial nitric oxide synthase.....	19
2.6.2 Sirtuin 1	20
3 Material and Methods	22
3.1 Study group, collection and preparation of tissue samples.....	22
3.2 Analysis of gene expression by RT-qPCR.....	23
3.2.1 Synthesis of cDNA	23
3.2.2 Reverse transcriptase quantitative polymerase chain reaction	24
3.2.3 Data analysis and quality requirements	25
3.3 Statistical analysis.....	26
3.4 Immunohistochemical Mac2 staining.....	26
4 Results	31
4.1 Characteristics of the study group	31
4.2 Analysis of gene expression in diseased and non-diseased aortic tissue	34
4.2.1 Cell markers	34
4.2.2 NOS3 and SIRT1	36
4.3.2 S1P receptors.....	37
4.3 Correlation analyses between the expression of cell markers and the..... expression of NOS3, SIRT1 and the S1P receptors 1-3.....	38
4.4 Correlation analysis between the expression of SIRT1, NOS3 and the	39
expression of S1PR1-3.....	39
4.5 Frequency and distribution of macrophages in diseased and non-diseased	40
aortic specimens	40
5 Discussion	43

5.1 Study design and study group	43
5.2 Epidemiological characteristics of the study subgroups	44
5.3 Prevalence of multiple vascular pathologies in the AA	46
5.3.1 Aneurysm and atherosclerosis in the AA	46
5.3.2 Dissection and atherosclerosis in the AA	47
5.4 The role of vascular cells in the aortic pathologies	47
5.4.1 Endothelial cells in the aortic pathologies	48
5.4.2 Vascular smooth muscle cells in the aortic pathologies	49
5.4.2.1 SIRT1 – regulator of Myh11 expression in aortic pathologies?	51
5.5 The role of immune cells in the aortic pathologies	53
5.5.1 Localization of macrophages in diseased aortic tissue	54
5.6 S1P receptors in the aortic pathologies	55
5.7 Conclusion and outlook.....	56
5.8 Limitations	57
6 Summary	59
7 List of figures	61
8 List of tables	62
9 List of references.....	63
10 Appendix	78
11 Acknowledgment (Danksagung).....	102
12 Curriculum vitae	104
13 Declaration on oath (Eidesstattliche Erklärung)	105

List of abbreviations

α -SMA	α -smooth muscle actin
AA	Abdominal aorta
AAA	Abdominal aortic aneurysm
AAD	Abdominal aortic dissection
ABC	Avidin-Biotin Complex
AC	Adenylate cyclase
AD	Aortic dissection
AEC	3-amino-9-ethylcarbazole
ApoE	Apolipoprotein E
BMI	Body mass index
cDNA	Complementary DNA
CD31	Cluster of differentiation 31
CD45	Cluster of differentiation 45
CD68	Cluster of differentiation 66
EC	Endothelial cell
ECM	Extracellular matrix
eNOS	Endothelial nitric oxide synthase
EPC	Endothelial progenitor cell
GAPDH	Glyceraldehyde 3-phosphate dehydrogenase
GPCR	G-protein coupled receptor
HDL	High-density lipoprotein
HUVEC	Human umbilical vein endothelial cells
IA	Intracranial aneurysm
IAAD	Isolated abdominal aortic dissection
ICAM1	Intercellular adhesion molecule 1
LDL	Low-density lipoprotein
LGALS3	Lectin galactoside-binding soluble 3 or galectin 3
MMP	Matrix metalloproteinase
Myh11	Myosin heavy chain 11
MYLK	Myosin light chain kinase
NAD	Nicotinamide adenine dinucleotide
NF- κ B	Nuclear factor 'kappa-light-chain-enhancer' of activated B-cells
NO	Nitric oxide
NOS3	Nitric oxide synthase 3
PECAM1	Platelet endothelial cell adhesion molecule 1
PI3K	Phosphoinositide 3-kinase
PKC	Protein kinase C

PLC	Phospholipase C
ROS	Reactive oxygen species
RT-qPCR	Reverse-transcriptase quantitative polymerase chain reaction
SIRT1	Sirtuin 1
SPHK	Sphingosine kinase
S1P	Sphingosine 1-phosphate
S1PR	Sphingosine 1-phosphate receptor
TIMP	Tissue inhibitor of metalloproteinase
VSMC	Vascular smooth muscle cell

1 Objectives

Aneurysm, dissection and atherosclerosis all are vascular pathologies that arise in the abdominal aorta with a high incidence (atherosclerosis) and high mortality rates (aneurysm and dissection). Therefore, the elucidation of underlying pathomechanisms, that are not fully understood at present, is of great clinical interest.

The main objective of this study is to investigate specific associations between aortic pathologies and the expression of cell markers including CD31 for endothelial cells, myosin heavy chain (Myh11) for smooth muscle cells, CD68 for macrophages and CD45 for leukocytes. In addition, the expression levels of nitric oxide synthase 3 (NOS3/eNOS) and sirtuin 1 (SIRT1) as well as the sphingosine 1-phosphate (S1P) receptors (S1PR1-3) were also measured. These genes have been shown to regulate various physiological as well as pathophysiological processes in the vasculature.

By correlating expression levels of cell markers with those of eNOS, SIRT1 and S1P receptors, I also attempted to gain insight which cells regulate the expression of these genes in association with abdominal aortic pathologies.

2 Introduction

Aneurysm and dissection both are vascular pathologies that mainly arise in the aorta. The two pathologies are relatively rare but potentially life-threatening due to the risk of heart failure, rupture and ischemic complications. Aortic aneurysm and dissection, both associated with typical cardiovascular risk factors, are considered extremely treacherous: In the case of an aortic aneurysm, clinical symptoms often occur late and, in the case of aortic dissection the onset is an acute event which can progress rapidly (Kent et al. 2010, Nienaber et al. 2016). Mortality rates for both pathologies climb over 50% when complications occur (Howard et al. 2013, Sakalihasan et al. 2018). In Germany, 4-5/100,000 deaths due to these two aortic vascular pathologies were reported in 2019 (Destatis 2019). Despite these alarmingly high mortality rates, detailed knowledge of the pathophysiology and the molecular mechanisms underlying these vascular diseases is still incomplete.

Aneurysms are characterized as a localized dilation of the artery due to processes that weaken the vessel wall. Over 90% of the aortic aneurysms occur in the abdominal aorta (AA) (Debus et al. 2020). Abdominal aortic aneurysms (AAA) are most often diagnosed incidentally in imaging diagnostics for other purposes or in screening programs. Aneurysms can progress in growth and in worst case rupture, which is associated with a high mortality (Kühnl et al. 2017). For AAA, co-prevalence with atherosclerosis is reported frequently (Siasos et al. 2015).

Dissections are characterized by an intimal tear and subsequent bleeding in the arterial wall, which leads to a progressive separation of the wall layers and the formation of a false lumen. In the aorta, dissections mainly occur in the thoracic aorta but can tear down to the abdominal aorta. An isolated abdominal aortic dissection is a very rare pathology (Liu et al. 2020). Complications of aortic dissections include aortic rupture, pericardial tamponade, or obstruction of the aortic branches with resulting ischemia of downstream organs (Nienaber et al. 2016, Gawinecka et al. 2017).

For both pathologies, treatment options include conservative management, such as strict blood pressure control, as well as open-surgical or endovascular therapy, depending on location, size and clinical course of the pathology (Kühnl et al. 2017, Nienaber and Clough 2015). Research continues on pharmacological agents to treat or to prevent the onset of these pathologies (Wang et al. 2018, Zhang et al. 2016). Recently, evidence was provided for a beneficial use of beta-blockers in patients with

a thoracic aortic dissection (Brikman and Dori 2019). In the case of AAA, prescriptions of the anti-diabetic drug metformin had been associated with reduced AAA growth, presumably due to antiinflammatory effects of this drug (Unosson et al. 2021).

2.1 Anatomical and physiological aspects of the abdominal aorta

The human aorta can be classified into three anatomical segments: (I) Aorta ascendens, (II) Arcus aortae and (III) Aorta descendens with a thoracic and an abdominal section. The aorta below the diaphragm until the bifurcation, as one section of the descending aorta, is referred to as abdominal aorta (AA). Vascular pathologies affect the aortic segments to differing extents and do often occur at predilection sites (Tillmann 2020). All tissue samples investigated in this study were taken from the abdominal aorta distal to the renal arteries (infrarenal aorta).

Human arteries are characterized by a three-layered structure of intima, media, and adventitia (from inside to outside). These layers are separated by the Lamina elastica interna and externa, respectively (Figure 1).

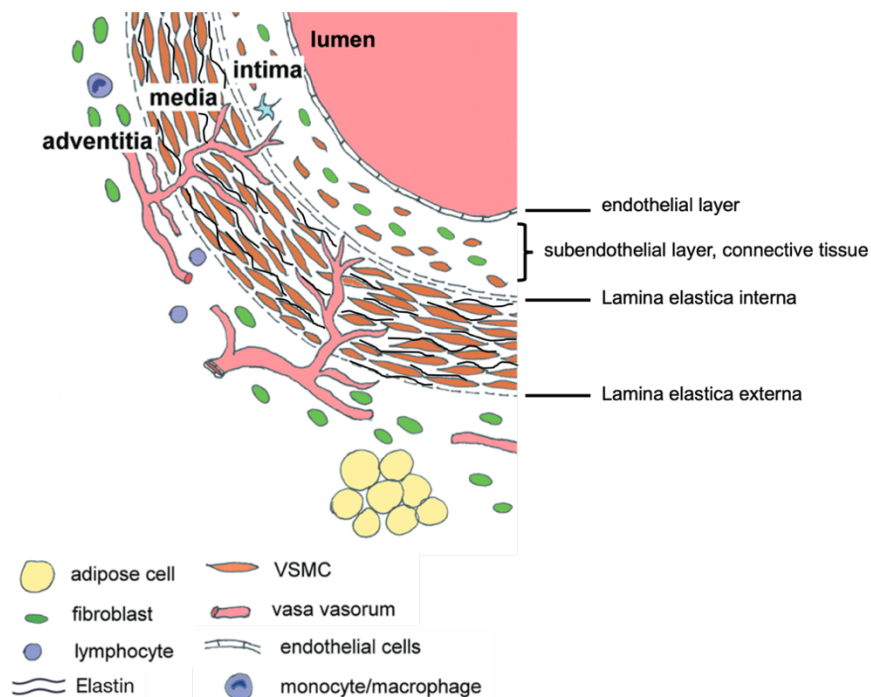


Figure 1. Structure of the arterial wall. VSMC, vascular smooth muscle cell; *modified from Milutinovic et al. 2020.*

The intima of the abdominal aorta consists of the endothelium and subendothelial connective tissue with loosely connected fibroblasts, collagen and elastic fibers. The endothelium, a monolayer of continuous epithelial cells connected by specific adhesion molecules, constitutes the inner lining of the abdominal aorta (Kummer and Welsch 2018). One endothelial adhesion molecule largely expressed at intercellular junctions is PECAM1, also known as cluster of differentiation gene 31 (CD31). Expressed in endothelial cells (ECs), CD31 regulates leukocyte trafficking but primarily functions as a mechanosensory protein and promotes the endothelial barrier (Privratsky and Newman 2014). In ECs, eNOS (endothelial nitric oxide synthase, encoded by the gene NOS3) synthesizes nitric oxide (NO), which promotes vasodilation and, generally, has a vasoprotective effect (Siasos et al. 2015, Zhao et al. 2015).

The medial layer of the abdominal aorta constitutes the largest share of the vessel wall and primarily consists of vascular smooth muscle cells (VSMCs), elastic fibers and extracellular matrix (ECM). VSMCs are positioned concentrically or lengthwise between the elastic lamellae and regulate the vascular tone. VSMCs are not terminally differentiated but can alternate between two major phenotypes (contractile and quiescent or proliferative and secretory), and thus, can adjust to the varying conditions in the vascular system (Owens et al. 2004, Hulsmans and Nahrendorf 2020). In the physiological state of healthy arteries, differentiated VSMCs remain quiescent and express specific genes and proteins, known as differentiation markers. These include, for example, myosin heavy chain11 (Myh11) or α -smooth muscle actin (α -SMA), both important for contraction. Upon vascular injury, VSMCs can dedifferentiate, characterized by increased migratory as well as proliferative capacities and a loss of expression of the contractile proteins. Generally, VSMC dedifferentiation and dysbalance of the VSMC phenotypes is a hallmark of vascular pathologies (Kwartler et al. 2014, Frismantiene et al. 2018). VSMCs and fibroblasts synthesize the non-cellular components of the ECM, mainly elastin, collagen, proteoglycans and glycoproteins. The ECM also strongly impacts the mechanical characteristics of the aorta (Jana et al. 2019).

The adventitia is the outermost layer of the aortic wall and mainly consists of collagen fibers, fibroblasts and can also host immune cells, neuronal cells and small vessels (Kummer and Welsch 2018).

2.2 Abdominal aortic aneurysms

Aortic aneurysms are characterized by a local dilation of the aortic wall, mostly due to degenerative mechanisms that weaken the vessel wall and promote dilation (Larena-Avellaneda and Debus 2020). Over 90% of all aortic aneurysms occur in the abdominal aorta (abdominal aortic aneurysm, AAA) (Debus et al. 2020). Thereby, several factors might predispose the AA to the formation of an aneurysm. These include mechanical risk factors such as profile of blood flow and shear stress. Further, the developmental origin of cells may be relevant, as abdominal aortic VSMCs stem from mesodermal precursors, while VSMCs of the thoracic aorta are in part derived from neural crest precursor cells (Majesky 2007, Pfaltzgraff and Bader 2015).

In current practice guidelines from the German Society for Vascular surgery, an abdominal aortic aneurysm is defined as a local dilation of the abdominal aorta of at least 30 mm (Debus et al. 2018). AAA diagnosis is often made incidentally in imaging diagnostics for another medical condition or in screening programs for men of 65 or more years of age and for women of 65 or more years of age with a smoking history (Debus et al. 2018). Main risk factors for AAA are male gender, age over 65 years, and smoking. AAA symptoms include abdominal pain, hypotension or shock and a pulsatile abdominal tumor (Sakalihasan et al. 2018). Kühnl et al. analyzed data from the German DRG (diagnosis-related-groups) statistics (2005 – 2014) and reported a standardized incidence rate for AAA in German hospitals of 27.9 per 100,000 men and 3.3 per 100,000 women (Kühnl et al. 2017). The global incidence and prevalence rates of AAA both decreased over the past 30 years (Sampson et al. 2014, Oliver-Williams et al. 2018). However, AAA is still associated with high mortality rates and must be considered a worldwide concern. Although the male gender is a main risk factor for AA, once diagnosed, females have a worse prognosis for AAA including a higher risk for rupture (Sampson et al. 2014).

Above a defined aneurysm size of 5.5 cm in men and 5 cm in women, AAA is treated interventionally, either by endovascular repair or by open surgical techniques (practice guideline, German society for Vascular surgery 2018) (Debus et al. 2018). Mortality rates for AAA patients in hospitals range from 3 – 5% for non-ruptured AAA up to > 50% for ruptured AAA (Kühnl et al. 2017, Parkinson et al. 2015, Sakalihasan et al. 2018). Conservative treatment of small, asymptomatic aneurysms comprises lifestyle modifications for minimization of risk factors, clinical surveillance and control of blood pressure (Debus et al. 2018). One approach for drug treatment of AAA is the anti-

diabetic agent metformin, which had been associated with reduced AAA progression (Unosson et al. 2021). Ongoing studies aim to confirm the benefit as well as the underlying mechanisms, presumably antiinflammatory, of metformin use in AAA, and seek other pharmacological treatments for AAA (Wang et al. 2018).

2.2.1 Pathophysiology of abdominal aortic aneurysms

The pathogenesis of AAA is complex and multifactorial, most commonly caused by degeneration and inflammation of the aortic wall (Larena-Avellaneda and Debus 2020). Although polymorphisms in some genes have been associated with AAA, the influence of genetics in developing AAA is generally low and mainly associated with AAA in younger individuals (Davis et al. 2015, Larena-Avellaneda and Debus 2020). A variety of pathological processes lead to degenerative remodeling, subsequently weakening the aortic wall and promoting dilation (Gurung et al. 2020). Fundamental pathological mechanisms in AAA formation include endothelial dysfunction and impaired VSMC function, leukocytic infiltration, chronic wall inflammation and ECM degradation (Figure 2) (Raffort et al. 2017, Liu et al. 2019a, Davis et al. 2015, Gurung et al. 2020).

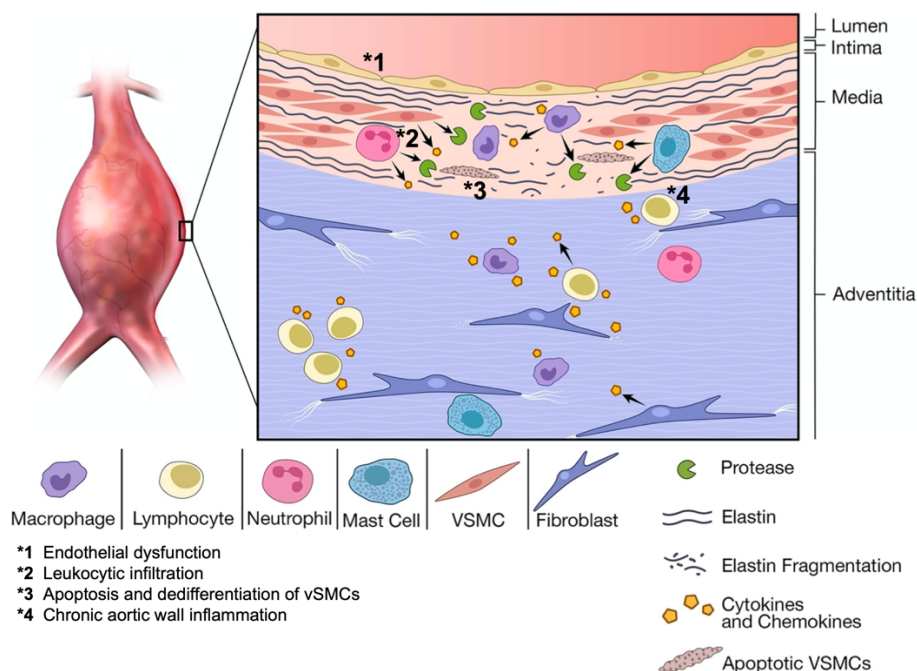


Figure 2. Pathophysiology of AAA. Fundamental mechanisms in AAA pathogenesis are endothelial dysfunction (*1), leukocytic infiltration (*2), cell death and dedifferentiation of vSMCs (*3), chronic aortic wall inflammation (*4) and degradation of connective tissue, all weakening the aortic wall and promoting the dilation. VSMC, vascular smooth muscle cell; *modified from Davis et al. 2014.*

In early AAA formation, the inner layer of the aortic wall is damaged leading to endothelial dysfunction. Dysfunctional endothelial cells lose the ability of adequate NO production due to uncoupling of eNOS, resulting in increased production of reactive oxygen species (ROS) (Gao et al. 2012). The increasing imbalance of NO and ROS production promotes aortic wall inflammation (Gao et al. 2012, Siasos et al. 2015). Further, upon stimulation by proinflammatory cytokines, dysfunctional endothelial cells increasingly express adhesion molecules (Saito et al. 2013). This leads to reduced endothelial wall integrity and promotes the migration and accumulation of inflammatory cells in the aortic wall (Figure 2) (Privratsky and Newman 2014, Raffort et al. 2017). In those inflammatory cell infiltrates, macrophages account for the largest subset of leukocytic cells identified in the aortic wall of AAA (Raffort et al. 2017). Activated macrophages produce reactive oxygen species and inflammatory cytokines (interleukin-1 β , interleukin 6, tumor-necrosis-factor α , epidermal growth factor, tumor-growth-factor β) (Siasos et al. 2015, Rabkin 2017). Key mechanisms attributed to the monocyte-macrophage cell line in AAA pathogenesis are degradation of extracellular matrix components, activation of proinflammatory cells and vascular remodeling, generally promoting inflammation and AAA formation. In later stages of the disease, monocytes and macrophages also induce tissue healing (Raffort et al. 2017).

The proteolytic and oxidative environment in the aortic wall also affects aortic VSMCs, resulting in a loss of contractile VSMCs, primarily due to cell death (Figure 2) (Henderson et al. 1999, Riches et al. 2013, Golledge 2019). Proinflammatory cytokines as well as increased level of ROS promote apoptosis of VSMCs (López-Candales et al. 1997, Gurung et al. 2020). In AAA tissue, VSMCs can acquire a macrophage-like phenotype expressing macrophage markers such as cluster of differentiation gene 68 (CD68) and LGALS3 (Lectin galactoside-binding soluble 3 or galectin-3), while VSMC differentiation markers are downregulated (Shankman et al. 2015, Gurung et al. 2020). In AAA, ECs, VSMCs and immune cells express matrix metalloproteinases (MMPs). Tilting the balance between MMPs and TIMPs (tissue inhibitor of metalloproteinases) in favor of MMPs, in consequence promotes the degradation of connective tissue (Gurung et al. 2020). Gradually, the aortic wall loses its stability and integrity, and dilation progresses. As a life-threatening complication of an abdominal aortic aneurysm, the weakened aortic wall can rupture, leading to massive and often lethal bleeding (Sakalihasan et al. 2018).

2.3 Aortic dissection

Aortic dissection (AD) describes the pathologic condition of an intimal tear (entry) and ensuing blood flow within the aortic wall. Aortic layers are dissected and the blood flow in-between these layers (false lumen) can continue in antegrade or retrograde direction and potentially re-connect to the true lumen through a second intimal tear (re-entry). Potential complications of aortic dissections depend on the localization and include aortic rupture, pericardial tamponade, aortic valve insufficiency and ischemia of organs due to the compression of aortic branches (Nienaber et al. 2016, Böckler 2020). Aortic dissection is one of the pathologies referred to as acute aortic syndrome (AAS), a group of life-threatening aortic pathologies presenting with chest pain. Besides aortic dissection, AAS encompasses intramural hematoma and penetrating aortic ulcer (Clough and Nienaber 2015).

Generally, incidences of acute aortic dissection range from 3 – 6/100,000 per year, but the incidence increases rapidly with advanced age up to more than 30/100,000 in individuals aged 65 – 75 years (Howard et al. 2013, Nienaber et al. 2016). However, individuals with hereditary aortic diseases, e.g., Marfan syndrome, Ehler-Danlos syndrome or Loeys-Dietz syndrome are at high risk for AD at a much earlier age (Gawinecka et al. 2017). Data from the international registry of acute aortic dissection (IRAD) indicate declining mortality rates over the past two decades for acute aortic dissection. However, this pathology is still associated with high rates of preclinical death and, if complications occur, with high overall mortality of above 50% for all patients with acute AD of the ascending aorta (Howard et al. 2013, Pape et al. 2015). Most aortic dissections arise in the thoracic aorta, and can be classified according to the Stanford system, depending on their exact location. All dissections affecting the ascending aorta are classified Stanford A, whereas dissections arising in the arcus aortae and in the proximal sections of the thoracic aorta are classified Stanford B (Gawinecka et al. 2017). Thoracic dissections can progress and tear down to the abdominal aorta. These cases account for most dissections found in the AA, while isolated abdominal aortic dissections (IAAD) are extremely rare with an incidence below 5% of all aortic dissections (Howard et al. 2013, Liu et al. 2020).

Therapy of AD depends on the Stanford classification, the clinical presentation, and comorbidities. Immediate open surgical repair is the method of choice for acute Stanford A dissection, the most severe form of AD. Without adequate surgical treatment, these patients face an increase of mortality of 1 – 2% per hour after onset

of symptoms (Gawinecka et al. 2017). Unless life-threatening complications necessitate surgical repair, Stanford B dissections can be treated conservatively with adequate analgesia, blood pressure and heart rate control (Erbel et al. 2014, Gawinecka et al. 2017).

2.3.1 Pathophysiology of aortic dissections

Aortic dissection is most common in men over 65 years of age and the main risk factors are uncontrolled hypertension and smoking (Landenhed et al. 2015). Additional and less frequent risk factors include inflammation (aortitis), trauma or iatrogenic harm of the aorta. Congenital connective tissue disorders (see above) cause the majority of AD in younger patients (Gawinecka et al. 2017). In contrast, non-hereditary, degenerative AD is a multifactorial disease, and its pathogenesis is still not fully understood (Nienaber et al. 2016, Gawinecka et al. 2017).

Fundamental mechanisms identified for AD pathogenesis are an intimal tear in the aortic wall and degradation of the medial layer. Both mechanisms are associated with elevated shear stress (Mussa et al. 2016, Böckler 2020), above all promoted by uncontrolled hypertension, which is the main risk factor for AD. Subsequently, the intimal tear can progress as a dissection within the medial layer (Gawinecka et al. 2017). The separation of the aortic wall layers facilitates the infiltration of immune cells, which mainly accumulate in the medial layer. Macrophages account for the largest subset of infiltrating immune cells and contribute to aortic wall remodeling, neoangiogenesis and ECM degradation through the production of proinflammatory cytokines and proteolytic enzymes (Del Porto et al. 2014, Gawinecka et al. 2017). Subsequent degradation of the medial layer in AD pathogenesis is mainly characterized by fragmentation of the elastic lamellae, dysfunctional collagen fibrils and a thinned-out basement membrane of VSMCs (Ishii and Asuwa 2000). Downregulation of VSMC differentiation markers Myh11 and myosin light chain kinase (MYLK) had been reported in dissected aortic tissue (Zhang et al. 2016). Further, mutations in VSMC proteins involved in mechano-sensing and contractility had been identified as predisposing factors for dissections in the thoracic aorta (Milewicz et al. 2017).

Generally, AD can evolve in various ways. Stanford A and Stanford B dissections may remain restricted to their aortic origin site but can also progress throughout the descending aorta down to the AA and even into the iliac-femoral arteries (Böckler 2020,

Gawinecka et al. 2017). To date, the mechanisms and stimuli that control AD progression are not fully understood. Therefore, it is of great interest to identify factors and mechanisms of predisposition towards the progression of AD. For instance, atherosclerosis is a frequent pathology in the AAA and may predispose the AA to tear in case of a proximal dissection.

2.4 Atherosclerosis in the abdominal aorta

Atherosclerosis is a common vascular pathology and is the underlying cause for the majority of all cardiovascular deaths worldwide. The chronic inflammatory disease is characterized by the formation of lipid-containing plaques in the intimal layer of arterial vessels (Libby et al. 2019).

Most of the recent clinical research in the field of atherosclerosis focused on coronary and carotid arteries. The detection of atherosclerosis in the abdominal aorta is mostly incidental by abdominal imaging diagnostics for different medical reasons and is often associated with atherosclerosis in other vascular beds, e.g., coronary arteries (Gallino et al. 2014, Suh et al. 2018). Systemic risk factors for atherosclerosis are dyslipidemia, diabetes, smoking, and hypertension as well as the non-influenceable risk factors male gender, age, and positive family history (Libby et al. 2019). The risk factors for atherosclerosis overlap with those for aortic aneurysm and aortic dissection, and these pathologies also co-exist in many patients (Kent et al. 2010, Hashiyama et al. 2018). Atherosclerotic alterations have not only been found in the aneurysmatic wall, but AAA had also been associated with atherosclerosis in carotid and coronary arteries as well as with peripheral artery disease (Johnsen et al. 2010, Toghil et al. 2017). For instance, in a cohort study with over three million individuals in the United States of America, Kent et al. found significantly higher frequencies of atherosclerosis in carotid and coronary arteries as well as of peripheral artery disease in individuals with AAA, compared to individuals without AAA (Kent et al. 2010). It is subject of current research whether AAA evolves on the basis of atherosclerosis or whether the high co-prevalence of AAA and atherosclerosis is attributable to similar risk factors (Gawinecka et al. 2017, Johnsen et al. 2010).

An association between aortic dissection and atherosclerosis in the AA has been studied less intensively. As generally true, the prevalence of atherosclerosis in AD patients increases with the patients' age. Atherosclerosis appears more common in

patients with Stanford B dissection, as these patients present more frequently with coronary artery disease compared to patients with a Stanford A dissection (Tsai et al. 2009, Hashiyama et al. 2018). However, it remains unknown, whether the prevalence of atherosclerosis in the AA influences the progress of AD.

Generally, atherosclerosis occurs at predilection sites such as bifurcations or segments with turbulent blood flow (Libby et al. 2019). Atherosclerosis is a chronic inflammatory vascular disease and endothelial dysfunction, macrophage infiltration, VSMC dedifferentiation and cell death are considered fundamental, proinflammatory mechanisms in atherogenesis (Libby et al. 2019, Sosnowska et al. 2017). Cardiovascular risk factors promote endothelial cell damage and vascular permeability (Gimbrone and García-Cardena 2016). Dysfunctional endothelial cells show impaired eNOS function, leading to decreased NO production and vasoconstriction as well as increased leukocyte adhesion and platelet aggregation (Zhao et al. 2015). Infiltrating monocytes evolve into macrophages, which internalize oxidized lipoproteins in the subendothelial space and turn into foam cells (Müller and Kuhlencordt 2020). Macrophages and foam cells produce proinflammatory cytokines, growth factors and ROS, attracting more leukocytes to the site of lesion. The accumulation of foam cells (fatty streak) characterizes a preliminary stage of atherosclerosis which, at that point, is still reversible (Gimbrone and García-Cardena 2016). The role of macrophages in atherogenesis is closely tied to the various states of macrophage polarization. In early atherogenesis, proinflammatory M1 polarized macrophages are mostly present, whereas the antiinflammatory and profibrotic M2 macrophages become more prevalent in advanced stages of atherosclerosis (Yang et al. 2020).

VSMCs play an important role in the process of atherogenesis. VSMC cell death (apoptosis and necrosis) and VSMCs with an altered phenotype contribute to plaque formation (Bennett et al. 2016). With progression of the atherosclerotic lesions, medial VSMCs migrate into the subendothelial space, dedifferentiate, and proliferate upon atherogenic stimulation by dysfunctional ECs and immune cells. This process is also known as phenotypic modulation and is characterized by a downregulation of VSMC differentiation markers (Vengrenyuk et al. 2015). During atherogenesis, VSMCs can adopt various phenotypes, e.g., an ECM producing, synthetic phenotype or a proinflammatory, macrophage-like phenotype (Shankman et al. 2015, Wirka et al. 2019). VSMC-derived macrophage-like cells show upregulation of macrophage markers such as CD68, exhibit phagocytic activity and contribute to foam cell

populations in the arterial wall (Feil et al. 2014, Vengrenyuk et al. 2015). VSMCs of an altered synthetic phenotype increasingly produce ECM proteins during atherosclerosis and promote the formation of a fibrotic cap to stabilize the atherosclerotic lesion (Bentzon et al. 2006, Shankman et al. 2015). A feared complication of advanced atherosclerosis is plaque rupture with the risk of subsequent thrombosis and embolism (Müller and Kuhlencordt 2020).

2.5 The Sphingosine 1-phosphate (S1P)/S1P receptor system

Over the past two decades, sphingosine 1-phosphate (S1P) and the S1P receptors have attracted increasing attention in the field of cardiovascular research. S1P is a sphingolipid metabolite and functions as a bioactive lipid mediator. S1P has been shown to regulate several cellular functions and its vital function in the vasculature is based on its role in vascular development (vasculogenesis) (Gaengel et al. 2012), the effect on maintenance of the endothelial integrity and the regulation of the vascular tone (Lucke and Levkau 2010).

S1P is synthesized by the ATP-dependent phosphorylation of ceramide-derived sphingosine by sphingosine kinases 1 or 2 (SPHK1, SPHK2) in red blood cells, platelets and ECs (Spiegel and Milstien 2003). S1P is degraded by dephosphorylation or cleavage by a S1P-lyase (Figure 3).

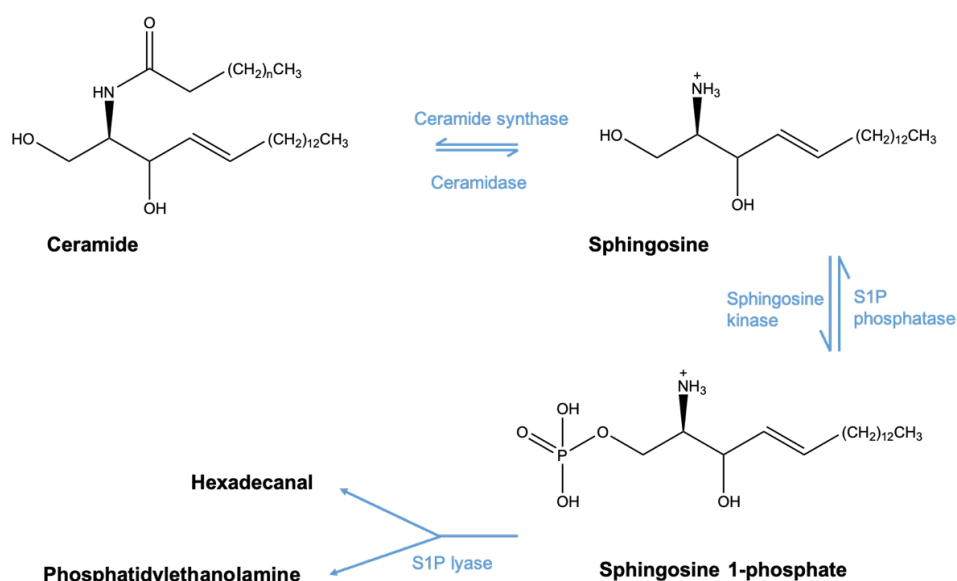


Figure 3. Sphingosine 1-phosphate metabolism. Synthesis and degradation pathways for sphingosine 1-phosphate (S1P) are shown. For details, see Section 2.5. Authors own presentation.

In blood, S1P is mainly bound to high-density lipoprotein (HDL) and albumin (Murata et al. 2000). HDL-bound S1P greatly contributes to the protective effects of HDL in the vasculature (Argraves and Argraves 2007). Importantly, a S1P gradient exists with high levels in lymph fluid and blood (~ 1 μ M) and low levels in tissue (nanomolar concentrations) (Schwab et al. 2005, Maceyka et al. 2012). This gradient is critical for lymphocytes to egress from lymphatic organs into the circulation towards a higher S1P concentration (Cyster and Schwab 2012). S1P functions are generally mediated by S1P receptors 1 – 5 (S1PR1-5), which all fall under the category of G-protein coupled receptors (GPCR) (Strub et al. 2010, Maceyka et al. 2012). Varying downstream effects of these receptors' signaling pathways are attributable to their coupling to different G-proteins G_{α_i} , G_{α_q} and $G_{\alpha_{12/13}}$ (Sanchez and Hla 2004) (Figure 4). S1PR1, S1PR2 and S1PR3 are ubiquitously expressed, while S1PR4 and S1PR5 are predominantly expressed in immune and neuronal cells respectively (Sanchez 2016).

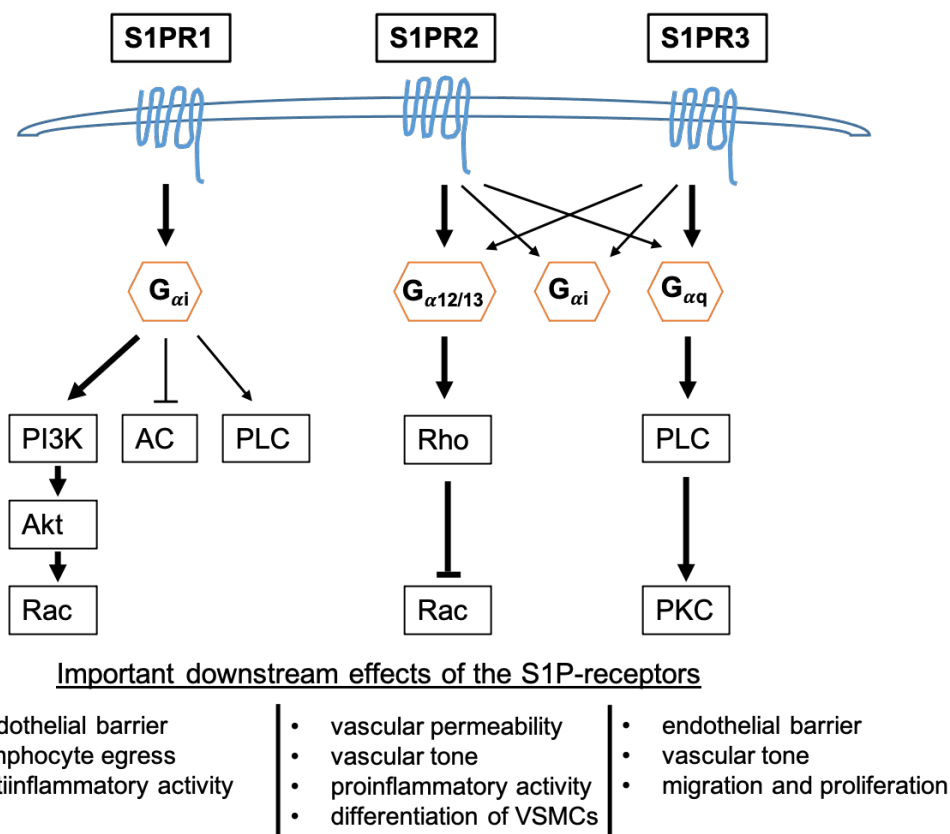


Figure 4. Downstream signaling pathways activated by S1PR1-3 in vascular cells. S1PR1 exclusively couples to G_{α_i} . S1PR2 and S1PR3 couple to G_{α_i} , G_{α_q} and $G_{\alpha_{12/13}}$ with dominant coupling to $G_{\alpha_{12/13}}$ (S1PR2) and G_{α_q} (S1PR3). S1PR, sphingosine 1-phosphate receptor; PI3K, phosphoinositide 3-kinase; Akt, Akt serine/threonine protein kinase (also called protein kinase B); Rac, rac-GTPase; AC, adenylate cyclase; PLC, phospholipase C; Rho, Rho-GTPase; PKC, protein kinase C.

2.5.1 Sphingosine 1-phosphate receptor 1

Sphingosine 1-phosphate receptor 1 (S1PR1) exclusively couples to G-protein $G_{\alpha i}$ with subsequent activation of Rac (Figure 4) (Hla and Maciag 1990, Sanchez and Hla 2004, Matloubian et al. 2004).

In ECs, S1PR1 is the predominantly expressed S1P receptor and promotes the integrity of the endothelial barrier (Lee et al. 1999, Garcia et al. 2001). S1PR1 leads to PI3K-dependent phosphorylation of Akt which, in turn, phosphorylates and activates eNOS, resulting in vasodilation (Morales-Ruiz et al. 2001, Sanchez 2016). Endothelial S1PR1 signaling is essential for the vascular development, since global as well as endothelial cell-specific knockout of S1PR1 in mice was shown to lead to in-utero death due to insufficient integrity of the vessel wall (Liu et al. 2000). S1PR1 activation is crucial for the inhibition of endothelial cell sprouting and for the stabilization of the endothelial barrier (Garcia et al. 2001, Gaengel et al. 2012).

S1PR1 expressed in lymphocytes is required for these cells to egress out of lymphatic organs towards a higher S1P gradient in the circulation (Schwab et al. 2005, Cyster and Schwab 2012). This mechanism is already used in the medical therapy of relapse remitting multiple sclerosis, employing the S1P analogue and functional S1PR1 antagonist FTY720 (Fingolimod) to inhibit lymphocyte egress and to suppress inflammation in the central nervous system (Brinkmann et al. 2002).

With regards to atherosclerosis, endothelial S1PR1 was shown to carry out primarily antiinflammatory functions and to protect against atherosclerosis, in particular through the enhancement of the endothelial barrier (Garcia et al. 2001, Blaho and Hla 2014). An induced deletion of endothelial S1PR1 in adult hypercholesterolemic apolipoprotein E (ApoE) knockout mice enhanced the expression of proinflammatory adhesion molecules such as ICAM1 and increased the atherosclerotic plaque burden in the descending aorta (Galvani et al. 2015). By the use of S1P analogues (FTY720) and S1PR1 agonists (KRP-203) it was shown that S1P/S1PR1 signaling inhibits the formation of atherosclerotic lesions. Thereby, KRP-203 application in LDL-receptor-deficient mice resulted in decreased recruitment and impaired function of lymphocytes (Potì et al. 2013). An overall reduction of lymphocytes and enhancement of the endothelial barrier was found upon FTY720 application in *in vitro* human and murine endothelial cells as well as in ApoE knockout mice (Sanchez et al. 2003, Keul et al. 2007). In a rat model for intracranial aneurysms (IA) in which IA was induced by ligation or wire injury of the carotid artery, the S1PR1 agonist ASP4058 was recently shown to

inhibit the formation of IA (Yamamoto et al. 2017). This effect was associated with a S1PR1-mediated reduction of vascular permeability and an inhibition of macrophage infiltration (Yamamoto et al. 2017).

Overall, S1PR1 plays an important role in maintaining vascular homeostasis. For intracranial aneurysm and atherosclerosis, S1PR1 may have a protective effect. However, to the best of my knowledge, no usable study has yet been performed to investigate the role of S1PR1, or of the other two S1PRs investigated in this study, in pathologies (abdominal) aortic aneurysm and dissection.

2.5.2 Sphingosine 1-phosphate receptor 2

Sphingosine 1-phosphate receptor 2 (S1PR2) couples to G-proteins $G_{\alpha i}$, $G_{\alpha q}$ and $G_{\alpha 12/13}$, whereby the $G_{\alpha 12/13}$ -dependent activation of Rho and the subsequent inhibition of Rac appears to be the dominant S1PR2-dependent pathway in vascular cells (Figure 4) (Pyne and Pyne 2000, Sanchez and Hla 2004). S1PR2 knockout mice are viable and fertile (Kono et al. 2004, Sanchez 2016), but present with inner ear deafness due to vascular defects in the stria vascularis. In these mice, capillaries were found to be dilated, suggesting a role of the S1PR2 in the regulation of the vascular tone (Kono et al. 2007, Proia and Hla 2015).

In vascular cells, S1PR2 generally appears to oppose S1PR1 signaling (see Section 2.5.1). Activation of endothelial S1PR2 is associated with a disruption of the endothelial barrier and enhanced vascular permeability (Zhang et al. 2013, Kim et al. 2015). S1PR2 antagonism in *in vitro* human endothelial cells of the umbilical vein (HUVECs) by using the specific pharmacological antagonist JTE-013 resulted in decreased endothelial permeability through modulation of actin cytoskeletal arrangements and VE-cadherin translocation to adherens junctions (Sanchez et al. 2007). Generally, S1PR2 expression was found upregulated in inflammation and atherosclerosis (Sanchez 2016). However, regarding atherosclerosis, S1PR2 appears to have potentially promoting as well as protective properties depending on the vascular cell type concerned. In direct contrast to the above-named observations of S1PR2 in ECs, in an arterial injury mouse model, where ligation of the common carotid artery causes the formation of neointimal lesions, S1PR2 knockout mice produced much larger lesions compared to wildtype animals, (Shimizu et al. 2007). This inhibitory effect of S1PR2 on intimal hyperplasia was later attributed to an S1PR2/RhoA-dependent

upregulation of VSMC differentiation genes and a concomitant inhibition of migration and proliferation (Grabski et al. 2009, Daum et al. 2009, Medlin et al. 2010). While S1PR2 signaling in VSMCs appears atheroprotective, overall, S1PR2 promotes atherosclerosis by enhancing vascular permeability (Jozefczuk et al. 2020) and S1PR2 expression is upregulated in atherosclerosis (Sanchez 2016). Moreover, S1PR2 also inhibits leukocyte migration which may lead to a retention of macrophages in atherosclerotic lesions resulting in increased foam cell accumulation (Michaud et al. 2010, Skoura et al. 2011, Baeyens et al. 2015).

2.5.3 Sphingosine 1-phosphate receptor 3

As is the case for S1PR2, sphingosine 1-phosphate receptor 3 (S1PR3) is not essential for embryonic development as S1PR3 knockout mice are viable (Kono et al. 2004). S1PR3 couples to $G_{\alpha i}$, $G_{\alpha 12/13}$ but mainly to $G_{\alpha q}$, resulting in activation of PLC and subsequently PKC (Figure 4) (Pyne and Pyne 2000, Sanchez 2016).

Shimizu et al. studied the role of S1PR3 in the vascular response to arterial injury. In S1PR3 knockout mice, smaller neointimal lesions as well as fewer intimal cells have been found upon denudation of the iliac-femoral arteries when compared to wild-type mice. Moreover, expression of S1PR3 in VSMCs resulted in an increased activation of Erk-, Akt- and Rac-signaling pathways by S1P. These cells also exhibited an increased migratory and proliferative potential (Shimizu et al. 2012). In a different arterial injury model with ligation of the carotid artery, S1PR3 appears to have an opposite role, as S1PR3 knockout mice produced larger lesions than wildtype animals (Keul et al. 2011, Shimizu et al. 2012). The reason of this apparent contradiction is to date unknown.

Depending on the cell type concerned, S1PR3 activation has varying effects on the vascular tone. Synergistically with S1PR1, endothelial S1PR3 mediates HDL-bound S1P-dependent vasodilation via the activation of eNOS (Nofer et al. 2004), whereas S1PR3 expressed in VSMCs promotes vasoconstriction through PLC activation and Ca^{2+} release (Hemmings 2006, Kerage et al. 2014).

S1PR3 has pro- as well as antiinflammatory activity. It stimulates leukocyte adhesion to ECs through NF- κ B activation and enhanced expression of adhesion molecules (Kimura et al. 2006). S1PR3 also seems to regulate macrophage recruitment to plaque upon carotid ligation. S1PR3/ApoE-double knockout mice presented with a reduced number of macrophages in atherosclerotic plaque but, interestingly, the overall plaque

burden was not affected (Keul et al. 2011). In murine aortae S1PR3 had been identified as the most relevant S1PR that mediates FTY720-induced vasodilation via the activation of eNOS. In S1PR3 as well as in eNOS knockout mice, this effect was no longer present (Tölle et al. 2005).

2.6 Vascular genes NOS3 and SIRT1

NOS3 and SIRT1, two genes with importance for vascular cells, have lately attracted great interest in vascular research. Generally, NOS3 (encoding eNOS) and SIRT1 generally protect the vasculature and prevent degenerative vascular pathologies (Kitada et al. 2016, Ota et al. 2010).

These two genes were included in this study to analyze cell-specific roles in the aortic pathologies aneurysm, dissection and atherosclerosis.

2.6.1 Endothelial nitric oxide synthase

NO synthases (NOS) produce NO in a five-electron oxidation of a guanidino nitrogen from L-arginine to L-citrulline. Three NOS isoforms have been described: eNOS is the predominantly expressed isoform in the endothelium. Inducible NOS (iNOS; NOS2) is mainly expressed in immune cells and neuronal NOS (nNOS; NOS1) is the major NOS isoform of the nervous system (Alderton et al. 2001).

The activity of eNOS is regulated through reversible phosphorylation and stimulated by fluid shear stress (Park et al. 2015, Gimbrone and García-Cardena 2016). eNOS activity is associated with its localization at cell-cell contact sites and *in vitro* studies found a co-expression of CD31 and eNOS at endothelial plasma membranes (Govers et al. 2002). Through the activation of the soluble guanylate cyclase, NO promotes vasodilation, cell survival and migration (Park et al. 2015). NO was shown to protect against atherosclerosis by vasodilation, inhibition of platelet and leukocyte adhesion and by decreased VSMC proliferation (Hong et al. 2019). Dysfunctional eNOS leads to reduced NO production and concomitant enhanced ROS production, both contributing to further endothelial dysfunction (Gao et al. 2012). eNOS/ApoE-double knockout mice present with enhanced leukocyte and platelet adhesion as well as increased levels of thrombosis and atherosclerosis compared to solely ApoE-deficient mice as controls (Kuhlen cordt et al. 2004, Kuhlen cordt et al. 2001, Gimbrone and García-Cardena 2016). The imbalance of enhanced ROS synthesis and reduced NO

synthesis has also been assumed to promote aortic wall inflammation and the formation of AAA (Siasos et al. 2015).

The activation of the eNOS/NO pathway still is considered a potential target for pharmacological therapy in vascular diseases including atherosclerosis and AAA (Hong et al. 2019, Sun et al. 2018).

2.6.2 Sirtuin 1

Sirtuin 1 (SIRT1), a member of the sirtuin (silent mating type information regulation 2 homolog) family, is a nicotinamide adenine dinucleotide (NAD)-dependent histone deacetylase. Sirtuins are highly expressed in the nucleus and cytoplasm of vascular cells including ECs, endothelial progenitor cells (EPCs) and VSMCs. Sirtuins modulate a wide variety of critical biological processes, e.g., metabolism and apoptosis in vascular aging. SIRT1 regulates the expression of inflammatory, metabolic, and cardiovascular transcription factors via deacetylation of histones (Winnik et al. 2015, Sosnowska et al. 2017). Age-dependent downregulation of SIRT1 in ECs and VSMCs had been associated with reduced capacity for vascular repair and diminished stress responses (Thompson et al. 2014).

SIRT1 mediates atheroprotective activities as shown in transgenic ApoE-deficient mice, in which an adenovirus-induced endothelial cell-specific overexpression of SIRT1 diminished atherosclerotic plaque formation (Zhang et al. 2008). Thereby, endothelial SIRT1 regulates eNOS activity and ROS synthesis with subsequent beneficial effects on endothelial repair processes and decreased cellular senescence (D'Onofrio et al. 2015, Kitada et al. 2016). Activation of SIRT1 in ECs also promotes the endothelial barrier by upregulation of adhesion molecule expression, e.g., of CD31 (D'Onofrio et al. 2015, Liu et al. 2019b). Moreover, in LDL-receptor-deficient mice SIRT1 had been shown to prevent atherosclerosis through inhibition of the senescence of ECs (Warboys et al. 2014).

Similarly, decreased expression of SIRT1 in VSMCs is associated with vascular dysfunction (Thompson et al. 2014). In VSMCs, SIRT1 expression prevents atherosclerosis or hypertension by attenuating DNA damage and medial degeneration (Gorenne et al. 2013, Winnik et al. 2015). In transgenic mice with overexpression of human SIRT1 specifically in VSMCs, decreased VSMC proliferation and decreased neointimal formation was found upon ligation or wire injury of the carotid artery (Li et al. 2011, D'Onofrio et al. 2015).

Besides atherosclerosis, SIRT1 had been associated with a protective role in the formation of aneurysm as well as dissection. Chen et al. found decreased expression and activity of SIRT1 in human AAA tissue. Further, transgenic mice with ApoE- and VSMC-specific SIRT1-double knockout showed higher susceptibility for AAA (Chen et al. 2016). Moreover, in mice with a macrophage-specific SIRT1 knockout, angiotensin II-induced AAA formation was accelerated (Zhang et al. 2018).

Similar findings for SIRT1 were reported in studies on AD. In tissue samples from AD patients undergoing surgery, significantly decreased expression levels of SIRT1, as well as of activator protein 1 and decorin, two proteins involved in SIRT1 downstream signaling, were found compared to healthy controls (Zhang et al. 2020). Moreover, in mice with β -aminopropionitrile-induced AD, application of a SIRT1 activator partially inhibited pathological processes such as medial degeneration. Results from a western blot analysis indicated for SIRT1 activity to protect against AD by enhanced AP-1/decorin signaling (Zhang et al. 2020).

Taken together, these studies all indicate an important role for SIRT1 in protecting the vasculature from various pathologies. However, the underlying mechanisms are not fully understood, and further research is required to determine whether SIRT1 might be a potential therapeutic target in the medical therapy of vascular pathologies.

3 Material and Methods

3.1 Study group, collection and preparation of tissue samples

Tissue collection for research purposes during autopsies at the University Hospital Hamburg-Eppendorf is permitted upon written notification of local authorities and under the premise that all person-related data recorded (see below) are anonymized. Accordingly, local authorities were informed about this study on February 13, 2015. An additional ethics vote was not necessary. Human abdominal aortic tissue from 95 deceased study subjects was collected at the Institute for Forensic Medicine at the University Hospital Hamburg-Eppendorf between 2014 and 2017. The sole inclusion criterium was the prevalence of an aneurysm or dissection in the aorta ascendens or/and aorta descendens. Children under 18 years of age, burn victims and bodies with an advanced stage of decay were excluded. Tissue was collected in formalin and RNAlater. Total RNA was prepared and RNAlater samples were stored at -80 °C until processing. Based on autopsy protocols, the following data were recorded: Age, gender, height and weight. The body mass index (BMI) was then calculated by the following formula: $BMI = \text{body weight [kg]} / \text{height [m]}^2$. Also based on autopsy protocols, tissue samples from the AA were initially classified according to the prevalence of an aneurysm (A), a dissection (D) or the absence of the two pathologies (0) in the abdominal aorta (AA). It should be noted that study subjects classified as "0" still had an aortic aneurysm or a dissection at another section of the aorta. The status of pathologies in the other aortic sections was not considered in this analysis of AA specimens.

All formalin-fixed tissue samples were processed for histology and tissue sections were subjected to Elastica-van-Gieson staining. Each aortic specimen was assessed for the prevalence and extent of atherosclerotic plaque (intimal lesions, medial lesions, medial degeneration and hemorrhages). A binary plaque score was finally generated whereby "0" comprised all specimens with no atherosclerotic changes or minor lesions restricted to the intimal layer only. "1" (= P) was chosen when the medial layer was affected. Finally, each aortic specimen was assigned to pathology subgroups aneurysm (A), dissection (D), plaque (P) or no pathology (0). It became obvious that all but one specimen with an aneurysm were also scored positive for atherosclerotic plaque. For better clarification, this subgroup will be referred to as subgroup AP in the following, as aortic pathology aneurysm can only be considered in the presence of plaque.

3.2 Analysis of gene expression by RT-qPCR

Gene expression was measured by reverse-transcriptase quantitative polymerase chain reaction (RT-qPCR) using total RNA that had previously been prepared. Briefly, this three-step method includes synthesis of complementary DNA (cDNA) from total RNA, amplification of a target cDNA fragment using specific primers and the quantitative measurement of the amplicon in real time (Nolan et al. 2006). Reaction kits and laboratory equipment are listed in the appendix (Table A1, Table A2).

3.2.1 Synthesis of cDNA

Complementary DNA (cDNA) is a single strand DNA molecule, synthesized by the enzyme reverse transcriptase from an RNA template. RNA extraction and photometric measurement of RNA concentration in the samples had been performed. Prior to further usage, samples with an RNA concentration higher than 14.3 ng/μl were diluted to this concentration with nuclease-free water. The „Maxima First Strand cDNA Synthesis Kit for RT-qPCR (Thermo Scientific; Table A1) was used for the cDNA synthesis and oligo-dT primers were used to selectively transcribe mRNA molecules with a poly-A tail. Following the producer’s protocol, reaction mixtures were pipetted on ice in sterile reaction tubes (Table 1).

Table 1. Reaction mixtures for cDNA synthesis.

Volume of nuclease-free water added depended on the concentration of the RNA-sample. Desired RNA concentration in the samples: 14.3 ng/μL. When necessary, samples were diluted with nuclease-free water, less concentrated samples were used without further dilution.

	Volume
5X Reaction Mix	4 μL
Maxima Enzyme Mix	2 μL
<i>Total RNA</i> -sample in Nuclease-free water	14 μL
Total volume	20 μL

After pipetting, the reagents were mixed by vortexing. The T100™ Thermal Cycler (BIO-RAD; Table A2) was used for the cDNA synthesis reaction. The samples were incubated at 25 °C for 10 min for annealing and subsequently at 50 °C for 15 min for reverse transcription. Reactions were terminated by incubating the assays at 85 °C for 5 min. Finally, 20 μl RNase-free water was added to each reaction mix before storage at -80 °C until further usage.

3.2.2 Reverse transcriptase quantitative polymerase chain reaction

The expression of CD31, Myh11, CD68, CD45, NOS3 and SIRT1 were measured by reverse transcriptase quantitative polymerase chain reaction (RT-qPCR) using the Rotor-Gene-Q-System and the Rotor-Gene SYBR Green PCR Kit by Qiagen (Table A1, Table A2). All primers used are listed below (Table 2).

Table 2. Primers used for RT-qPCR.

Dilution refers to 100 μ M stock solution of primers. All primers were supplied by Sigma-Aldrich.

Gene	Dilution	Forward primer	Reverse primer
GAPDH	1:20	5'-TCCTGCACCACCAACTGCTT-488	3'-AGGGGCCATCCACAGTCTTC-592
CD31	1:10	AACAGTGTTGACATGAAGAGCC	TGTA AACAGCAGCAGTCATCCTT
CD68	1:20	CTTCTCTCATTCCCCTATGGACA	GAAGGACACATTGTACTCCACC
Myh11	1:20	CGCCAAGAGACTCGTCTGG	TCTTTCCCAACCGTGACCTTC
CD45	1:10	ACCACAAGTTTACTAACGCAAGT	TTTGAGGGGGATTCCAGGTAAT
NOS3	1:10	TGATGGCGAAGCGAGTGAAG	ACTCATCCATACACAGGACCC
SIRT1	1:20	TGTGTCATAGGTTAGGTGGTGA	AGCCAATTCTTTTTGTGTTCTG

As a reference gene, glyceraldehyde 3-phosphate dehydrogenase (GAPDH) was included. For amplicon measurements, SYBR Green I (Qiagen) was used, a fluorescent dye that specifically binds to double-stranded DNA. Amplicon generation was monitored by real-time measurements of SYBR Green I fluorescence, displayed in a fluorescence intensity-number of cycles diagram. The number of cycles to reach a predetermined threshold (ct = cycle threshold) was then used to calculate the relative template concentration of the sample (see Section 3.2.3).

Lyophilized primers (Sigma-Aldrich; Table 2) were dissolved in nuclease-free water to obtain 100 μ M stock solutions. Primer concentrations were chosen so that a doubled template concentration gave a by one decreased ct-value. Additionally, melting curves were recorded at the end of every qPCR run to demonstrate assay specificity. When more than a single peak was detected, qPCR runs were repeated with fresh solution aliquots (see below). In every RT-qPCR run, 72 samples were analyzed. These included triplicates of four genes (three genes of interest plus GAPDH as the reference gene) in five specimens (= 60 samples), two water controls for each gene (eight samples) and one positive control, consisting of a corresponding DNA fragment for each gene (four samples). To prepare the reaction mixture, 1 μ l of cDNA solution was added to 9 μ l of the reaction master-mix (Table 3) whereby each master-mix contained the appropriate primer pairs.

Table 3. Schema of the preparation of the master-mix for one cDNA sample.

	Volume
RNAse free water	3 μ L
Primer	1 μ L
Rotor-Gene SYBR Green PCR Master-Mix	5 μ L
Total volume	9 μ L

For the initial DNA polymerase activation and denaturation of cDNA, samples were incubated at 95 °C for 10 min. Subsequently, 40 cycles of qPCR with denaturation (10 s at 95 °C; Table 4), annealing (15 s at 60 °C), elongation (20 s at 72 °C) and the recording of melting curves (5 s/step at 72 – 95 °C) were performed by the Rotor-Gene-Q-System (Qiagen; Table A2).

Table 4. Steps of one RT-qPCR run.

	Duration	Temperature	Repetitions
Initial PCR activation and denaturation	10 min	95 °C	1x (initial)
Denaturation	10 s	95 °C	40x
Annealing	15 s	60 °C	
Elongation	20 s	72 °C	
Recording of melting curves	5 s/step	72 - 95 °C	

3.2.3 Data analysis and quality requirements

Expression of the target genes in the cDNA-samples was calculated in relation to the expression of the reference gene GAPDH by using the delta-ct method. Gene expression is then given in % GAPDH.

$$\text{Gene expression (in \% GAPDH)} = 2^{(-\text{ct}(\text{target gene}) - \text{ct}(\text{GAPDH}))} * 100$$

For this calculation, the mean ct-value of the triplicate measurements was used. If an individual ct-value deviated by more than 0.5 ct from the average ct-value, the corresponding RT-qPCR run was repeated. If three measurements failed to fulfil these criteria, the average of all nine individual measurements was used. RT-qPCR runs were also repeated if one of the two negative controls showed any amplicon generation, or if the positive control was not properly amplified.

3.3 Statistical analysis

For statistical analyses, Microsoft Excel 2011 (Microsoft) and Prism 6.07 (GraphPad Software Inc.) were utilized. All gene expression data were logarithmized (\log_2). Data are presented as mean \pm standard deviation (SD) or median with interquartile ranges (IQR), the 5 - 95 percentiles and outliers. Data distribution was tested for normality by the D'Agostino & Pearson omnibus normality test. T-tests or Mann-Whitney tests were used for group comparisons of parametric and non-parametric data sets, respectively. Analyses of variance were performed by one-way Anova followed by the Tukey's multiple comparison test for parametric data and by the Kruskal-Wallis test followed by the Dunn's comparisons test for non-parametric data. For correlation analyses, the Spearman correlation coefficient r_s and corresponding significance value P were calculated. For all statistical analyses, $P < 0.05$ was considered significant. More details are given in respective figure legends.

3.4 Immunohistochemical Mac2 staining

To stain for macrophages, an antibody against the macrophage/monocyte surface antigen Mac2 was used (Figure 5). All reagents utilized for the immunohistochemical Mac2 stain are listed in Table A3. Staining details are given in Table 5.

Paraffin blocks of all tissue specimens used in this study had previously been prepared. Using a sliding microtome (pfm medical; Table A2) 3 μm sections were cut from paraffin-embedded tissue blocks and were then transferred onto microscope slides. For each tissue sample, ten slides with two sections each were generated. The slides were then incubated at 37 °C for 12 h and stored at room temperature in the dark until further usage. Prior to the staining procedures the tissue sections were deparaffinized by incubating the slides in a series of xylene and a gradient of alcohol solutions and finally rehydrated with distilled water (Table 5).

Table 5. Mac2 staining.

Procedure/reagent		Duration
Deparaffinization and rehydration		
Xylol		3 x 5 min
Ethanol 99%		2 x 5 min
Ethanol 96%		5 min
Ethanol 70%		5 min
Aqua destillata		5 min
Staining		
Incubation with Antigen Retrieval Citra Plus in a water bath at 95 °C (1:10 diluted in distilled water)		40 min
Cooling slides at room temperature		20 min
Cooling slides on ice		20 min
Washing in Tris-buffered saline (TBS)	TBS 0,05 M, pH 7,6: - 88 g crystalline sodium chloride > 99,8% and 61 g Trizma® base (> 99,9%) diluted in 800 ml distilled water - pH adjustment with 50 ml of hydrochloride acid - fill up to 1 l with distilled water	3 x 5 min
Quenching of endogenous peroxidase (3% H ₂ O ₂)		15 min
Washing in TBS		5 min
Avidin-Biotin-Blocking Kit		
Avidin		15 min
Washing in TBS		3 x 5 min
Biotin		15 min
Washing in TBS		3 x 5 min
Protein block with rabbit serum		20 min
Application of antibodies		
Primary antibody	MAC-2 (rat-anti-mouse/human 1:1000) or Isotype control (rat IgG2a)	Overnight incubation (12-16 h)
Washing in TBS		3 x 5 min
Secondary antibody	rabbit-anti-rat 1:200	45 min
Washing in TBS		3 x 5 min
Avidin-Biotin Complex	Vectastain® Elite ABC Reagent: - 50 µl reagent A - 50 µl reagent B mixed in 2500 ml antibody diluent - allow to stand for 30 min	30 min
Washing in TBS		3 x 5 min
AEC 2 components kit (substrate)	Components: - 1 drop of AEC concentrate - 2 ml of substrate buffer	microscopic control
Washing in distilled water		3 x 5 min
Counterstaining with hematoxylin Mayer		30 sec
Washing in tap water		10 min
Cover: coverslip with permanent mounting medium (Aquamount®)		

To unmask antigens, Antigen Retrieval Citra Plus stock solution (10x concentrated, BioGenex) was diluted 1:10 in distilled water and then applied to the slides. The slides, covered with the antigen retrieval solution, were then incubated in a water bath at 95 °C for 40 min. After cooling down, the slides were washed in 50 mM Tris-buffered saline (TBS, Sigma® Life Science, Roth, for preparation see Table 5) three times for 5 min. For staining, the Avidin-Biotin-Complex method (ABC-method) was utilized. This detection method is based on the high affinity of the glycoprotein Avidin to the hydrophilic vitamin Biotin, which has been covalently linked to an antibody prior to its application (Figure 5).

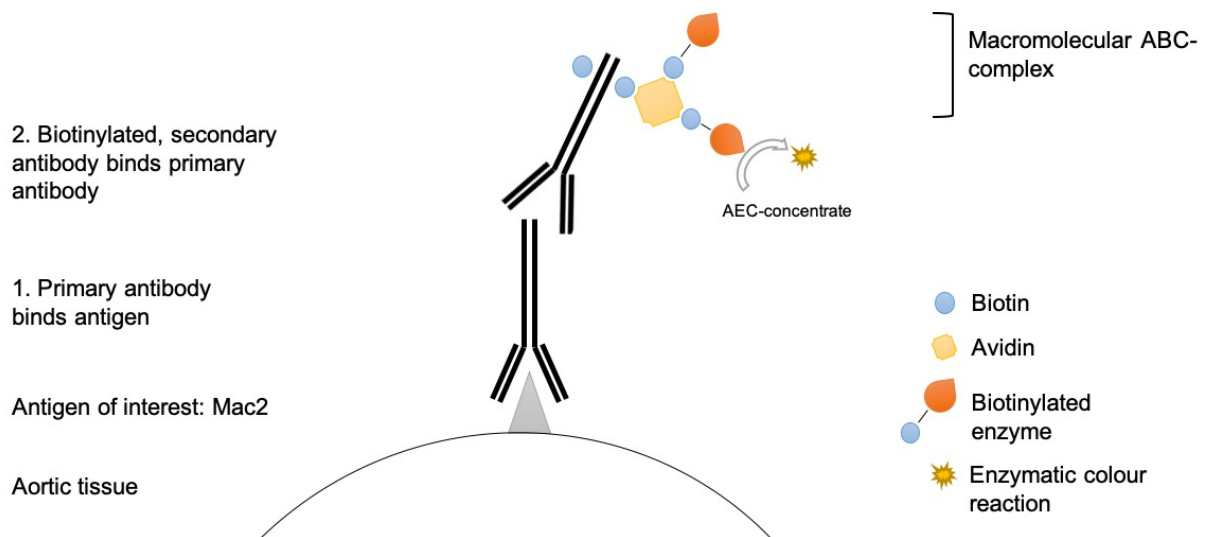


Figure 5. Principles of Mac2 staining using the Avidin-Biotin complex method. Aortic tissue samples were stained for Mac2 antigen. After unmasking of the Mac2 antigen and blocking of endogenous enzyme activity, a specific primary antibody was applied and let incubate overnight (1). Then, a biotinylated secondary antibody was added that specifically binds the primary antibody (2). Macromolecular avidin-biotin-complexes (ABC), consisting of glycoprotein Avidin and biotinylated enzymes, were applied. These complexes bind the secondary antibody. After the application of the 3-amino-9-ethylcarbazole-concentrate (AEC) a detectable, enzymatic color reaction occurred. For detailed staining protocol see Table 5 and Table A3 for reagents.

Prior to the application of the primary antibody (see 1. Primary antibody in Figure 5), the activity of endogenous peroxidase as well as non-specific binding sites for avidin, biotin and antibodies were blocked by successively incubating slides with (a) 3% hydrogen peroxide (Merck KGaA) for 15 min, (b) with avidin and biotin (Avidin/Biotin Blocking Kit, life technologies) for 15 min each, and (c) with rabbit serum (BioGenex) for 20 min. In between the slides were washed with 50 mM TBS three times for 5 min (Table 5). The monoclonal rat Mac2-antibody (Cedarlane,

catalogue number CL 8942AP, LOT number 104227A; Table A3) was then applied to slides in a 1:1000 dilution. After an over-night incubation (12 – 16 h), slides were washed in 50 mM TBS for 5 min and a biotinylated rabbit anti-rat IgG antibody (H+L; 1:200; Vector Laboratories, cat. number BA-4000, LOT number W0720) was applied for 45 min (see 2. Secondary antibody in Figure 5). Subsequently, the slides were washed in 50 mM TBS three times for 5 min. For staining, Vectastain® Elite ABC Reagent (Vector Laboratories) was used. Prior to application, the reagents Avidin (reagent A) and biotinylated enzyme (reagent B) were mixed and kept for 30 min at room temperature to allow complex formation between avidin and biotinylated peroxidase (ABC; Figure 5).

When applied to the tissue sample, the ABC binds to the biotinylated secondary antibody. Vectastain® Elite ABC Reagent was applied for 30 min. The slides were then washed in 50 mM TBS three times for 5 min afterwards to remove unbound ABC.

The peroxidase substrate, 3-Amino-9-ethylcarbazole (AEC-concentrate, DCS Chromoline, DCS Innovative), was then added onto the slides and a color reaction was monitored under a light microscope to prevent over-staining. The reaction was terminated by washing slides in distilled water three times for 5 min (Table 5). Color development generally took 8 – 13 min. Nuclei were visualized by counterstaining slides with hematoxylin (Medite) for 30 s. To terminate the staining reaction with hematoxylin, the slides were washed in tap water for 10 min. Finally, stained tissue sections were covered with coverslips using Aquamount (Polysciences) as mounting medium.

Ten tissue samples were stained in each batch. For each tissue sample, one slide with two tissue sections was utilized, whereof one section was incubated with monoclonal Mac2 rat antibody (see above) and the other with a monoclonal isotype control antibody (rat IgG2a, concentrated 1 mg/ml, in a 1:1000 dilution; R&D Systems, cat. number MAB006, LOT number CAO2414021). Each batch also included one negative control without primary antibody and one positive control for macrophage staining (tonsil or colon tissue).

The stained tissue sections were analyzed with an inverted light microscope at different magnifications (Keyence Biozero BZ-8100). For documentation, overview images at 40x magnification and, supplementary for some samples, images of areas of interest at 200x magnification were taken with the camera integrated in the microscope. Images

of the corresponding areas were also taken from the adjacent tissue sections with control antibody (isotype control). All images were saved as JPEG files.

4 Results

4.1 Characteristics of the study group

Sample collection (see Section 3.1), as well as the analysis of the expression of S1P receptors in the aortic tissues (see Section 4.2.3) had been completed prior to this work by members of our group. In total, tissue samples from the infrarenal abdominal aorta (AA) from 95 study subjects were examined whereof 61 samples (64%) were from men and 34 (36%) from women. Tissues were initially assigned to five pathology subgroups: A (aneurysm, $n = 49$) and D (dissection, $n = 19$), both according to data from autopsy protocols, and P (plaque, $n = 67$), based on our histological evaluation (the presence of medial lesions, medial degeneration, or hemorrhage; Figure 6B-C). Subgroup 0 ($n = 18$) included tissue with no pathology or minor atherosclerotic lesions that were restricted to the intimal layer (Figure 6).

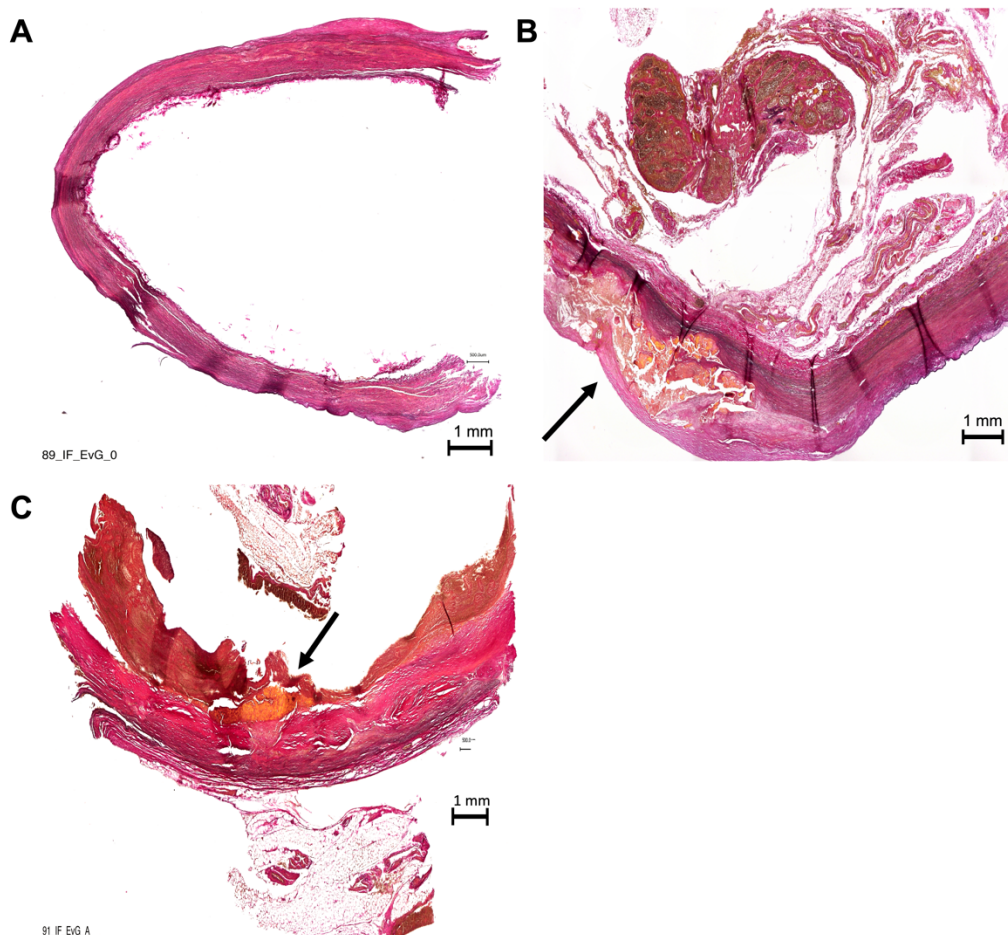


Figure 6. Elastica-van-Gieson staining of infrarenal aortic tissue sections. All tissue samples were subjected to histology and scored for the prevalence of plaque. Representative tissue samples (with sample number) illustrating differentiating criteria for plaque score group 0 and 1 are shown. A: Small intimal lesion with intact media, plaque score group 0 (#89). B: Medial lesion, plaque score group 1 (#74). C: Hemorrhage, plaque score group 1, (#91).

Finally, subgroup ADP (n = 77) was defined to consist of specimens with at least one out of the three pathologies investigated. During the evaluation of pathologies, it became apparent that many specimens presented with multiple vascular pathologies. All but one specimen in the subgroup A also presented with atherosclerotic plaque. For clarity, I therefore refer to this subgroup as AP rather than A. About half of the dissection samples (52%) were also scored positive for plaque, whereas no specimen displayed an aneurysm and a dissection together. Table 6 gives an overview of the five pathology subgroups. The defined pathology subgroups were then compared regarding epidemiological parameters (gender, age and BMI) using tests for group comparison (t-test), analyses of variances (ANOVA) and post-hoc tests (Tukey's multiple comparison test; Table 6, Figure 7).

Table 6. Epidemiological data of the study subgroups.

Abdominal aortic tissue samples (N = 95, all) were classified according to the prevalence of vascular pathologies: 0 (none), ADP (at least one pathology), D (dissection), P (plaque) and AP (aneurysm and plaque; see Section 3.1). For each subgroup, number of specimens is shown (n), as well as gender (n, %), age (median, min-max) and BMI (mean \pm standard deviation SD). #, differences between pathology subgroups were analyzed by a One-way ANOVA; respective P-values: 0.72 (gender, n.s.), $9,1864 \times 10^{-5}$ (age, for post-hoc analysis see Figure 7) and 1 (BMI, n.s.). ****P<0.0001; n.s., non-significant. BMI, body mass index; m, male; f, female.

	all	0	ADP	D	P	AP
n	95	18	77	19	67	49
Gender # (n, %)	m:61(64%) f:34(36%)	m:10(56%) f:8(44%)	m:51(66%) f:26(34%)	m:11(58%) f:8(42%)	m:43(64%) f:24(36%)	m:35(71%) f:14(29%)
Age # (years) median (min-max)	71 (33 – 91)	59 (33–86)	72 (43 – 91)	65 (43 – 88)	72 (43 – 91)	74 (57 –91)
BMI # (kg/m²) mean \pm SD	27 \pm 5.7	28 \pm 4.2	27 \pm 5.9	27 \pm 4.8	26 \pm 6	27 \pm 6.5

A one-way ANOVA showed that neither the gender distribution nor the BMI varied significantly among the pathology subgroups and when compared to subgroup 0 (Table 6).

In contrast, significant differences between the subgroups were found regarding age: Study members from subgroups AP and P were significantly older than those from subgroups 0 and D (Figure 7).

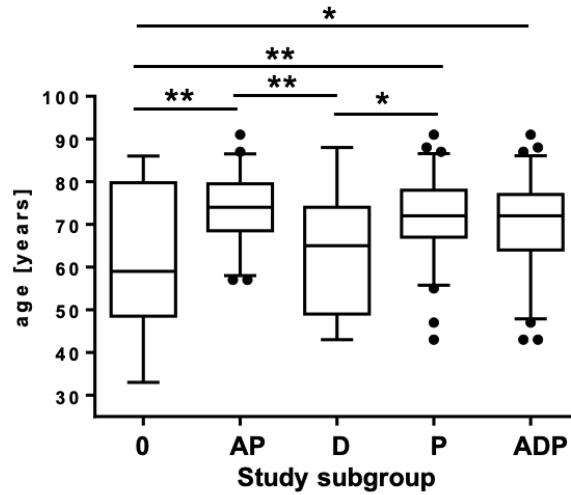


Figure 7. Age in study subgroups. For each subgroup, age is shown as median, IQR and 5 - 95 percentiles with outliers. Differences were analyzed by a One-way ANOVA and a post-hoc Tukey's multiple comparisons test. * $P < 0.05$, ** $P < 0.01$. 0, no pathologies (n = 18); AP, aneurysm and plaque (n = 49); D, dissection (n = 19); P, plaque (n = 67); ADP, either A, D, or P (n = 77).

4.2 Analysis of gene expression in diseased and non-diseased aortic tissue

4.2.1 Cell markers

To identify potential alterations on a cellular level associated with aortic aneurysm, dissection or atherosclerotic plaque, the expression of the following four cell markers was measured: CD31 (endothelial cells), CD45 (leukocytes), CD68 (monocytes/macrophages) and Myh11 (vascular smooth muscle cells). Gene expression was measured by RT-qPCR (see Section 3.2). Initially, cell marker expression was compared between subgroups 0 and ADP (Figure 8), followed by an analysis including pathology subgroups 0, AP, D and P (Figure 9).

The only difference between subgroups 0 and ADP was found for VSMC marker Myh11, with a significantly lower expression in subgroup ADP (Figure 8B).

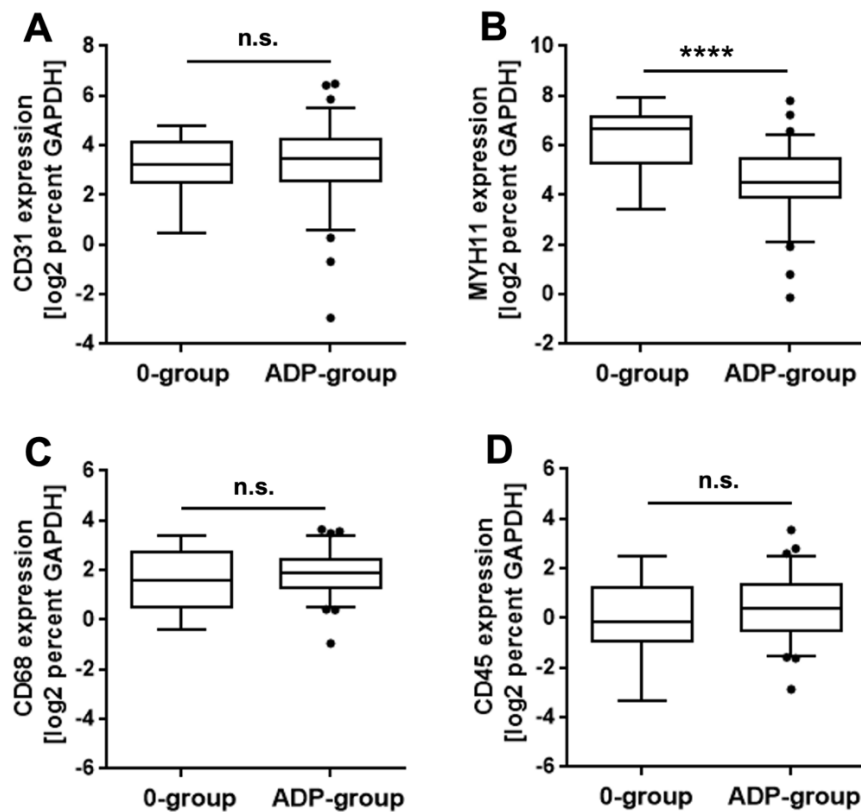


Figure 8. Expression of cell markers in study subgroups 0 and ADP. The expression of CD31 (A), Myh11 (B), CD68 (C) and CD45 (D) was measured in infrarenal aortic tissue by RT-qPCR (N = 95). Data are presented as log2 percent of GAPDH expression. Data (median, IQR and 5 - 95 percentiles including outliers) are shown for two subgroups: 0 (no pathology, n = 18) and ADP (aneurysm, dissection or plaque, n = 77). Significance (P-value) was calculated using the Mann-Whitney test. The P-value is indicated on top of error bar. *P<0.05, ***P<0.001, ****P<0.0001; n.s., non-significant.

When cell marker expression was compared between subgroup 0 and subgroups AP, D or P, a test for variances showed significant differences for Myh11 and CD68 (Figure 9B-C).

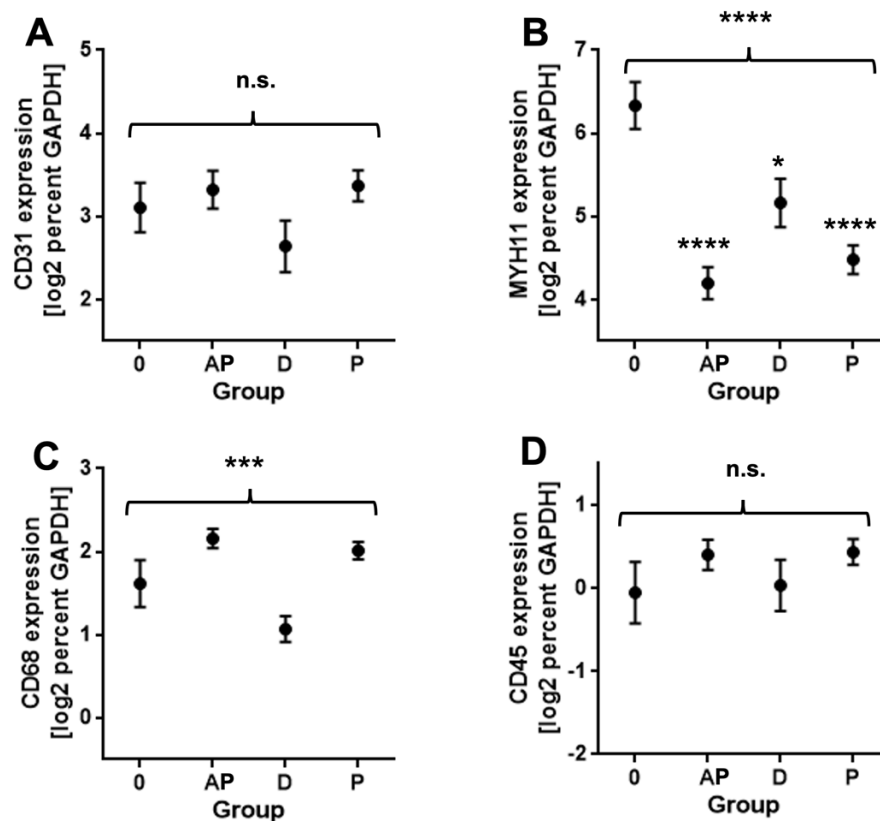


Figure 9. Expression of cell markers in study subgroups 0, AP, D and P. The expression of CD31 (A), Myh11 (B), CD68 (C) and CD45 (D) was measured in infrarenal aortic tissue by qPCR (N = 95). Data are presented as log2 percent of GAPDH expression. Data (mean +/- standard error of the mean (SEM)) are shown for four subgroups: 0 (no pathology, n = 18), AP (aneurysm and plaque, n = 49), D (dissection, n = 19) and P (plaque, n = 67). Analysis of variance was calculated by the Kruskal-Wallis test and the P-value is shown above parentheses. The Dunn's multiple comparisons test was performed for significance of differences of an individual pathology (AP, D, or P) to subgroup 0. The P-value is indicated on top of error bar. *P<0.05, ***P<0.001, ****P<0.0001; n.s., non-significant.

After applying post-hoc tests, significant differences were only seen for Myh11 (Figure 9B). Compared to subgroup 0, Myh11 expression was decreased in all pathology subgroups with the highest degree in subgroups AP and P. Although without significance, expression of all other marker genes (CD31, CD68 and CD45) was found higher in subgroups AP and P compared to 0 and D (Figure 9A, C and D).

4.2.2 NOS3 and SIRT1

Analogous to the cell markers, the expression of NOS3 and SIRT1 was measured and compared between pathology subgroups (Figure 10). These two genes were chosen for their known role in the vasculature and vascular pathologies (see Section 2.6).

For NOS3, no significant difference in the expression was found between subgroup 0 and any of the pathology subgroups (Figure 10A, B). The expression of SIRT1 was significantly decreased in subgroup ADP compared to subgroup 0 (Figure 10C) and significantly differing among the pathology subgroups (Figure 10C). More detailed analysis then revealed a significant decrease of SIRT1 expression in subgroups AP and P, but not in D when compared to subgroup 0 (Figure 10D).

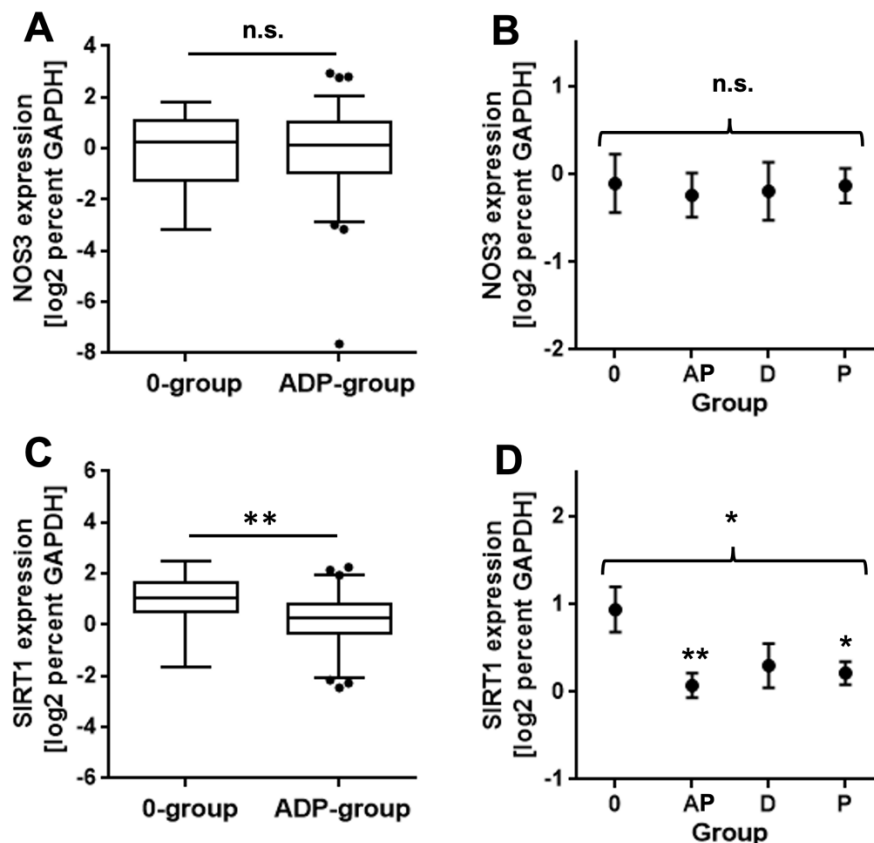


Figure 10. Expression of NOS3 and SIRT1. The expression of NOS3 (A, B) and SIRT1 (C, D), was measured in infrarenal aortic tissue by RT-qPCR (N = 95). Data are presented as log2 percent of GAPDH expression. A and C, Data (median, IQR and 5 - 95 percentiles including outliers) are shown for subgroups 0 (no pathology, n = 18) and ADP (aneurysm, dissection or plaque, n = 77). Significance (P-value) was calculated using the Mann-Whitney test. B and D, Data (mean +/- SEM) are shown for subgroups 0 (no pathology, n = 18), AP (aneurysm and plaque, n = 49), D (dissection, n = 19) and P (plaque, n = 67). Analysis of variance was calculated by the Kruskal-Wallis test and the P-value is shown above parentheses. The Dunn's multiple comparisons test was performed for significance of differences of an individual pathology (AP, D, or P) to the 0-subgroup. The P-value is indicated on top of error bar. *P<0.05, **P<0.01; n.s., non-significant.

4.3.2 S1P receptors

Prior to this study, the expression of S1PR1, S1PR2 and S1PR3 in the aortic tissue samples had been measured and analyzed for associations with the aortic pathologies aneurysm and dissection. Here, subgroup P was added to the correlation analysis.

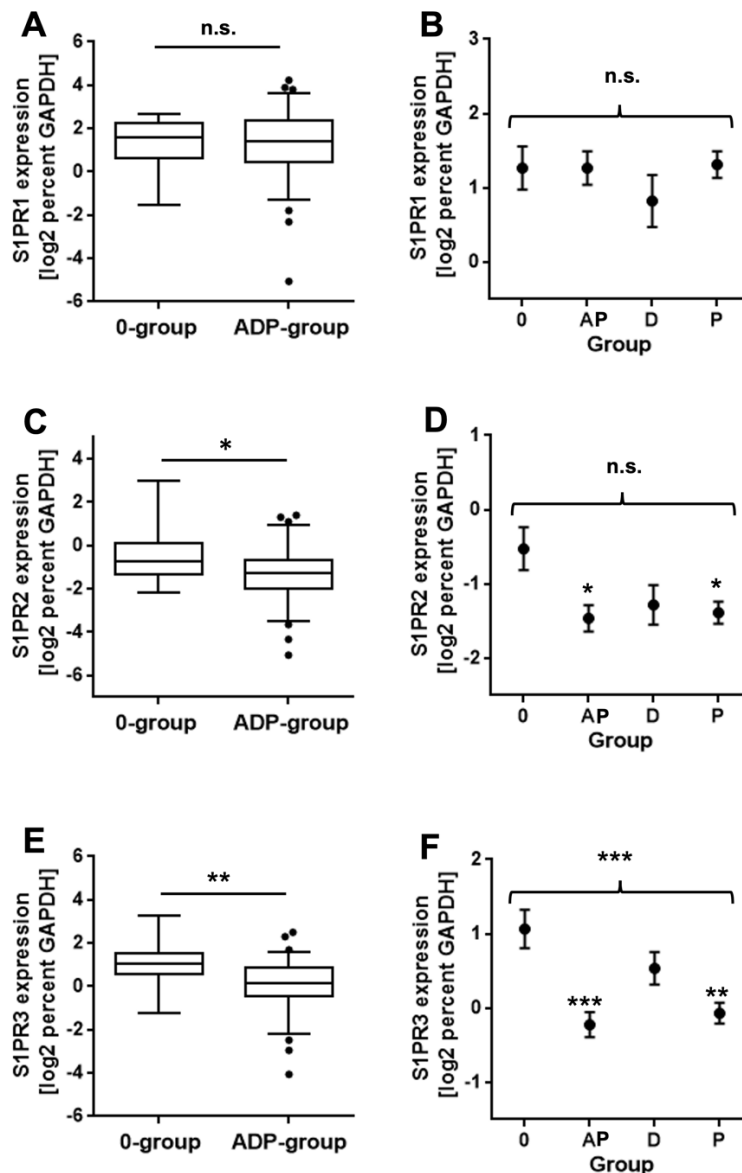


Figure 11. S1P receptor expression. The expression of S1PR1 (A, B), S1PR2 (C, D) and S1PR3 (E, F) was measured in infrarenal aortic tissue by RT-qPCR (N = 95). Data are presented as log2 percent of GAPDH expression. A, C, E (left column), Data (median, IQR and 5 - 95 percentiles including outliers) are shown for two groups: 0 (no pathology, n = 18) and ADP (aneurysm, dissection or plaque, n = 77). Significance (P) was calculated using the Mann-Whitney test. B, D, F (right column), Data (mean +/- SEM) are shown for four groups: 0 (no pathology, n = 18), AP (aneurysm and plaque, n = 49), D (dissection, n = 19) and P (plaque, n = 67). Analysis of variance was calculated by the Kruskal-Wallis test and the P-value is shown above parentheses. The Dunn's multiple comparisons test was performed for significance of differences of an individual pathology (AP, D, or P) to the 0-group. The P-value is indicated on top of error bar. *P<0.05, **P<0.01, ***P<0.001; n.s., non-significant. S1PR, sphingosine 1-phosphate receptor.

As shown in Figure 11A-B, the S1PR1 expression did not significantly differ among the pathology subgroups. The expression of S1PR2 as well as S1PR3 was significantly lower in subgroup ADP compared to subgroup 0 (Figure 11C,E). In post-hoc group comparisons of the variance analysis, both receptors showed decreased expression in subgroups AP and P compared to subgroup 0 (Figure 11D,F). A trend of lower expression was also seen for subgroup D, however, without statistical significance.

4.3 Correlation analyses between the expression of cell markers and the expression of NOS3, SIRT1 and the S1P receptors 1-3

To identify potential cell- or pathology-specific expression of a gene or S1P receptor of interest, correlation analyses were performed between cell marker expression and the expression of NOS3, SIRT1 and S1P receptors (Figure 12, Figure 13).

For both NOS3 and SIRT1, significant associations were found with CD31, CD45 and Myh11, but not with CD68 (Figure 12). Differences in the Spearman coefficient r_s between NOS3 and SIRT1 were noted for CD31 expression with $r_s(\text{CD31}/\text{NOS3}; 0.78) > r_s(\text{CD31}/\text{SIRT1}; 0.55)$ and for Myh11 expression with $r_s(\text{Myh11}/\text{NOS3}; 0.35) < r_s(\text{Myh11}/\text{SIRT1}; 0.6)$.

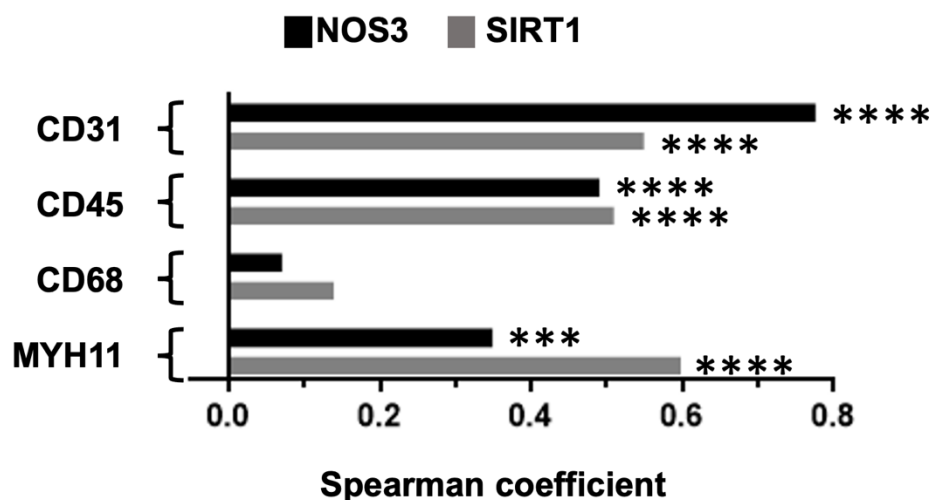


Figure 12. Correlations between the expression of NOS3, SIRT1 and cell marker genes. The expression of all genes was measured in infrarenal aortic tissue by RT-qPCR (N = 95). The Spearman coefficient r_s as well as the corresponding P-value were calculated for the indicated gene pairs. ***P<0.001, ****P<0.0001.

For CD31 as well as Myh11 expression, significant positive associations with the expression of all three S1P receptors were found (Figure 13). The most significant association for CD31 was found with S1PR1 and for Myh11 with S1PR3. CD45 expression was associated with S1PR1 and S1PR2 on a similar level of significance. For CD68 expression, no significant association with the expression of one of the S1P receptors was found.

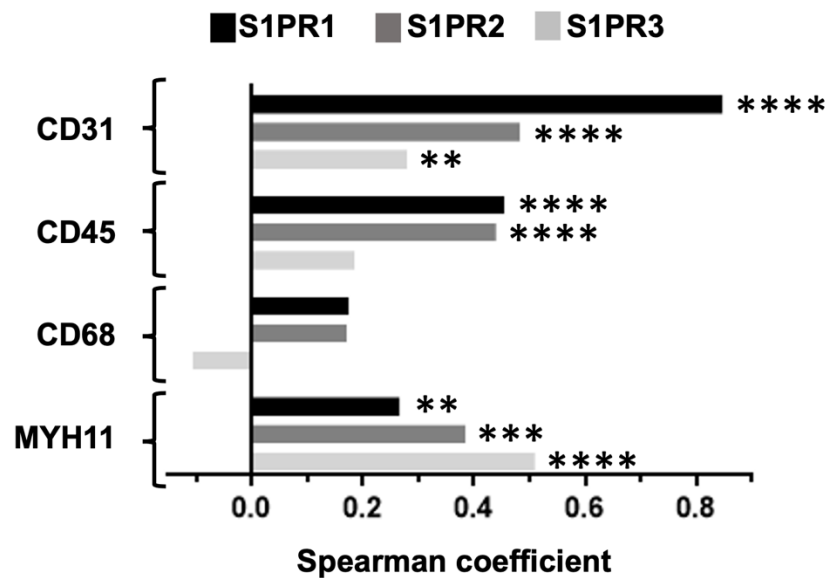


Figure 13. Correlations between the expression of S1P receptors and cell marker genes. The expression of all genes was measured in infrarenal aortic tissue by RT-qPCR (N = 95). The Spearman coefficient r_s as well as the corresponding P-value were calculated for the indicated gene pairs. **P<0.01, ***P<0.001, ****P<0.0001

4.4 Correlation analysis between the expression of SIRT1, NOS3 and the expression of S1PR1-3

Finally, correlation analyses were performed between the expression of NOS3 and SIRT1 and the S1P receptors to potentially gain insight about which of the genes are similarly regulated. For all S1P receptors a highly significant association with the expression of NOS3 and SIRT1 was found, although with varying Spearman coefficients r_s (Figure 14). For NOS3 and SIRT1 the highest association was obtained with S1PR1 and S1PR2, respectively.

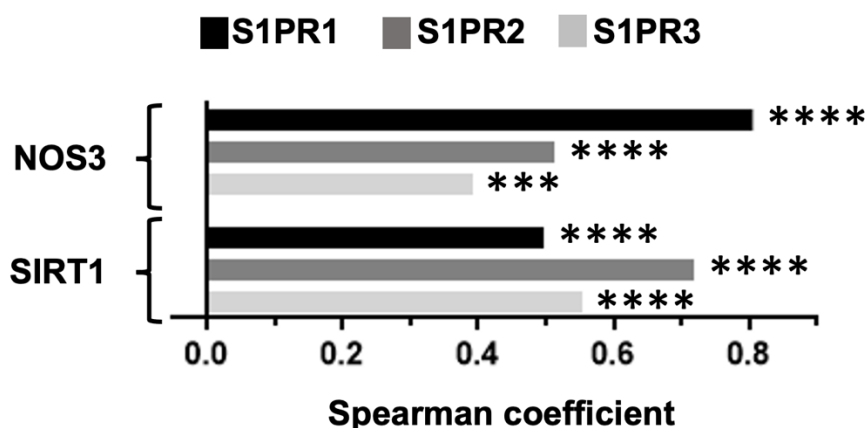


Figure 14. Correlations between the expression of S1P receptors and genes NOS3, SIRT1. The expression of all genes was measured in infrarenal aortic tissue by RT-qPCR (N = 95). The Spearman coefficient r_s as well as the corresponding P-value were calculated for the indicated gene pairs. **P<0.01, ***P<0.001, ****P<0.0001.

4.5 Frequency and distribution of macrophages in diseased and non-diseased aortic specimens

After the quantitative analysis of the expression of macrophage marker CD68 in the tissue samples, selected tissue samples (13 - 23 slides per pathology subgroup) were stained for Mac2 (see Section 3.4), to study potential pathology-specific localization of macrophages in diseased aortic tissue. Representative tissue slides had been selected based on EvG staining results and tissue quality of the study specimens. In total, 47 tissue samples have been used: 13 with aneurysm and plaque (AP), 14 with dissection (D), 4 with plaque only (P) and 16 without pathology (0; Table 7). In subgroup D, 6 out of all 14 stained tissue slides did present with co-existing plaque, but no differences were obtained when comparing the distribution and localization of macrophages in tissue samples from subgroup D with or without co-existing plaque. Macrophages were detected in 28 out of 31 tissue samples with a pathology (subgroups AP, P or D, 90%), but also in 12 out of 16 tissue samples with no pathology (subgroups 0, 75%; Table 7).

Table 7. Results of the Mac2 staining for macrophages.

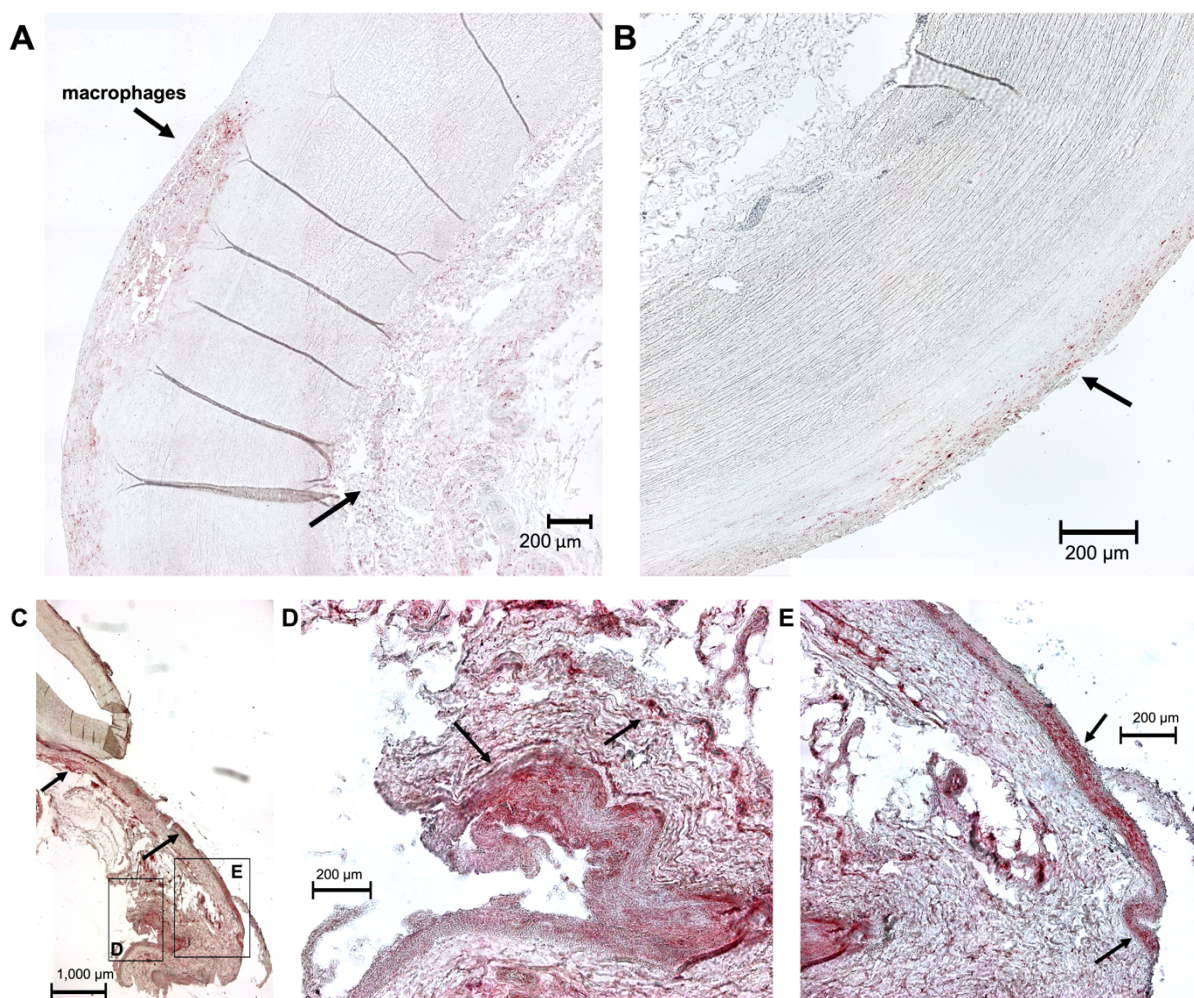
Based on EvG staining results and quality of the tissue samples, a total of 47 tissue samples comprising of all pathology subgroups were selected for Mac2 staining. Note that all tissue samples selected for the aneurysm group also presented with plaque. For each subgroup, the total number of tissue samples stained, and the number of tissues stained positive for Mac2 (n, %).

	Subgroups			
	0	AP	D	P
Total number	16	13	14	4
Positive for Mac2 (%)	12 (75%)	11 (85%)	13 (93%)	4 (100%)

In Figure 15, representative tissue sections illustrate pathology-specific localizations of macrophages for each pathology subgroup.

When comparing frequency and distribution of macrophages between the subgroups, it was obvious that in non-diseased tissue (subgroup 0) fewer macrophages were present per tissue sample than in diseased tissue (compare Figure 15A, B to Figure 15C-I). In tissues of subgroup 0, macrophages were generally restricted to the intima (Figure 15A, B).

In tissue samples from both subgroups AP and P, macrophages were identified in all arterial layers (Figure 15C-G). In all AP/P samples, macrophages were detected in plaque areas (Figure 15G) and in more than 50% of the AP/P tissues samples, macrophages were also seen in the adventitia and in the adjacent fibrous tissue (Figure 15C-E). In the media, macrophages were the least frequently seen (Figure 15E).



Continued on page 42

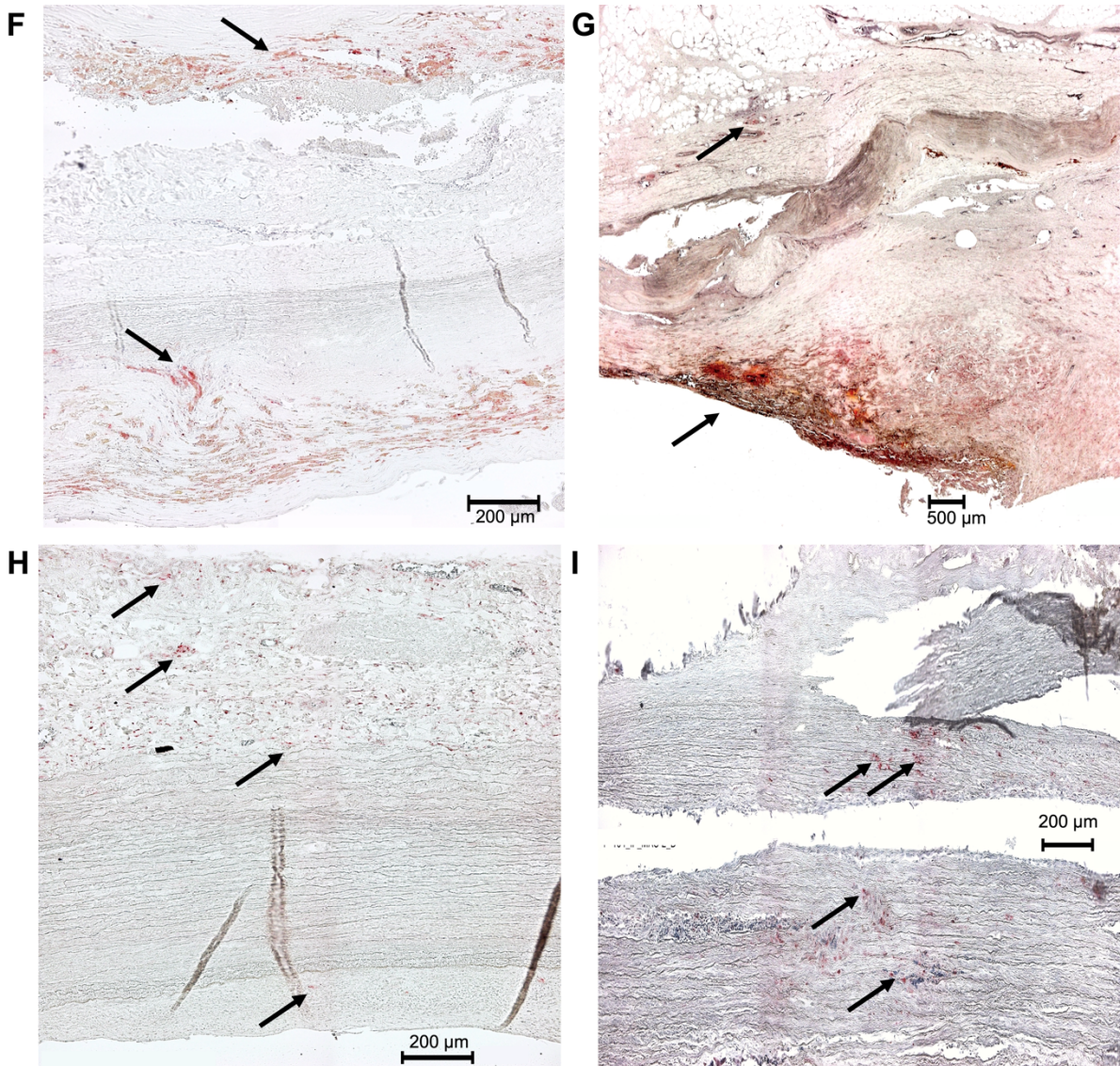


Figure 15. Macrophage staining of infrarenal aortic tissue sections. Representative tissue sections for each pathology subgroup (no pathology 0, plaque P, aneurysm and plaque AP, dissection D) were stained with Mac2 antibody (see methods 3.4). A, B: subgroup 0, A (#42) and B (#27), both at 200x magnification. C, D, E: subgroup P, (#78), magnification at 40x (C) and 200x (D, E) magnification. F, G: subgroup AP, F (#25) at 200x magnification and G (#102) at 40x magnification. H, I: subgroup D, H, (#24) and I (#104), both at 200x magnification. For all samples, isotype control stains were negative (see appendix, Figure A1). #, sample number. Arrows point to Mac2 positive cells.

Compared to tissue samples from subgroups AP and P (Figure 15F, G), macrophages were stained more frequently in the medial layer in samples from subgroup D (Figure 15H, I). This finding was independent of co-existing plaque. In 5 of the 14 tissue samples from subgroup D, macrophages were found to accumulate around tear edges of the dissection (Figure 15I).

5 Discussion

Vascular pathologies atherosclerosis, aneurysm and dissection can all arise in the abdominal aorta (AA). Despite their high mortality (Destatis 2019), to date, the pathophysiology and the molecular mechanisms underlying these vascular diseases remain to be fully elucidated.

The major aim of this study was to investigate mRNA expression levels of vascular cell markers in human abdominal aortic tissue samples to detect specific associations between their expression and the prevalence of aneurysms, dissections, or atherosclerosis. Further, this study aimed to investigate associations between the expression of these selected cell markers and the expression of vascular genes sirtuin 1 (SIRT1) and the nitric oxide synthase 3 (NOS3) as well as the expression of the S1P receptors 1-3 (S1PR1-3) in order to identify cell types of interest, in which these genes potentially play a role in regulating aortic pathologies.

SIRT1 and NOS3 have been chosen for this study as both mediate protective effects in the pathophysiology of degenerative vascular diseases (Kitada et al. 2016, Ota et al. 2010). Lipid mediator S1P and its receptors are of great interest as they play an essential role in the regulation of embryonic vascular development and in maintaining the vascular integrity (Proia and Hla 2015). To date, however, no study has been published relating S1P receptor expression to specific aortic pathologies except one, which relied on antibodies of insufficient quality as S1PR1 protein could not be detected in vascular tissue (Qu et al. 2012). Unpublished data from our laboratory, obtained from S1P receptor measurements in this study cohort, show a significant reduction of S1PR2 as well as S1PR3 expression in association with aneurysm and atherosclerosis in the abdominal aorta (Figure 11). These results from earlier S1PR measurements were further analyzed in this study.

5.1 Study design and study group

Although atherosclerotic plaque was one of the pathologies investigated in this study, atherosclerosis in the AA was not defined as an inclusion criterium. Only specimens from deceased individuals with an aortic aneurysm or dissection were included because of the relative rareness of these pathologies when compared to atherosclerosis. It should be noted that aneurysms or dissections have been located in any aortic section to fulfill inclusion criteria (see Section 3.1). As this study focuses

on the mechanisms of vascular pathologies in the AA only, potential pathologies in the other aortic sections were not considered any further. Here, tissue samples from the abdominal aorta only were investigated and a total of 95 specimens were included. Besides yielding a sufficient number of tissue samples with aneurysm and dissection for gene measurements, another advantage of this study design is that all samples were derived from people with an aortic pathology and therefore, fundamental epidemiological risk factors for cardiovascular pathologies such as age and gender were found similar among all subgroups and are less confounding in statistical analyses (Table 6).

To form pathology subgroups including atherosclerotic plaque, all tissue samples were processed for histology, EvG-stained, and then scored for the prevalence of atherosclerotic plaque in the AA (see Section 4.1; Figure 6). Plaque was found in all tissue samples but one from study subjects with an aneurysm. Thus, in this study, abdominal aortic aneurysm could not be analyzed separately from atherosclerosis. One could compare, however, tissue specimens with atherosclerotic plaque burden, without further consideration of co-existing (vascular) pathologies, and specimens specific with plaque and aneurysm (subgroup P vs AP). However, in no cases any differences between these two groups were found. From 19 samples with dissection (subgroup D), 10 also showed atherosclerotic plaque and it should be noted that these samples were included in subgroup D as well as in subgroup P.

5.2 Epidemiological characteristics of the study subgroups

Given that study subjects had originally been selected based on the prevalence of an aortic aneurysm or a dissection, it was no surprise to find more men ($n = 61$) than women ($n = 34$), an increased BMI in all study subgroups (mean: 27 kg/m^2) and an advanced age of the entire study group (median age 71 years; Table 6), as male gender, advanced age and obesity are general risk factors for cardiovascular pathologies (Roth et al. 2020).

Here, male study subjects represented the majority in all pathology subgroups (Table 6), and this is in agreement with the epidemiological data for these aortic pathologies found in previous studies. For instance, Kent et al. screened over three million individuals in the United States for AAA and 79% of the individuals with an AAA were men (Kent et al. 2010). Analyses of data from the international registry of acute aortic dissection revealed a proportion of males of 67.5% in individuals with Stanford A AD

and of 65.8% in individuals with Stanford B AD (Pape et al. 2015). For atherosclerosis a higher prevalence in men has long been recognized (Man et al. 2020).

As shown in Table 6, the BMI was elevated in all pathology subgroups with values between 26 and 28 kg/m², but did not vary significantly between the subgroups. Obesity, defined by an elevated BMI \geq 25 kg/m² has become a problem of worldwide concern and is a frequent finding in individuals with cardiovascular diseases. Atherosclerosis and obesity are co-existing in many (cardiovascular) patients and share pathophysiological mechanisms as both are considered lipid-storage diseases (Rocha and Libby 2009). Kent et al. reported for almost 75% of the individuals with an AAA to present with a BMI > 25 kg/m² (Kent et al. 2010). In a Swedish cohort study on aortic pathologies, an elevated BMI > 25 kg/m² was also reported frequently for individuals with AAA and AD. However, in this particular study, an elevated BMI was also seen for the entire study cohort (Landenhed et al. 2015).

Although all study subjects, including those in subgroup 0, presented with an aortic pathology (see Section 3.1 for inclusion criteria), subjects presenting with a pathology in the AA (subgroup ADP) were generally older than those without a pathology in the AA (subgroup 0) (72 versus 59 years; Figure 7). Notably, study subjects in subgroup 0 either presented with an aneurysm or a dissection in the thoracic aorta. It had previously been observed that individuals with an aneurysm in the thoracic aorta are younger (baseline age of 60.9 years) than individuals with an aneurysm in the abdominal aorta (baseline age 62.1 years) (Landenhed et al. 2015).

Further, study members with an aneurysm and plaque (subgroup AP, 74 years) or plaque alone in the AA (subgroup P, 72 years) were found to be significantly older than those with a dissection in the AA, regardless of the respective plaque status of study members of subgroup D (subgroup D, 65 years; Figure 7). This is also in line with previous studies, which found an even higher mean age in AAA patients (71 years) (Kent et al. 2010) compared to patients with AD (62 – 64 years) (Pape et al. 2015) or isolated abdominal aortic dissections (64 years) (Liu et al. 2020).

Taken together, although advanced age is associated with all three vascular pathologies (Kent et al. 2010, Wang and Bennett 2012, Pape et al. 2015), results from this study confirm that age appears to play a less important role in aortic dissections compared to atherosclerosis and abdominal aortic aneurysms and that generally, age appears as a more vital risk factor for vascular pathologies arising in the abdominal aorta compared to the other aortic sections.

5.3 Prevalence of multiple vascular pathologies in the AA

Several study subjects presented with multiple vascular pathologies.

5.3.1 Aneurysm and atherosclerosis in the AA

The observation that abdominal aortic aneurysm (AAA) frequently coincides with atherosclerotic plaque, agrees with existing data (Kent et al. 2010, Toghil et al. 2017). Generally, atherosclerosis in the AA is often found incidentally in imaging diagnostics of the abdomen for other medical purposes or in histologic analyses of tissue samples from the AA (Gallino et al. 2014). Atherosclerosis in the AA also has to be considered a frequent condition in presumably healthy adults, as shown in a Korean screening study with over 1,400 healthy individuals (mean age 55.9 years, 62.2% male gender). In their study cohort, plaque with or without stenosis in the AA was found in 75% of all study subjects. Further, atherosclerosis in the AA was found significantly associated with stenosis of the coronary arteries (Suh et al. 2018).

Based on the apparent co-existence of abdominal aortic aneurysm and atherosclerosis, a causal relation of the two vascular pathologies has been assumed for many years (Reed et al. 1992, Johnsen et al. 2010, Siasos et al. 2015). Atherosclerosis and abdominal aortic aneurysms not only share typical cardiovascular risk factors, such as advanced age, male gender, and smoking, but also pathophysiological mechanisms. Hallmarks involved in the pathogenesis of both diseases are endothelial dysfunction, apoptosis and phenotypic modulation of vascular smooth muscle cells, chronic inflammation, and degradation of extracellular matrix (Toghil et al. 2017, Siasos et al. 2015). However, it remains to be elucidated whether aneurysms in the abdominal aorta develop on the basis of atherosclerosis or whether the association of the two pathologies is only a result of shared risk factors and pathomechanisms.

Results from the present study promote the view of an aneurysm as a complication of atherosclerosis in the AA, as here, no aneurysm without co-existing plaque (except one case) was encountered, but vice versa, atherosclerotic plaque was frequently seen without an aneurysm. Further, compared to the other aortic sections, the AA is the most common aortic section for atherosclerotic lesions to develop (Thej et al. 2012), potentially contributing to the AA as a predilection site for aortic aneurysms. Atherosclerosis also appears to be a risk factor for aneurysms in the thoracic aorta,

but co-prevalence of the two pathologies is generally less frequent (65%) (Juraszek et al. 2013).

5.3.2 Dissection and atherosclerosis in the AA

Aortic dissections found in the AA most frequently originate from the thoracic aorta, as isolated abdominal aortic dissections are very rare (Howard et al. 2013, Liu et al. 2020) and this is likely true for our study cohort as well. Aortic dissections and atherosclerosis share common and overlapping risk factors such as male gender, age, hypertension and smoking (Gawinecka et al. 2017). To date, most studies on the link between atherosclerosis and AD focused on the thoracic aorta, where most aortic dissections originate. In those studies, atherosclerotic alterations were found more frequently in older patients and in patients with a Stanford B AD compared to Stanford A AD (Juraszek et al. 2013, Hashiyama et al. 2018). Here, only about half of the specimens (52%) of dissected AA also presented with atherosclerotic plaque. In contrast to aneurysm, it therefore seems less likely that atherosclerosis is a major determinant for dissection in the AA. However, it is an interesting possibility that early, age-associated atherosclerotic alterations in the abdominal aorta facilitate tearing of the abdominal aortic wall in the case of a thoracic aortic dissection.

5.4 The role of vascular cells in the aortic pathologies

The main focus of this study was the analysis of pathology-associated alterations in the mRNA expression of cell markers CD31 (marker for ECs), Myh11 (marker for VSMCs), CD45 (leukocyte marker) and CD68 (marker for monocytes and macrophages). Therein, the differences in the cell marker expression comparing diseased and non-diseased abdominal aortic tissue as well as differences between the individual aortic pathologies were analyzed. When compared to non-diseased tissue (subgroup 0), I generally expected the expression of CD31 and Myh11 to decrease with the prevalence of any pathology (subgroup ADP), which might be due to cell death or, in case of Myh11, a dedifferentiation of VSMCs.

As mentioned above, all aneurysmal tissue also presented with atherosclerotic plaque and potential differences in gene expression for abdominal aortic aneurysm compared to other subgroups could only be observed in the context of co-existing plaque in the AA (subgroup AP). The comparison of cell marker as well as vascular gene and

S1P receptor expression in subgroups AP and P never yielded significant differences (see Figures 9, 10 and 11) as plaque-mediated alterations apparently overshadow any potential alterations specific for aneurysm.

5.4.1 Endothelial cells in the aortic pathologies

Here, the expression of the endothelial cell marker CD31 did not differ significantly between diseased and non-diseased aortic tissue (subgroup ADP vs. 0; Figure 8). This was unexpected at first as endothelial dysfunction is paradigmatic for the pathogenesis of vascular diseases, especially for AAA and atherosclerosis, where it is considered an early and critical event (Gao et al. 2012, Milutinović et al. 2020). The resulting question is, to what extent CD31 expression reflects endothelial cell coverage or adequate function of the adhesion receptor CD31 in our tissue samples.

With S1PR1 and NOS3, two additional genes which can be considered endothelial marker genes as both are highly expressed in ECs were measured. Accordingly, expression of both S1PR1 and NOS3 was strongly associated with CD31 expression (Figure 12, Figure 13). Like CD31, neither NOS3 nor S1PR1 expression differed significantly between non-diseased and diseased AA tissue (Figure 10, Figure 11).

In summary, results from this study showed no association of endothelial gene expression with the aortic pathologies investigated. One reason for this finding may lie in the fact that in this study diseased tissue samples were compared to samples that have also been derived from vascular patients (subgroup 0) which presented with an aneurysm or a dissection in a different aortic section (see Section 3.1). Thus, systemic disease parameters may have affected endothelial gene expression in the AA, even in subjects without obvious pathology in this aortic section. One possibility for instance, is arterial hypertension that predisposes for other vascular pathologies and has been associated with reduced expression of endothelial genes (Good et al. 2015, Cantalupo et al. 2017). Pulmonary ECs have been found to lose expression of endothelial cell markers such as CD31, and to transform into mesenchymal cells when exposed to hypertension (Good et al. 2015). Similarly, endothelial S1PR1 appears to protect against hypertension and loss of endothelial S1PR1 was found to be associated with increasing blood pressure in a murine model (Cantalupo et al. 2017).

Further, none of the three genes (CD31, NOS3 or S1PR1) is truly EC-specific, as they can also be found expressed in other cell types. For instance, CD31 is also expressed in leukocytes, platelets, and endothelial progenitor cells (EPCs) and these cells might

well contribute to the expression levels of CD31 measured in the present study. Expressed in leukocytes, CD31 promotes interaction with ECs and promotes leukocyte adhesion and migration into the artery wall (Privratsky and Newman 2014, Caligiuri 2020), both vital mechanisms in the pathogenesis of vascular diseases (Raffort et al. 2017, Libby et al. 2019). Therefore, in case of CD31, expression might increase in diseased tissue based on an increased number of leukocytes or EPCs.

Taken together, aortic pathologies involve mechanisms that potentially increase or decrease the prevalence of CD31-expressing cells resulting in seemingly unaltered CD31 expression levels when comparing diseased and non-diseased tissue from the AA. To further address this question, immunohistology for CD31 may be a good strategy to identify and localize CD31-positive cells to analyze potential differences in healthy and diseased aortic tissue.

Although no significant differences in CD31 expression were found when comparing the various pathology subgroups, it was interesting to us that expression levels in dissection appeared lower, compared to aneurysm, plaque or control specimens (subgroups D vs AP, P and 0; Figure 9A). Notably, a similar pattern was also found for S1PR1 expression (Figure 11B), but not for NOS3 (Figure 10B). As both CD31 and S1PR1 regulate vascular permeability (Garcia et al. 2001, Privratsky and Newman 2014), loss of expression may point to the critical function of the endothelial barrier in aortic dissection, where an intimal tear is considered the initial event (Mussa et al. 2016, Gawinecka et al. 2017). Given the current literature on the typical location of aortic dissections (Howard et al. 2013, Li et al. 2020), it is likely for most dissections found in the AA to originate from a more upstream section of the aorta. Decreased expression of CD31 and S1PR1 in abdominal aortic ECs then perhaps promotes vascular leakage and medial changes that subsequently facilitate tearing of the wall. Thereby, hypertension, as a vital systemic risk factor for aortic dissection, might well promote the initial loss of endothelial genes as previously stated.

5.4.2 Vascular smooth muscle cells in the aortic pathologies

Myh11 was the only gene whose expression significantly differed between diseased (subgroup ADP) and non-diseased aortic tissues (subgroup 0) with lower expression in the former (Figure 8B). This finding suggests that differentiated VSMCs generally play a major role in the pathogenesis of vascular diseases and that decreased Myh11 expression is associated with the aortic pathologies investigated in this study.

When Myh11 expression of each pathology subgroup (AP, P and D) was compared to subgroup 0, Myh11 expression was found decreased in all three pathology subgroups (Figure 9B). Thereby, the biggest differences, compared to subgroup 0, were found for subgroups AP and P, and the least for subgroup D.

The finding of decreased Myh11 expression in vascular pathologies can be interpreted in at least two ways: (1) Loss of Myh11 expression stems from a loss of VSMCs for instance by cell death or (2) it reflects a downregulation of expression by a process described as phenotypic modulation that characterizes an injury-induced change in VSMC phenotype from a contractile and quiescent to a synthetic and pro-proliferative phenotype. This phenotypic modulation of VSMCs is characterized by the downregulation of differentiation markers, e.g., Myh11, and the gain of proliferative and migratory capacity. Decreased Myh11 expression in atherosclerotic tissue (subgroup P) is likely attributable to both processes, whereby quantifying the contribution of each process has not been attempted in our study. Both dedifferentiated and apoptotic VSMCs have been reported to promote plaque formation (Bennett et al. 2016). Moreover, VSMCs also can transdifferentiate into macrophage-like cells with downregulation of VSMC differentiation markers and upregulation of typical markers for macrophages, e.g., CD68 (Feil et al. 2014, Vengrenyuk et al. 2015, Shankman et al. 2015). These cells can take up lipoproteins and also turn into foam cells in atherogenesis (Campbell et al. 1983, Allahverdian et al. 2018). Although apoptosis accounts for most of VSMC death in atherosclerosis and is strongly associated with plaque vulnerability, necrosis has also been described and is stimulated by highly oxidized lipoproteins (Kockx and Knaapen 2000, Grootaert et al. 2018).

For the pathogenesis of AAA (subgroup AP), loss of VSMCs by cell death, mainly apoptosis, and the subsequent impairment of the aortic wall integrity is of great importance for the progressive dilation of the aorta (Henderson et al. 1999). The main mechanism, apoptosis of VSMCs, is stimulated by the upregulation of proinflammatory cytokines (interleukin 1 β , tumor-necrosis factor α and interferon λ) as well as by the increased production of ROS in dysfunctional ECs (Geng et al. 1996, Gurung et al. 2020). A recent study reported Myh11 to be released from dying VSMCs and the authors found a correlation between circulatory Myh11 levels and aortic diameter (Yokoyama et al. 2018). In addition, VSMCs in AAA show impaired contractility (Bogunovic et al. 2019).

As stated previously, in this study, all specimens with an aneurysm (but one) also presented with atherosclerotic plaque. Thus, it can be assumed that mechanisms of both pathologies contributed to the loss of Myh11 expression in the tissue samples from subgroup AP. The prevalence of both pathologies might explain the slightly stronger decrease of Myh11 expression in subgroup AP compared to subgroup P (Figure 9B).

Compared to subgroups AP and P, decrease of Myh11 expression is less pronounced in subgroup D (Figure 9B). Previous studies also reported a significantly decreased Myh11 expression in tissue samples from aortic dissection, however, these tissue samples were derived from the thoracic aorta (Zhang et al. 2016). Similar to atherosclerosis and aneurysm, loss of Myh11 expression in AD tissue is likely due to both VSMC dedifferentiation and apoptosis. Together with the loss of collagen and elastin fibers, VSMC dedifferentiation characterizes medial degeneration which is critical in the pathogenesis of AD (Wang et al. 2019). Aortic dissections, particularly in the thoracic aorta, are strongly impacted by genetic components: Mutations in VSMC differentiation genes including Myh11 have been associated with syndromic and non-syndromic thoracic aortic diseases (Zhu et al. 2006, Milewicz et al. 2017). Considering VSMC biology in AA dissections, one needs to consider again that tearing likely originates in the thoracic aorta and that most studies performed so far addressed VSMC biology in thoracic aortic dissections (Howard et al. 2013, Liu et al. 2020). Whether the state of VSMC differentiation and Myh11 expression in the AA, as well as predisposing genetic mutations, promote progression of tear may be an interesting question for future studies.

5.4.2.1 SIRT1 – regulator of Myh11 expression in aortic pathologies?

Sirtuin 1 (SIRT1), a NAD⁺-dependent deacetylase acting on histone and non-histone proteins, is highly expressed in vascular (EC, EPC, VSMC) and immune cells (Kitada et al. 2016). Accordingly, in this study, SIRT1 expression was strongly associated with the expression of cell markers for ECs (CD31), VSMCs (Myh11) as well as lymphocytes (CD45; Figure 12).

When the expression of SIRT1 was compared between the various pathology subgroups it was found significantly decreased in diseased aortic tissue compared to non-diseased aortic tissue (Figure 10C). These findings are in line with previous studies, showing decreased SIRT1 expression in ECs, VSMCs as well as in immune

cells to be associated with vascular aging, vascular dysfunction and pathologies (Donato et al. 2011, Kitada et al. 2016, Thompson et al. 2014). The analysis of SIRT1 expression in the individual pathology subgroups revealed a decrease in all pathology subgroups compared to subgroup 0 (Figure 10D). The greatest decrease of SIRT1 expression was found in subgroup AP, followed by subgroups P and D, possibly suggesting a greater involvement of SIRT1 activity in aneurysmatic and atherosclerotic disease of the AA compared to aortic dissection. These results also agree with previous studies, as all three aortic pathologies had been associated with reduced SIRT1 expression (Chen et al. 2016, Zhang et al. 2020). With importance for this work, SIRT1 overexpression in transgenic mice was shown to prevent atherosclerotic plaque: In ApoE knockout mice with adenoviral-mediated EC-specific overexpression of SIRT1, atherosclerotic plaque formation was diminished (Zhang et al. 2008). This endothelial SIRT1-mediated prevention of atherosclerosis and endothelial senescence has been found attributable to the activation of various signaling pathways, e.g., stimulation of NO production, inhibition of arterial remodeling, and inhibition of foam cell formation (Mattagajasingh et al. 2007, Bai et al. 2016, Zeng et al. 2013, Kitada et al. 2016). Moreover, VSMC-specific induced overexpression of SIRT1 in mice inhibited VSMC proliferation and neointima formation, thus protecting against atherosclerotic plaque (Li et al. 2011).

Notably, the pattern of SIRT1 expression among the various pathology subgroups was similar to that of Myh11 (Figure 9B and Figure 10D) and expression of these two genes was also found strongly associated (Figure 12). These findings may indicate an association of SIRT1 downregulation with dedifferentiation or apoptosis of VSMCs. For instance, one study previously reported lower expression levels of SIRT1 in human AAA tissue and identified VSMCs as the main cell type concerned. SIRT1 knockout in murine VSMCs was found to promote not only the formation of angiotensin II- as well as calcium chloride-induced AAA through enhanced vascular senescence and inflammation, but also to increase the risk of AAA rupture in the angiotensin II model (Chen et al. 2016). Moreover, SIRT1 had previously been found to promote the expression of VSMC differentiation genes, e.g., Myh11 (Yu et al. 2015) and might therefore be considered a regulator of VSMC differentiation. Taken together, it is possible to assume that loss of SIRT1 expression in aortic pathologies may be functionally linked to the dedifferentiation of VSMCs.

SIRT1 expression was also found associated with the expression of leukocyte marker CD45 (Figure 12). This is in line with previous studies that report SIRT1 expression in leukocytes where it stimulates differentiation. A reduction of SIRT1 expression in leukocytes, has been associated with ageing (Donato et al. 2011, Yu et al. 2018). In this study no association of macrophage marker CD68 with SIRT1 expression was found. This might be attributable to the prevalence of both M1 and M2 polarized macrophages in the aortic tissue samples which presumably regulates SIRT1 expression in opposing manner in association with the aortic pathologies, e.g., AAA (Zhang et al. 2018).

5.5 The role of immune cells in the aortic pathologies

Besides markers for vascular cells, two markers for immune cells were measured in the study specimens. Generally, I expected the expression of CD45 (marker for leukocytes) and CD68 (marker for macrophages) to increase with the prevalence of aortic pathologies reflecting immune cell infiltration.

To our surprise, no significant differences were found when comparing the expression of CD68 and CD45 between subgroup 0 and subgroup ADP (Figure 8C, D). When comparing the individual pathology subgroups, the One-way ANOVA showed significant differences for CD68; all post-hoc tests, however, were non-significant (Figure 9C). The pattern for CD68 and CD45 expression among the various subgroups was similar with slightly higher expression levels in subgroups AP and P compared to subgroups 0 and D (Figure 9C, D). This pattern may be explained by the higher prevalence of inflammation in atherosclerosis and aneurysm than in dissection. The lack of clear expression differences for CD45 among the study subgroups may be attributable to its expression in multiple cell types (Pilling et al. 2009), which may be differentially regulated throughout the formation of the aortic pathologies, overall resulting in non-significant alterations of CD45 expression in the diseased tissue. As mentioned above, particularly for CD68, I would have expected to find significant expression differences between the pathology subgroups because an essential role for macrophages in aneurysm and atherosclerosis is well established (Raffort et al. 2017, Gimbrone and García-Cardena 2016). It should also be of further notice, that – as aforementioned – transdifferentiated VSMCs also acquire a macrophage-like phenotype in atherosclerosis (Rong et al., 2003, Shankman et al., 2015) and contribute to increased CD68 expression.

The reduction of macrophages in tissue from aortic dissection also came as a surprise, as macrophages are just as well instrumental in the pathogenesis of aortic dissection. Macrophages are known to promote wall inflammation and degradation of ECM and, thus, are strongly related to rupture (Del Porto et al. 2010, Gawinecka et al. 2017). Additionally, macrophages were identified as the most abundant cells in the leukocytic infiltrates in the wall of aortic dissections and depletion of monocytes and macrophages successfully inhibited aortic dissection in a murine model (Li et al. 2020).

In summary, the main explanation for the lack of significant expression differences for CD45 and CD68 lies in the fact that all study members suffered a severe aortic disease, namely an aneurysm or dissection. Therefore, it can be assumed that all suffered a systemic aortic inflammation that overshadowed specific associations in the AA.

5.5.1 Localization of macrophages in diseased aortic tissue

Based on the unexpected lack of differences in CD68 expression in the pathology subgroups (see above), the location of macrophages in the various aortic pathologies were further investigated by immunohistology (see Section 3.4 and 4.5). For each pathology subgroup, representative tissue slides were chosen and stained with an antibody against the macrophage antigen Mac2.

Overall, as one may expect, more macrophage staining was found in slides from diseased tissue (subgroups AP, P and D) when compared to controls (subgroup 0; Table 7, Figure 15) which underlines the important role for macrophages in aortic pathologies. No obvious differences in macrophage expression levels were seen among the selected tissue samples of the individual pathology subgroups (Table 7, Figure 15).

Notable differences, however, were found between the pathology subgroups regarding the localization of macrophages. In tissue samples from subgroups AP and P, macrophages were detected in all arterial layers with foremost prevalence in plaque areas and adventitial tissue (Figure 15C-G), generally supporting previous observations (Robbins et al. 2013, Dutertre et al. 2014, Rao et al. 2015). In contrast, tissue samples from subgroup D displayed more macrophages in the medial layer where these cells accumulated around tear edges (Figure 15H, I). Similar observations had been made in dissected thoracic aortae (Del Porto et al. 2014, Ye et al. 2018). Taken together, although AD rarely originates in the AA, macrophages in the AA also seem to play an important role in AA dissection. Thereby, the accumulation of

macrophage may facilitate tearing of the abdominal aortic wall but may also represent inflammatory tissue reaction in response to a dissection in the AA.

5.6 S1P receptors in the aortic pathologies

The S1P/S1P receptor system plays a critical role in vascular development as well as the maintenance of vascular integrity and is associated with vascular pathologies (Proia and Hla 2015). Important for this work, S1P receptor expression had previously been investigated in the study specimens and pathology-associated expression was identified: In subgroups AP and P, expression of both S1PR2 and S1PR3 were significantly decreased whereas, surprisingly, S1PR1 expression was not altered in any of the pathology subgroups (Figure 11). Based on these findings, correlations between the expression of S1P receptors and cell markers as well as genes SIRT1 and NOS3 were analyzed to address the questions (1) which cells may regulate S1P receptor expression in aortic pathologies and (2) whether S1P signaling may regulate the expression of SIRT1 or NOS3. In the correlation analyses with cell marker expression, for S1PR1, the strongest association was found with CD31. For both S1PR2 and S1PR3 strong associations with Myh11 were present (Figure 13). These results confirm the generally assumed pattern of S1P receptor expression in the vasculature with S1PR1 as the predominant receptor in ECs whereas S1PR2 and S1PR3 are mainly expressed in VSMCs (Sanchez 2016). Expressed in VSMCs, S1PR2 and S1PR3 signaling may have opposing effects: S1PR2 stimulates VSMC differentiation and inhibits growth and migration (Grabski et al. 2009, Medlin et al. 2010), whereas, depending on the vascular bed (see Section 2.5.3), S1PR3 can stimulate VSMC migration and proliferation (Shimizu et al. 2012).

As S1P/S1PR2 induces the expression of VSMC-specific genes, such as smooth muscle cell alpha actin (Grabski et al. 2009), it is conceivable that loss of S1PR2, associated with aneurysmatic and atherosclerotic aortic tissue in this study, contributes to the dedifferentiation of VSMCs with decreased Myh11 expression observed in these pathologies (Figure 9B).

Interestingly, of all S1P receptors, expression of S1PR2 was the strongest associated with the expression of SIRT1 (Figure 14). The existence of a S1P/SIRT1 axis, with SIRT1 as a downstream molecule in this signaling pathway, was first reported in ECs (Gao et al. 2016). In that particular model with human umbilical vein endothelial cells (HUVECs), exogenous S1P stimulated SIRT1 expression via phosphorylation of p38

MAPK (p38 mitogen-activated protein kinases), ERK (extracellular-signal regulated kinases) and AKT (protein kinases), regulating proliferation and migration of ECs. The authors, however, did not specify which of the S1P receptors is the decisive one in this signaling network (Gao et al. 2016). Data from the here presented study might indicate the possibility that S1PR2/SIRT1 signaling in VSMCs is promoting a differentiated state of these cells and that loss of this signaling domain contributes to atherosclerosis and aneurysm in the AA.

5.7 Conclusion and outlook

The understanding of the pathomechanisms of the vascular pathologies aneurysm, dissection and atherosclerosis in the abdominal aorta is still lacking. Here, cellular alterations, varying S1P receptor expression and alterations of NOS3 and SIRT1 expression, specific for these vascular pathologies were identified.

For aneurysm and atherosclerosis, characteristic parameters for inflammatory vascular pathologies including loss of VSMC differentiation marker Myh11, accumulation of macrophages and downregulation of SIRT1 expression were found. Data from this study support the idea of AAA to arise as a complication of atherosclerosis in the AA. Further, the results might indicate for S1PR2/SIRT1 signaling to promote VSMC differentiation. The loss of this signaling domain might promote the formation of aneurysm and atherosclerosis in the AA. This finding warrants further investigation as S1PR2 agonism might be a potential approach for pharmacological treatment of aortic pathologies.

Aortic dissections found in the AA originate to a large extent from the thoracic aorta, but the mechanisms leading to tearing in the AA are not fully understood, leaving a lack of preventive and therapeutic options in pharmacological therapy. This study identified a number of alterations in cell marker expression, specific for dissection in the AA. These alterations might facilitate the tearing of the aortic wall in the case of a thoracic aortic dissection. Loss of differentiated VSMCs as well as endothelial dysfunction might contribute to the destabilization of the aortic wall and facilitate subsequent tearing. In case of VSMC biology, future studies will be of great interest to identify the role of genetic mutations and the state of VSMC dedifferentiation in AA dissection, as these aspects have been identified as crucial factors in thoracic aortic dissections. The histological analysis of macrophage prevalence in the aortic tissue showed accumulation of these cells around the dissection edges in the medial layer,

but surprisingly, measurements of CD68, a marker for monocytes/macrophages, did not indicate an accumulation of these cells in dissected tissue. These results stress the need for further analyses: First, analysis of macrophage expression in these tissue samples will have to be repeated with healthy control specimens in order to rule out the impact of any other aortic pathology. Second, macrophages found in the aortic pathologies might vary in the expression of specific cell markers and therefore, the use of more than one cell marker will be necessary to evaluate the expression and the role of macrophages in the aortic pathologies.

5.8 Limitations

To obtain a sufficient number of aneurysmal or dissected aortic specimens, the study subjects were selected based on the criterium of an existing aortic aneurysm or a dissection in any aortic section. This way, the study design resulted in sufficient numbers of specimens to compare the different pathologies, but the lack of “healthy” study specimens as controls may be seen as a limitation. Further, no data was available regarding the prevalence of thoracic aortic aneurysm and dissection in study subjects from subgroup 0. The upstream pathologies might well have had an impact on cell marker biology in the AA, and therefore, a cautious interpretation of these tissue samples as the control group is indicated. Further, no clinical data beyond the study members’ age, gender and BMI were available to control for potentially confounding parameters such as co-morbidities, risk-factors, or medication.

Taken together, the interpretation of the results is limited by the lack of patient-related data to control for potentially confounding parameters and by using non-healthy but also diseased individuals as control specimens.

Due to the method of sample collection and subgroup formation, aneurysm in the AA could not be analyzed as an individual pathology in this study, as the corresponding tissue samples always presented with co-prevalent atherosclerosis. This can be seen as a limitation to the individual analysis of pathologies, but, however, is somewhat close to the clinical reality, as the overall co-prevalence of the two pathologies is high and omnipresent.

An inherent limitation of studies using quantitative measurements of gene expression is the challenging interpretation of the results. Differential gene expression may not only be due to up- or downregulation of genes but also to relative changes in a cell population in tissue by cell death, proliferation, or invasion. Another limitation is seen

in the use of the individual cell markers. On one hand, a cellular phenotype is usually defined by many genes, on the other hand, markers are generally not restricted to a single cell type.

6 Summary

Aneurysm, dissection, and atherosclerosis are vascular diseases that can also arise in the abdominal aorta (AA). Due to high prevalence and high mortality rates, they are worldwide of concern. Detailed cellular pathomechanisms have not been fully elucidated and drug therapy as well as preventive strategies are still lacking.

This study investigated associations of the expression of cell markers, vascular genes and S1P receptors (S1PR) with the named AA pathologies. AA tissue specimens (N = 95) were harvested during autopsies from people that had suffered a dissection or aneurysm in any aortic section. Analyses of the expression of selected genes was performed by RT-qPCR and in addition, selected tissues were stained for macrophages.

Our data support the assumption that AA aneurysms arise as a complication of atherosclerosis in the AA. In the pathogenesis of dissection, atherosclerosis appeared less critical. For all pathologies, downregulation of VSMC differentiation marker Myh11 was observed indicating a loss of differentiated VSMCs due to phenotypic change and cell death. Expression levels of histone-deacetylase SIRT1 were found to correlate to those of Myh11, suggesting a functional link between SIRT1 loss and VSMC dedifferentiation in aortic pathologies. Surprisingly, expression of macrophage marker CD68 was not significantly altered in any of the pathology subgroups. Staining of selected tissues with the macrophage marker Mac2 showed macrophages accumulating in the intima and in plaque areas in tissue samples from aneurysm and atherosclerosis. In dissected tissues macrophages were also found in the medial layer and around dissection edges.

S1PRs are critical in vascular development and homeostasis, however their cell-specific role in the named aortic pathologies has not been studied yet. Here, we show a significant decrease of S1PR2 and S1PR3 expression in aneurysm and atherosclerosis. The loss of S1PR2 might well contribute to the dedifferentiation of VSMCs, as S1PR2/RhoA signaling is known to promote the expression of VSMC differentiation genes. Our data may suggest the existence of a S1PR2/SIRT1 axis in VSMCs that may regulate atherosclerosis and aneurysm in the AA. Future work may define the potential of S1P receptor agonism or antagonism for pharmacological treatment of AA pathologies.

Zusammenfassung

Aneurysma, Dissektion und Atherosklerose kommen alle in der abdominellen Aorta (AA) vor und sind wegen der hohen Prävalenz- und Mortalitätsraten von weltweiter Bedeutung. Die Pathomechanismen sind dabei unvollständig untersucht und effektive medikamentöse Therapien fehlen mitunter.

In dieser Studie wurde die Expression von Zellmarkern, vaskulären Genen und S1P Rezeptoren (S1PR), sowie deren Assoziation mit den o.g. Pathologien untersucht. Gewebeproben (N = 95) aus der AA wurden in Autopsien gewonnen und mittels RT-qPCR sowie Makrophagenfärbung untersucht. Einschlusskriterium für diese Studie war ein Aneurysma oder eine Dissektion in einem Abschnitt der Aorta.

Die vorliegenden Ergebnisse stützen die Annahme, dass Aneurysmen in der AA (AAA) aus atherosklerotischen Läsionen entstehen, während Dissektionen in der AA (AAD) weniger stark von diesen abhängen. Der Verlust glatter Muskelzellen (GMZ) durch Zelltod und/oder Dedifferenzierung zeigte sich für alle untersuchten Pathologien. Dabei wurde ein ähnliches Muster für die Expression des GMZ Differenzierungsmarker Myh11 sowie für SIRT1 gefunden, was ein Hinweis auf eine funktionelle Verbindung der beiden sein könnte. Überraschenderweise war die Expression des Makrophagenmarkers CD68 in den einzelnen Pathologien nicht signifikant verändert. Die Färbung des Makrophagen-Antigens Mac2 zeigte eine Akkumulation von Makrophagen in der Intima und in Plaque-Arealen in AAA und Atherosklerose sowie in der Media und entlang der Dissektionsränder in Geweben mit AAD.

S1PR spielen eine wichtige Rolle in der Entwicklung und der Homöostase des Gefäßsystems. Die Ergebnisse dieser Studie zeigen eine signifikante Abnahme der S1PR2 sowie S1PR3 Expression in AAA und Atherosklerose. Der Verlust der Expression des S1PR2 könnte dabei zu der Abnahme der differenzierten GMZ in den erkrankten Geweben beitragen. Für die Aktivierung des S1PR2/RhoA Signalweges wurde bereits gezeigt, dass dieser die Differenzierung von GMZ fördert. Die Ergebnisse dieser Studie zeigen nun, dass ein S1PR2/SIRT1 Signalweg an der Differenzierung der GMZ beteiligt sein könnte, und ein Verlust dieses Signalweges möglicherweise eine Rolle in der Entstehung von Aneurysmen und Atherosklerose in der AA spielt. Zusammenfassend weisen diese Ergebnisse auf eine Rolle des S1P/S1PR Systems in der Regulation von endothelialer und GMZ-Funktion in den Aortenpathologien hin, die in weiteren Untersuchungen, auch im Hinblick auf den potentiellen Nutzen in der pharmakologischen Therapie, überprüft werden sollte.

7 List of figures

FIGURE 1. STRUCTURE OF THE ARTERIAL WALL.	5
modified from MILUTINOVIĆ A, ŠUPUT D & ZORC-PLESKOVIČ R (2020) Pathogenesis of atherosclerosis in the tunica intima, media, and adventitia of coronary arteries: An updated review. Bosn J Basic Med Sci, 20(1): 21-30.	
FIGURE 2. PATHOPHYSIOLOGY OF AAA.	8
modified from DAVIS F M, RATERI D L & DAUGHERTY A (2015) Abdominal aortic aneurysm: novel mechanisms and therapies. Curr Opin Cardiol, 30(6): 566-73.	
FIGURE 3. SPHINGOSINE 1-PHOSPHATE METABOLISM.....	14
FIGURE 4. DOWNSTREAM SIGNALING PATHWAYS ACTIVATED BY S1PR1-3 IN VASCULAR CELLS.	15
FIGURE 5. PRINCIPLES OF MAC2 STAINING USING THE AVIDIN-BIOTIN COMPLEX METHOD..	28
FIGURE 6. ELASTICA-VAN-GIESON STAINING OF INFRARENAL AORTIC TISSUE SECTIONS....	31
FIGURE 7. AGE IN STUDY SUBGROUPS..	33
FIGURE 8. EXPRESSION OF CELL MARKERS IN STUDY SUBGROUPS 0 AND ADP.....	34
FIGURE 9. EXPRESSION OF CELL MARKERS IN STUDY SUBGROUPS 0, AP, D AND P.....	35
FIGURE 10. EXPRESSION OF NOS3 AND SIRT1.....	36
FIGURE 11. S1P RECEPTOR EXPRESSION..	37
FIGURE 12. CORRELATIONS BETWEEN THE EXPRESSION OF NOS3, SIRT1 AND CELL MARKER GENES..	38
FIGURE 13. CORRELATIONS BETWEEN THE EXPRESSION OF S1P RECEPTORS AND CELL MARKER GENES.	39
FIGURE 14. CORRELATIONS BETWEEN THE EXPRESSION OF S1P RECEPTORS AND GENES NOS3, SIRT1.....	40
FIGURE 15. MACROPHAGE STAINING OF INFRARENAL AORTIC TISSUE SECTIONS.	42

8 List of tables

TABLE 1. REACTION MIXTURES FOR CDNA SYNTHESIS.	23
TABLE 2. PRIMERS USED FOR RT-QPCR.	24
TABLE 3. SCHEMA OF THE PREPARATION OF THE MASTER-MIX FOR ONE CDNA SAMPLE.	25
TABLE 4. STEPS OF ONE RT-QPCR RUN.	25
TABLE 5. MAC2 STAINING.	27
TABLE 6. EPIDEMIOLOGICAL DATA OF THE STUDY SUBGROUPS.	32
TABLE 7. RESULTS OF THE MAC2 STAINING FOR MACROPHAGES.	40

9 List of references

- ALDERTON W K, COOPER C E & KNOWLES R G (2001) Nitric oxide synthases: structure, function and inhibition. *Biochem J*, 357(Pt 3): 593-615.
- ALLAHVERDIAN S, CHAABANE C, BOUKAIS K, FRANCIS G A & BOCHATON-PIALLAT M L (2018) Smooth muscle cell fate and plasticity in atherosclerosis. *Cardiovasc Res*, 114(4): 540-550.
- ARGRAVES K M & ARGRAVES W S (2007) HDL serves as a S1P signaling platform mediating a multitude of cardiovascular effects. *J Lipid Res*, 48(11): 2325-33.
- BAEYENS A, FANG V, CHEN C & SCHWAB S R (2015) Exit Strategies: S1P Signaling and T Cell Migration. *Trends Immunol*, 36(12): 778-787.
- BAI B, MAN A W, YANG K, GUO Y, XU C, TSE H F, HAN W, BLOKSGAARD M, DE MEY J G, VANHOUTTE P M et al. (2016) Endothelial SIRT1 prevents adverse arterial remodeling by facilitating HERC2-mediated degradation of acetylated LKB1. *Oncotarget*, 7(26): 39065-39081.
- BENNETT M R, SINHA S & OWENS G K (2016) Vascular Smooth Muscle Cells in Atherosclerosis. *Circ Res*, 118(4): 692-702.
- BENTZON J F, WEILE C, SONDERGAARD C S, HINDKJAER J, KASSEM M & FALK E (2006) Smooth muscle cells in atherosclerosis originate from the local vessel wall and not circulating progenitor cells in ApoE knockout mice. *Arterioscler Thromb Vasc Biol*, 26(12): 2696-702.
- BLAHO V A & HLA T (2014) An update on the biology of sphingosine 1-phosphate receptors. *J Lipid Res*, 55(8): 1596-608.
- BÖCKLER D (2020) Akute Aortensyndrome. In: Operative und interventionelle Gefäßmedizin. *DEBUS, E S & GROSS-FENGELS, W (eds.)* 2. ed, Springer, Berlin Heidelberg, 601-613.
- BOGUNOVIC N, MEEKEL J P, MICHA D, BLANKENSTEIJN J D, HORDIJK P L & YEUNG K K (2019) Impaired smooth muscle cell contractility as a novel concept of abdominal aortic aneurysm pathophysiology. *Sci Rep*, 9(1): 6837.
- BRIKMAN S & DORI G (2019) Beta-blockers in non-surgical patients with type A aortic dissection. *Med Hypotheses*, 128: 76-77.
- BRINKMANN V, DAVIS M D, HEISE C E, ALBERT R, COTTENS S, HOF R, BRUNS C, PRIESCHL E, BAUMRUKER T, HIESTAND P et al. (2002) The immune modulator FTY720 targets sphingosine 1-phosphate receptors. *J Biol Chem*, 277(24): 21453-7.
- CALIGIURI G (2020) CD31 as a Therapeutic Target in Atherosclerosis. *Circ Res*, 126(9): 1178-1189.

- CAMPBELL J H, POPADYNEC L, NESTEL P J & CAMPBELL G R (1983) Lipid accumulation in arterial smooth muscle cells. Influence of phenotype. *Atherosclerosis*, 47(3): 279-95.
- CANTALUPO A, GARGIULO A, DAUTAJ E, LIU C, ZHANG Y, HLA T & DI LORENZO A (2017) S1PR1 (Sphingosine-1-Phosphate Receptor 1) Signaling Regulates Blood Flow and Pressure. *Hypertension*, 70(2): 426-434.
- CHEN H Z, WANG F, GAO P, PEI J F, LIU Y, XU T T, TANG X, FU W Y, LU J, YAN Y F et al. (2016) Age-Associated Sirtuin 1 Reduction in Vascular Smooth Muscle Links Vascular Senescence and Inflammation to Abdominal Aortic Aneurysm. *Circ Res*, 119(10): 1076-1088.
- CLOUGH R E & NIENABER C A (2015) Management of acute aortic syndrome. *Nat Rev Cardiol*, 12(2): 103-14.
- CYSTER J G & SCHWAB S R (2012) Sphingosine-1-phosphate and lymphocyte egress from lymphoid organs. *Annu Rev Immunol*, 30: 69-94.
- D'ONOFRIO N, VITIELLO M, CASALE R, SERVILLO L, GIOVANE A & BALESTRIERI M L (2015) Sirtuins in vascular diseases: Emerging roles and therapeutic potential. *Biochim Biophys Acta*, 1852(7): 1311-22.
- DAUM G, GRABSKI A & REIDY M A (2009) Sphingosine 1-phosphate: a regulator of arterial lesions. *Arterioscler Thromb Vasc Biol*, 29(10): 1439-43.
- DAVIS F M, RATERI D L & DAUGHERTY A (2015) Abdominal aortic aneurysm: novel mechanisms and therapies. *Curr Opin Cardiol*, 30(6): 566-73.
- DEBUS E S, BEHRENDT C-A, GROSS-FENGELS W & KÖLBEL T (2020) Aneurysmen der infrarenalen Aorta: Klinik, Diagnostik einschließlich Screening und Therapieindikationen. In: *Operative und interventionelle Gefäßmedizin. DEBUS, E S & GROSS-FENGELS, W (eds.) 2. ed*, Springer, Berlin Heidelberg, 673-689.
- DEBUS E S, HEIDEMANN F, GROSS-FENGELS W, MAHLMANN A, MUHL E, PFISTER K, ROTH S, STROSZCZYNSKI C, WALTHER A, WEISS N et al. (2018) S3-Leitlinie zu Screening, Diagnostik, Therapie und Nachsorge des Bauchortenaneurysmas. Berlin [Online]. Available: https://www.awmf.org/uploads/tx_szleitlinien/004-014l__S3_Bauchortenaneurysma_2018-08.pdf [Accessed 05.05 2021].
- DEL PORTO F, DI GIOIA C, TRITAPEPE L, FERRI L, LEOPIZZI M, NOFRONI I, DE SANTIS V, DELLA ROCCA C, MITTERHOFER A P, BRUNO G et al. (2014) The multitasking role of macrophages in Stanford type A acute aortic dissection. *Cardiology*, 127(2): 123-9.
- DEL PORTO F, PROIETTA M, TRITAPEPE L, MIRALDI F, KOVERECH A, CARDELLI P, TABACCO F, DE SANTIS V, VECCHIONE A, MITTERHOFER A P et al. (2010) Inflammation and immune response in acute aortic dissection. *Ann Med*, 42(8): 622-9.

- DESTATIS 2019. Health report of the federal government in Germany. Berlin: German federal statistic office.
- DONATO A J, MAGERKO K A, LAWSON B R, DURRANT J R, LESNIEWSKI L A & SEALS D R (2011) SIRT-1 and vascular endothelial dysfunction with ageing in mice and humans. *J Physiol*, 589(Pt 18): 4545-54.
- DUTERTRE C A, CLEMENT M, MORVAN M, SCHÄKEL K, CASTIER Y, ALSAC J M, MICHEL J B & NICOLETTI A (2014) Deciphering the stromal and hematopoietic cell network of the adventitia from non-aneurysmal and aneurysmal human aorta. *PLoS One*, 9(2): e89983.
- ERBEL R, ABOYANS V, BOILEAU C, BOSSONE E, BARTOLOMEO R D, EGGBRECHT H, EVANGELISTA A, FALK V, FRANK H, GAEMPERLI O et al. (2014) 2014 ESC Guidelines on the diagnosis and treatment of aortic diseases: Document covering acute and chronic aortic diseases of the thoracic and abdominal aorta of the adult. The Task Force for the Diagnosis and Treatment of Aortic Diseases of the European Society of Cardiology (ESC). *Eur Heart J*, 35(41): 2873-926.
- FEIL S, FEHRENBACHER B, LUKOWSKI R, ESSMANN F, SCHULZE-OSTHOFF K, SCHALLER M & FEIL R (2014) Transdifferentiation of vascular smooth muscle cells to macrophage-like cells during atherogenesis. *Circ Res*, 115(7): 662-7.
- FRISMANTIENE A, PHILIPPOVA M, ERNE P & RESINK T J (2018) Smooth muscle cell-driven vascular diseases and molecular mechanisms of VSMC plasticity. *Cell Signal*, 52: 48-64.
- GAENGEL K, NIAUDET C, HAGIKURA K, LAVIÑA B, MUHL L, HOFMANN J J, EBARASI L, NYSTRÖM S, RYMO S, CHEN L L et al. (2012) The sphingosine-1-phosphate receptor S1PR1 restricts sprouting angiogenesis by regulating the interplay between VE-cadherin and VEGFR2. *Dev Cell*, 23(3): 587-99.
- GALLINO A, ABOYANS V, DIEHM C, COSENTINO F, STRICKER H, FALK E, SCHOUTEN O, LEKAKIS J, AMANN-VESTI B, SICLARI F et al. (2014) Non-coronary atherosclerosis. *Eur Heart J*, 35(17): 1112-9.
- GALVANI S, SANSON M, BLAHO V A, SWENDEMAN S L, OBINATA H, CONGER H, DAHLBÄCK B, KONO M, PROIA R L, SMITH J D et al. (2015) HDL-bound sphingosine 1-phosphate acts as a biased agonist for the endothelial cell receptor S1P1 to limit vascular inflammation. *Sci Signal*, 8(389): ra79.
- GAO L, SIU K L, CHALUPSKY K, NGUYEN A, CHEN P, WEINTRAUB N L, GALIS Z & CAI H (2012) Role of uncoupled endothelial nitric oxide synthase in abdominal aortic aneurysm formation: treatment with folic acid. *Hypertension*, 59(1): 158-66.
- GAO Z, WANG H, XIAO F J, SHI X F, ZHANG Y K, XU Q Q, ZHANG X Y, HA X Q & WANG L S (2016) SIRT1 mediates Sphk1/S1P-induced proliferation and migration of endothelial cells. *Int J Biochem Cell Biol*, 74: 152-60.

- GARCIA J G, LIU F, VERIN A D, BIRUKOVA A, DECHERT M A, GERTHOFFER W T, BAMBERG J R & ENGLISH D (2001) Sphingosine 1-phosphate promotes endothelial cell barrier integrity by Edg-dependent cytoskeletal rearrangement. *J Clin Invest*, 108(5): 689-701.
- GAWINECKA J, SCHÖNRATH F & VON ECKARDSTEIN A (2017) Acute aortic dissection: pathogenesis, risk factors and diagnosis. *Swiss Med Wkly*, 147: w14489.
- GENG Y J, WU Q, MUSZYNSKI M, HANSSON G K & LIBBY P (1996) Apoptosis of vascular smooth muscle cells induced by in vitro stimulation with interferon-gamma, tumor necrosis factor-alpha, and interleukin-1 beta. *Arterioscler Thromb Vasc Biol*, 16(1): 19-27.
- GIMBRONE M A, Jr. & GARCÍA-CARDEÑA G (2016) Endothelial Cell Dysfunction and the Pathobiology of Atherosclerosis. *Circ Res*, 118(4): 620-36.
- GOLLEDGE J (2019) Abdominal aortic aneurysm: update on pathogenesis and medical treatments. *Nat Rev Cardiol*, 16(4): 225-242.
- GOOD R B, GILBANE A J, TRINDER S L, DENTON C P, COGHLAN G, ABRAHAM D J & HOLMES A M (2015) Endothelial to Mesenchymal Transition Contributes to Endothelial Dysfunction in Pulmonary Arterial Hypertension. *Am J Pathol*, 185(7): 1850-8.
- GORENNE I, KUMAR S, GRAY K, FIGG N, YU H, MERCER J & BENNETT M (2013) Vascular smooth muscle cell sirtuin 1 protects against DNA damage and inhibits atherosclerosis. *Circulation*, 127(3): 386-96.
- GOVERS R, BEVERS L, DE BREE P & RABELINK T J (2002) Endothelial nitric oxide synthase activity is linked to its presence at cell-cell contacts. *Biochem J*, 361(Pt 2): 193-201.
- GRABSKI A D, SHIMIZU T, DEOU J, MAHONEY W M, Jr., REIDY M A & DAUM G (2009) Sphingosine-1-phosphate receptor-2 regulates expression of smooth muscle alpha-actin after arterial injury. *Arterioscler Thromb Vasc Biol*, 29(10): 1644-50.
- GROOTAERT M O J, MOULIS M, ROTH L, MARTINET W, VINDIS C, BENNETT M R & DE MEYER G R Y (2018) Vascular smooth muscle cell death, autophagy and senescence in atherosclerosis. *Cardiovasc Res*, 114(4): 622-634.
- GURUNG R, CHOONG A M, WOO C C, FOO R & SOROKIN V (2020) Genetic and Epigenetic Mechanisms Underlying Vascular Smooth Muscle Cell Phenotypic Modulation in Abdominal Aortic Aneurysm. *Int J Mol Sci*, 21(17).
- HASHIYAMA N, GODA M, UCHIDA K, ISOMATSU Y, SUZUKI S, MO M, NISHIDA T & MASUDA M (2018) Stanford type B aortic dissection is more frequently associated with coronary artery atherosclerosis than type A. *J Cardiothorac Surg*, 13(1): 80.

- HEMMINGS D G (2006) Signal transduction underlying the vascular effects of sphingosine 1-phosphate and sphingosylphosphorylcholine. *Naunyn Schmiedebergs Arch Pharmacol*, 373(1): 18-29.
- HENDERSON E L, GENG Y J, SUKHOVA G K, WHITTEMORE A D, KNOX J & LIBBY P (1999) Death of smooth muscle cells and expression of mediators of apoptosis by T lymphocytes in human abdominal aortic aneurysms. *Circulation*, 99(1): 96-104.
- HLA T & MACIAG T (1990) An abundant transcript induced in differentiating human endothelial cells encodes a polypeptide with structural similarities to G-protein-coupled receptors. *J Biol Chem*, 265(16): 9308-13.
- HONG F F, LIANG X Y, LIU W, LV S, HE S J, KUANG H B & YANG S L (2019) Roles of eNOS in atherosclerosis treatment. *Inflamm Res*, 68(6): 429-441.
- HOWARD D P, BANERJEE A, FAIRHEAD J F, PERKINS J, SILVER L E & ROTHWELL P M (2013) Population-based study of incidence and outcome of acute aortic dissection and premorbid risk factor control: 10-year results from the Oxford Vascular Study. *Circulation*, 127(20): 2031-7.
- HULSMANS M & NAHRENDORF M (2020) Proliferative, degradative smooth muscle cells promote aortic disease. *J Clin Invest*, 130(3): 1096-1098.
- ISHII T & ASUWA N (2000) Collagen and elastin degradation by matrix metalloproteinases and tissue inhibitors of matrix metalloproteinase in aortic dissection. *Hum Pathol*, 31(6): 640-6.
- JANA S, HU M, SHEN M & KASSIRI Z (2019) Extracellular matrix, regional heterogeneity of the aorta, and aortic aneurysm. *Exp Mol Med*, 51(12): 1-15.
- JOHNSEN S H, FORSDAHL S H, SINGH K & JACOBSEN B K (2010) Atherosclerosis in abdominal aortic aneurysms: a causal event or a process running in parallel? The Tromsø study. *Arterioscler Thromb Vasc Biol*, 30(6): 1263-8.
- JOZEF CZUK E, GUZIK T J & SIEDLINSKI M (2020) Significance of sphingosine-1-phosphate in cardiovascular physiology and pathology. *Pharmacol Res*, 156: 104793.
- JURASZEK A, BAYER G, DZIODZIO T, KRAL A, LAUFER G & EHRLICH M (2013) Evaluation of the intraoperative specimens of the thoracic and abdominal aorta. *J Cardiothorac Surg*, 8: 110.
- KENT K C, ZWOLAK R M, EGOROVA N N, RILES T S, MANGANARO A, MOSKOWITZ A J, GELIJNS A C & GRECO G (2010) Analysis of risk factors for abdominal aortic aneurysm in a cohort of more than 3 million individuals. *J Vasc Surg*, 52(3): 539-48.

- KERAGE D, BRINDLEY D N & HEMMINGS D G (2014) Review: novel insights into the regulation of vascular tone by sphingosine 1-phosphate. *Placenta*, 35 Suppl: S86-92.
- KEUL P, LUCKE S, VON WNUCK LIPINSKI K, BODE C, GRÄLER M, HEUSCH G & LEVKAU B (2011) Sphingosine-1-phosphate receptor 3 promotes recruitment of monocyte/macrophages in inflammation and atherosclerosis. *Circ Res*, 108(3): 314-23.
- KEUL P, TÖLLE M, LUCKE S, VON WNUCK LIPINSKI K, HEUSCH G, SCHUCHARDT M, VAN DER GIET M & LEVKAU B (2007) The sphingosine-1-phosphate analogue FTY720 reduces atherosclerosis in apolipoprotein E-deficient mice. *Arterioscler Thromb Vasc Biol*, 27(3): 607-13.
- KIM G S, YANG L, ZHANG G, ZHAO H, SELIM M, MCCULLOUGH L D, KLUK M J & SANCHEZ T (2015) Critical role of sphingosine-1-phosphate receptor-2 in the disruption of cerebrovascular integrity in experimental stroke. *Nat Commun*, 6: 7893.
- KIMURA T, TOMURA H, MOGI C, KUWABARA A, DAMIRIN A, ISHIZUKA T, SEKIGUCHI A, ISHIWARA M, IM D S, SATO K et al. (2006) Role of scavenger receptor class B type I and sphingosine 1-phosphate receptors in high density lipoprotein-induced inhibition of adhesion molecule expression in endothelial cells. *J Biol Chem*, 281(49): 37457-67.
- KITADA M, OGURA Y & KOYA D (2016) The protective role of Sirt1 in vascular tissue: its relationship to vascular aging and atherosclerosis. *Aging (Albany NY)*, 8(10): 2290-2307.
- KOCKX M M & KNAAPEN M W (2000) The role of apoptosis in vascular disease. *J Pathol*, 190(3): 267-80.
- KONO M, BELYANTSEVA I A, SKOURA A, FROLENKOV G I, STAROST M F, DREIER J L, LIDINGTON D, BOLZ S S, FRIEDMAN T B, HLA T et al. (2007) Deafness and stria vascularis defects in S1P2 receptor-null mice. *J Biol Chem*, 282(14): 10690-6.
- KONO M, MI Y, LIU Y, SASAKI T, ALLENDE M L, WU Y P, YAMASHITA T & PROIA R L (2004) The sphingosine-1-phosphate receptors S1P1, S1P2, and S1P3 function coordinately during embryonic angiogenesis. *J Biol Chem*, 279(28): 29367-73.
- KUHLENCORDT P J, GYURKO R, HAN F, SCHERRER-CROSBIE M, ARETZ T H, HAJJAR R, PICARD M H & HUANG P L (2001) Accelerated atherosclerosis, aortic aneurysm formation, and ischemic heart disease in apolipoprotein E/endothelial nitric oxide synthase double-knockout mice. *Circulation*, 104(4): 448-54.
- KUHLENCORDT P J, ROSEL E, GERSZTEN R E, MORALES-RUIZ M, DOMBKOWSKI D, ATKINSON W J, HAN F, PREFFER F, ROSENZWEIG A, SESSA W C et al. (2004) Role of endothelial nitric oxide synthase in endothelial

- activation: insights from eNOS knockout endothelial cells. *Am J Physiol Cell Physiol*, 286(5): C1195-202.
- KÜHNL A, ERK A, TRENNER M, SALVERMOSER M, SCHMID V & ECKSTEIN H H (2017) Incidence, Treatment and Mortality in Patients with Abdominal Aortic Aneurysms. *Dtsch Arztebl Int*, 114(22-23): 391-398.
- KUMMER W & WELSCH U (2018) *Organe des Kreislaufs und Lymphgefäße*, Elsevier GmbH, Deutschland, München.
- KWARTLER C S, CHEN J, THAKUR D, LI S, BASKIN K, WANG S, WANG Z V, WALKER L, HILL J A, EPSTEIN H F et al. (2014) Overexpression of smooth muscle myosin heavy chain leads to activation of the unfolded protein response and autophagic turnover of thick filament-associated proteins in vascular smooth muscle cells. *J Biol Chem*, 289(20): 14075-88.
- LANDENHED M, ENGSTRÖM G, GOTTSÄTER A, CAULFIELD M P, HEDBLAD B, NEWTON-CHEH C, MELANDER O & SMITH J G (2015) Risk profiles for aortic dissection and ruptured or surgically treated aneurysms: a prospective cohort study. *J Am Heart Assoc*, 4(1): e001513.
- LARENA-AVELLANEDA A & DEBUS E S (2020) Aneurysmatische Gefäßerkrankungen: Terminologie, Ätiologie und Lokalisation. In: *Operative und interventionelle Gefäßmedizin*. DEBUS, E S & GROSS-FENGELS, W (eds.) 2. ed, Springer Berlin Heidelberg, 91-104.
- LEE M J, THANGADA S, CLAFFEY K P, ANCELLIN N, LIU C H, KLUK M, VOLPI M, SHA'AFI R I & HLA T (1999) Vascular endothelial cell adherens junction assembly and morphogenesis induced by sphingosine-1-phosphate. *Cell*, 99(3): 301-12.
- LI L, ZHANG H N, CHEN H Z, GAO P, ZHU L H, LI H L, LV X, ZHANG Q J, ZHANG R, WANG Z et al. (2011) SIRT1 acts as a modulator of neointima formation following vascular injury in mice. *Circ Res*, 108(10): 1180-9.
- LI X, LIU D, ZHAO L, WANG L, LI Y, CHO K, TAO C & JIANG B (2020) Targeted depletion of monocyte/macrophage suppresses aortic dissection with the spatial regulation of MMP-9 in the aorta. *Life Sci*, 254: 116927.
- LIBBY P, BURING J E, BADIMON L, HANSSON G K, DEANFIELD J, BITTENCOURT M S, TOKGÖZOĞLU L & LEWIS E F (2019) Atherosclerosis. *Nat Rev Dis Primers*, 5(1): 56.
- LIU Y, HAN M, ZHAO J, KANG L, MA Y, HUANG B, YUAN D & YANG Y (2020) Systematic Review and Meta-analysis of Current Literature on Isolated Abdominal Aortic Dissection. *Eur J Vasc Endovasc Surg*, 59(4): 545-556.
- LIU Y, WADA R, YAMASHITA T, MI Y, DENG C X, HOBSON J P, ROSENFELDT H M, NAVA V E, CHAE S S, LEE M J et al. (2000) Edg-1, the G protein-coupled receptor for sphingosine-1-phosphate, is essential for vascular maturation. *J Clin Invest*, 106(8): 951-61.

- LIU Y, WANG X, WANG H & HU T (2019a) Identification of key genes and pathways in abdominal aortic aneurysm by integrated bioinformatics analysis. *J Int Med Res*: 300060519894437.
- LIU Z H, ZHANG Y, WANG X, FAN X F, ZHANG Y, LI X, GONG Y S & HAN L P (2019b) SIRT1 activation attenuates cardiac fibrosis by endothelial-to-mesenchymal transition. *Biomed Pharmacother*, 118: 109227.
- LÓPEZ-CANDALES A, HOLMES D R, LIAO S, SCOTT M J, WICKLINE S A & THOMPSON R W (1997) Decreased vascular smooth muscle cell density in medial degeneration of human abdominal aortic aneurysms. *Am J Pathol*, 150(3): 993-1007.
- LUCKE S & LEVKAU B (2010) Endothelial functions of sphingosine-1-phosphate. *Cell Physiol Biochem*, 26(1): 87-96.
- MACEYKA M, HARIKUMAR K B, MILSTIEN S & SPIEGEL S (2012) Sphingosine-1-phosphate signaling and its role in disease. *Trends Cell Biol*, 22(1): 50-60.
- MAJESKY M W (2007) Developmental basis of vascular smooth muscle diversity. *Arterioscler Thromb Vasc Biol*, 27(6): 1248-58.
- MAN J J, BECKMAN J A & JAFFE I Z (2020) Sex as a Biological Variable in Atherosclerosis. *Circ Res*, 126(9): 1297-1319.
- MATLOUBIAN M, LO C G, CINAMON G, LESNESKI M J, XU Y, BRINKMANN V, ALLENDE M L, PROIA R L & CYSTER J G (2004) Lymphocyte egress from thymus and peripheral lymphoid organs is dependent on S1P receptor 1. *Nature*, 427(6972): 355-60.
- MATTAGAJASINGH I, KIM C S, NAQVI A, YAMAMORI T, HOFFMAN T A, JUNG S B, DERICCO J, KASUNO K & IRANI K (2007) SIRT1 promotes endothelium-dependent vascular relaxation by activating endothelial nitric oxide synthase. *Proc Natl Acad Sci U S A*, 104(37): 14855-60.
- MEDLIN M D, STAUS D P, DUBASH A D, TAYLOR J M & MACK C P (2010) Sphingosine 1-phosphate receptor 2 signals through leukemia-associated RhoGEF (LARG), to promote smooth muscle cell differentiation. *Arterioscler Thromb Vasc Biol*, 30(9): 1779-86.
- MICHAUD J, IM D S & HLA T (2010) Inhibitory role of sphingosine 1-phosphate receptor 2 in macrophage recruitment during inflammation. *J Immunol*, 184(3): 1475-83.
- MILEWICZ D M, TRYBUS K M, GUO D C, SWEENEY H L, REGALADO E, KAMM K & STULL J T (2017) Altered Smooth Muscle Cell Force Generation as a Driver of Thoracic Aortic Aneurysms and Dissections. *Arterioscler Thromb Vasc Biol*, 37(1): 26-34.

- MILUTINOVIĆ A, ŠUPUT D & ZORC-PLESKOVIĆ R (2020) Pathogenesis of atherosclerosis in the tunica intima, media, and adventitia of coronary arteries: An updated review. *Bosn J Basic Med Sci*, 20(1): 21-30.
- MORALES-RUIZ M, LEE M J, ZÖLLNER S, GRATTON J P, SCOTLAND R, SHIOJIMA I, WALSH K, HLA T & SESSA W C (2001) Sphingosine 1-phosphate activates Akt, nitric oxide production, and chemotaxis through a Gi protein/phosphoinositide 3-kinase pathway in endothelial cells. *J Biol Chem*, 276(22): 19672-7.
- MÜLLER J G & KUHLENCORDT P (2020) Arteriosklerose: Ätiologie und Pathogenese. In: Operative und interventionelle Gefäßmedizin. *DEBUS, E S & GROSS-FENGELS, W (eds.)* 2. ed, Springer Berlin Heidelberg, 63-76.
- MURATA N, SATO K, KON J, TOMURA H, YANAGITA M, KUWABARA A, UI M & OKAJIMA F (2000) Interaction of sphingosine 1-phosphate with plasma components, including lipoproteins, regulates the lipid receptor-mediated actions. *Biochem J*, 352 Pt 3(Pt 3): 809-15.
- MUSSA F F, HORTON J D, MORIDZADEH R, NICHOLSON J, TRIMARCHI S & EAGLE K A (2016) Acute Aortic Dissection and Intramural Hematoma: A Systematic Review. *Jama*, 316(7): 754-63.
- NIENABER C A & CLOUGH R E (2015) Management of acute aortic dissection. *Lancet*, 385(9970): 800-11.
- NIENABER C A, CLOUGH R E, SAKALIHASAN N, SUZUKI T, GIBBS R, MUSSA F, JENKINS M P, THOMPSON M M, EVANGELISTA A, YEH J S et al. (2016) Aortic dissection. *Nat Rev Dis Primers*, 2: 16053.
- NOFER J R, VAN DER GIET M, TÖLLE M, WOLINSKA I, VON WNUCK LIPINSKI K, BABA H A, TIETGE U J, GÖDECKE A, ISHII I, KLEUSER B et al. (2004) HDL induces NO-dependent vasorelaxation via the lysophospholipid receptor S1P3. *J Clin Invest*, 113(4): 569-81.
- NOLAN T, HANDS R E & BUSTIN S A (2006) Quantification of mRNA using real-time RT-PCR. *Nat Protoc*, 1(3): 1559-82.
- OLIVER-WILLIAMS C, SWEETING M J, TURTON G, PARKIN D, COOPER D, RODD C, THOMPSON S G & EARNSHAW J J (2018) Lessons learned about prevalence and growth rates of abdominal aortic aneurysms from a 25-year ultrasound population screening programme. *Br J Surg*, 105(1): 68-74.
- OTA H, ETO M, OGAWA S, IIJIMA K, AKISHITA M & OUCHI Y (2010) SIRT1/eNOS axis as a potential target against vascular senescence, dysfunction and atherosclerosis. *J Atheroscler Thromb*, 17(5): 431-5.
- OWENS G K, KUMAR M S & WAMHOFF B R (2004) Molecular regulation of vascular smooth muscle cell differentiation in development and disease. *Physiol Rev*, 84(3): 767-801.

- PAPE L A, AWAIS M, WOZNICKI E M, SUZUKI T, TRIMARCHI S, EVANGELISTA A, MYRMEL T, LARSEN M, HARRIS K M, GREASON K et al. (2015) Presentation, Diagnosis, and Outcomes of Acute Aortic Dissection: 17-Year Trends From the International Registry of Acute Aortic Dissection. *J Am Coll Cardiol*, 66(4): 350-8.
- PARK S, SORENSON C M & SHEIBANI N (2015) PECAM-1 isoforms, eNOS and endoglin axis in regulation of angiogenesis. *Clin Sci (Lond)*, 129(3): 217-34.
- PARKINSON F, FERGUSON S, LEWIS P, WILLIAMS I M & TWINE C P (2015) Rupture rates of untreated large abdominal aortic aneurysms in patients unfit for elective repair. *J Vasc Surg*, 61(6): 1606-12.
- PFALTZGRAFF E R & BADER D M (2015) Heterogeneity in vascular smooth muscle cell embryonic origin in relation to adult structure, physiology, and disease. *Dev Dyn*, 244(3): 410-6.
- PILLING D, FAN T, HUANG D, KAUL B & GOMER R H (2009) Identification of markers that distinguish monocyte-derived fibrocytes from monocytes, macrophages, and fibroblasts. *PLoS One*, 4(10): e7475.
- POTÌ F, GUALTIERI F, SACCHI S, WEISSE-PLENZ G, VARGA G, BRODDE M, WEBER C, SIMONI M & NOFER J R (2013) KRP-203, sphingosine 1-phosphate receptor type 1 agonist, ameliorates atherosclerosis in LDL-R^{-/-} mice. *Arterioscler Thromb Vasc Biol*, 33(7): 1505-12.
- PRIVRATSKY J R & NEWMAN P J (2014) PECAM-1: regulator of endothelial junctional integrity. *Cell Tissue Res*, 355(3): 607-19.
- PROIA R L & HLA T (2015) Emerging biology of sphingosine-1-phosphate: its role in pathogenesis and therapy. *J Clin Invest*, 125(4): 1379-87.
- PYNE S & PYNE N (2000) Sphingosine 1-phosphate signalling via the endothelial differentiation gene family of G-protein-coupled receptors. *Pharmacol Ther*, 88(2): 115-31.
- QU Z, CHEUK B L & CHENG S W (2012) Differential expression of sphingosine-1-phosphate receptors in abdominal aortic aneurysms. *Mediators Inflamm*, 2012: 643609.
- RABKIN S W (2017) The Role Matrix Metalloproteinases in the Production of Aortic Aneurysm. *Prog Mol Biol Transl Sci*, 147: 239-265.
- RAFFORT J, LAREYRE F, CLÉMENT M, HASSEN-KHODJA R, CHINETTI G & MALLAT Z (2017) Monocytes and macrophages in abdominal aortic aneurysm. *Nat Rev Cardiol*, 14(8): 457-471.
- RAO J, BROWN B N, WEINBAUM J S, OFSTUN E L, MAKAROUN M S, HUMPHREY J D & VORP D A (2015) Distinct macrophage phenotype and collagen organization within the intraluminal thrombus of abdominal aortic aneurysm. *J Vasc Surg*, 62(3): 585-93.

- REED D, REED C, STEMMERMANN G & HAYASHI T (1992) Are aortic aneurysms caused by atherosclerosis? *Circulation*, 85(1): 205-11.
- RICHES K, ANGELINI T G, MUDHAR G S, KAYE J, CLARK E, BAILEY M A, SOHRABI S, KOROSSIS S, WALKER P G, SCOTT D J et al. (2013) Exploring smooth muscle phenotype and function in a bioreactor model of abdominal aortic aneurysm. *J Transl Med*, 11: 208.
- ROBBINS C S, HILGENDORF I, WEBER G F, THEURL I, IWAMOTO Y, FIGUEIREDO J L, GORBATOV R, SUKHOVA G K, GERHARDT L M, SMYTH D et al. (2013) Local proliferation dominates lesional macrophage accumulation in atherosclerosis. *Nat Med*, 19(9): 1166-72.
- ROCHA V Z & LIBBY P (2009) Obesity, inflammation, and atherosclerosis. *Nat Rev Cardiol*, 6(6): 399-409.
- ROTH G A, MENSAH G A, JOHNSON C O, ADDOLORATO G, AMMIRATI E, BADDOUR L M, BARENGO N C, BEATON A Z, BENJAMIN E J, BENZIGER C P et al. (2020) Global Burden of Cardiovascular Diseases and Risk Factors, 1990-2019: Update From the GBD 2019 Study. *J Am Coll Cardiol*, 76(25): 2982-3021.
- SAITO T, HASEGAWA Y, ISHIGAKI Y, YAMADA T, GAO J, IMAI J, UNO K, KANEKO K, OGIHARA T, SHIMOSAWA T et al. (2013) Importance of endothelial NF- κ B signalling in vascular remodelling and aortic aneurysm formation. *Cardiovasc Res*, 97(1): 106-14.
- SAKALIHASAN N, MICHEL J B, KATSARGYRIS A, KUIVANIEMI H, DEFRAIGNE J O, NCHIMI A, POWELL J T, YOSHIMURA K & HULTGREN R (2018) Abdominal aortic aneurysms. *Nat Rev Dis Primers*, 4(1): 34.
- SAMPSON U K, NORMAN P E, FOWKES F G, ABOYANS V, SONG Y, HARRELL F E, Jr., FOROUZANFAR M H, NAGHAVI M, DENENBERG J O, MCDERMOTT M M et al. (2014) Estimation of global and regional incidence and prevalence of abdominal aortic aneurysms 1990 to 2010. *Glob Heart*, 9(1): 159-70.
- SANCHEZ T (2016) Sphingosine-1-Phosphate Signaling in Endothelial Disorders. *Curr Atheroscler Rep*, 18(6): 31.
- SANCHEZ T, ESTRADA-HERNANDEZ T, PAIK J H, WU M T, VENKATARAMAN K, BRINKMANN V, CLAFFEY K & HLA T (2003) Phosphorylation and action of the immunomodulator FTY720 inhibits vascular endothelial cell growth factor-induced vascular permeability. *J Biol Chem*, 278(47): 47281-90.
- SANCHEZ T & HLA T (2004) Structural and functional characteristics of S1P receptors. *J Cell Biochem*, 92(5): 913-22.
- SANCHEZ T, SKOURA A, WU M T, CASSERLY B, HARRINGTON E O & HLA T (2007) Induction of vascular permeability by the sphingosine-1-phosphate

- receptor-2 (S1P2R) and its downstream effectors ROCK and PTEN. *Arterioscler Thromb Vasc Biol*, 27(6): 1312-8.
- SCHWAB S R, PEREIRA J P, MATLOUBIAN M, XU Y, HUANG Y & CYSTER J G (2005) Lymphocyte sequestration through S1P lyase inhibition and disruption of S1P gradients. *Science*, 309(5741): 1735-9.
- SHANKMAN L S, GOMEZ D, CHEREPANOVA O A, SALMON M, ALENCAR G F, HASKINS R M, SWIATLOWSKA P, NEWMAN A A, GREENE E S, STRAUB A C et al. (2015) KLF4-dependent phenotypic modulation of smooth muscle cells has a key role in atherosclerotic plaque pathogenesis. *Nat Med*, 21(6): 628-37.
- SHIMIZU T, DE WISPELAERE A, WINKLER M, D'SOUZA T, CAYLOR J, CHEN L, DASTVAN F, DEOU J, CHO A, LARENA-AVELLANEDA A et al. (2012) Sphingosine-1-phosphate receptor 3 promotes neointimal hyperplasia in mouse iliac-femoral arteries. *Arterioscler Thromb Vasc Biol*, 32(4): 955-61.
- SHIMIZU T, NAKAZAWA T, CHO A, DASTVAN F, SHILLING D, DAUM G & REIDY M A (2007) Sphingosine 1-phosphate receptor 2 negatively regulates neointimal formation in mouse arteries. *Circ Res*, 101(10): 995-1000.
- SIASOS G, MOUROUZIS K, OIKONOMOU E, TSALAMANDRIS S, TSIGKOU V, VLASIS K, VAVURANAKIS M, ZOGRAFOS T, DIMITROPOULOS S, PAPAIOANNOU T G et al. (2015) The Role of Endothelial Dysfunction in Aortic Aneurysms. *Curr Pharm Des*, 21(28): 4016-34.
- SKOURA A, MICHAUD J, IM D S, THANGADA S, XIONG Y, SMITH J D & HLA T (2011) Sphingosine-1-phosphate receptor-2 function in myeloid cells regulates vascular inflammation and atherosclerosis. *Arterioscler Thromb Vasc Biol*, 31(1): 81-5.
- SOSNOWSKA B, MAZIDI M, PENSON P, GLUBA-BRZÓZKA A, RYSZ J & BANACH M (2017) The sirtuin family members SIRT1, SIRT3 and SIRT6: Their role in vascular biology and atherogenesis. *Atherosclerosis*, 265: 275-282.
- SPIEGEL S & MILSTIEN S (2003) Sphingosine-1-phosphate: an enigmatic signalling lipid. *Nat Rev Mol Cell Biol*, 4(5): 397-407.
- STRUB G M, MACEYKA M, HAIT N C, MILSTIEN S & SPIEGEL S (2010) Extracellular and intracellular actions of sphingosine-1-phosphate. *Adv Exp Med Biol*, 688: 141-55.
- SUH B, SONG Y S, SHIN D W, LIM J, KIM H, MIN S H, LEE S P, PARK E A, LEE W, LEE H et al. (2018) Incidentally detected atherosclerosis in the abdominal aorta or its major branches on computed tomography is highly associated with coronary heart disease in asymptomatic adults. *J Cardiovasc Comput Tomogr*, 12(4): 305-311.
- SUN J, DENG H, ZHOU Z, XIONG X & GAO L (2018) Endothelium as a Potential Target for Treatment of Abdominal Aortic Aneurysm. *Oxid Med Cell Longev*, 2018: 6306542.

- THEJ M J, KALYANI R & KIRAN J (2012) Atherosclerosis in coronary artery and aorta in a semi-urban population by applying modified American Heart Association classification of atherosclerosis: An autopsy study. *J Cardiovasc Dis Res*, 3(4): 265-71.
- THOMPSON A M, WAGNER R & RZUCIDLO E M (2014) Age-related loss of SirT1 expression results in dysregulated human vascular smooth muscle cell function. *Am J Physiol Heart Circ Physiol*, 307(4): H533-41.
- TILLMANN B N (2020) Anatomie der Gefäße: Rumpf. In: Operative und interventionelle Gefäßmedizin. *DEBUS, E S & GROSS-FENGELS, W (eds.) 2. ed*, Springer Berlin Heidelberg, 549-561.
- TOGHILL B J, SARATZIS A & BOWN M J (2017) Abdominal aortic aneurysm-an independent disease to atherosclerosis? *Cardiovasc Pathol*, 27: 71-75.
- TÖLLE M, LEVKAU B, KEUL P, BRINKMANN V, GIEBING G, SCHÖNFELDER G, SCHÄFERS M, VON WNUCK LIPINSKI K, JANKOWSKI J, JANKOWSKI V et al. (2005) Immunomodulator FTY720 Induces eNOS-dependent arterial vasodilatation via the lysophospholipid receptor S1P3. *Circ Res*, 96(8): 913-20.
- TSAI T T, TRIMARCHI S & NIENABER C A (2009) Acute aortic dissection: perspectives from the International Registry of Acute Aortic Dissection (IRAD). *Eur J Vasc Endovasc Surg*, 37(2): 149-59.
- UNOSSON J, WÅGSÄTER D, BJARNEGÅRD N, DE BASSO R, WELANDER M, MANI K, GOTTSÄTER A & WANHAINEN A (2021) Metformin Prescription Associated with Reduced Abdominal Aortic Aneurysm Growth Rate and Reduced Chemokine Expression in a Swedish Cohort. *Ann Vasc Surg*, 70: 425-433.
- VENGRENYUK Y, NISHI H, LONG X, OUI MET M, SAVJI N, MARTINEZ F O, CASSELLA C P, MOORE K J, RAMSEY S A, MIANO J M et al. (2015) Cholesterol loading reprograms the microRNA-143/145-myocardin axis to convert aortic smooth muscle cells to a dysfunctional macrophage-like phenotype. *Arterioscler Thromb Vasc Biol*, 35(3): 535-46.
- WANG J C & BENNETT M (2012) Aging and atherosclerosis: mechanisms, functional consequences, and potential therapeutics for cellular senescence. *Circ Res*, 111(2): 245-59.
- WANG Y, DONG C Q, PENG G Y, HUANG H Y, YU Y S, JI Z C & SHEN Z Y (2019) MicroRNA-134-5p Regulates Media Degeneration through Inhibiting VSMC Phenotypic Switch and Migration in Thoracic Aortic Dissection. *Mol Ther Nucleic Acids*, 16: 284-294.
- WANG Y D, LIU Z J, REN J & XIANG M X (2018) Pharmacological Therapy of Abdominal Aortic Aneurysm: An Update. *Curr Vasc Pharmacol*, 16(2): 114-124.
- WARBOYS C M, DE LUCA A, AMINI N, LUONG L, DUCKLES H, HSIAO S, WHITE A, BISWAS S, KHAMIS R, CHONG C K et al. (2014) Disturbed flow promotes

- endothelial senescence via a p53-dependent pathway. *Arterioscler Thromb Vasc Biol*, 34(5): 985-95.
- WINNIK S, AUWERX J, SINCLAIR D A & MATTER C M (2015) Protective effects of sirtuins in cardiovascular diseases: from bench to bedside. *Eur Heart J*, 36(48): 3404-12.
- WIRKA R C, WAGH D, PAIK D T, PJANIC M, NGUYEN T, MILLER C L, KUNDU R, NAGAO M, COLLIER J, KOYANO T K et al. (2019) Atheroprotective roles of smooth muscle cell phenotypic modulation and the TCF21 disease gene as revealed by single-cell analysis. *Nat Med*, 25(8): 1280-1289.
- YAMAMOTO R, AOKI T, KOSEKI H, FUKUDA M, HIROSE J, TSUJI K, TAKIZAWA K, NAKAMURA S, MIYATA H, HAMAKAWA N et al. (2017) A sphingosine-1-phosphate receptor type 1 agonist, ASP4058, suppresses intracranial aneurysm through promoting endothelial integrity and blocking macrophage transmigration. *Br J Pharmacol*, 174(13): 2085-2101.
- YANG S, YUAN H Q, HAO Y M, REN Z, QU S L, LIU L S, WEI D H, TANG Z H, ZHANG J F & JIANG Z S (2020) Macrophage polarization in atherosclerosis. *Clin Chim Acta*, 501: 142-146.
- YE J, WANG M, JIANG H, JI Q, HUANG Y, LIU J, ZENG T, XU Y, WANG Z, LIN Y et al. (2018) Increased levels of interleukin-22 in thoracic aorta and plasma from patients with acute thoracic aortic dissection. *Clin Chim Acta*, 486: 395-401.
- YOKOYAMA U, ARAKAWA N, ISHIWATA R, YASUDA S, MINAMI T, GODA M, UCHIDA K, SUZUKI S, MATSUMOTO M, KOIZUMI N et al. (2018) Proteomic analysis of aortic smooth muscle cell secretions reveals an association of myosin heavy chain 11 with abdominal aortic aneurysm. *Am J Physiol Heart Circ Physiol*, 315(4): H1012-h1018.
- YU Q, DONG L, LI Y & LIU G (2018) SIRT1 and HIF1 α signaling in metabolism and immune responses. *Cancer Lett*, 418: 20-26.
- YU X, ZHANG L, WEN G, ZHAO H, LUONG L A, CHEN Q, HUANG Y, ZHU J, YE S, XU Q et al. (2015) Upregulated sirtuin 1 by miRNA-34a is required for smooth muscle cell differentiation from pluripotent stem cells. *Cell Death Differ*, 22(7): 1170-80.
- ZENG H T, FU Y C, YU W, LIN J M, ZHOU L, LIU L & WANG W (2013) SIRT1 prevents atherosclerosis via liver-X-receptor and NF- κ B signaling in a U937 cell model. *Mol Med Rep*, 8(1): 23-8.
- ZHANG K, PAN X, ZHENG J, LIU Y & SUN L (2020) SIRT1 protects against aortic dissection by regulating AP-1/decorin signaling-mediated PDCD4 activation. *Mol Biol Rep*, 47(3): 2149-2159.
- ZHANG L, YU C, CHANG Q, LUO X, QIU J & LIU S (2016) Comparison of gene expression profiles in aortic dissection and normal human aortic tissues. *Biomed Rep*, 5(4): 421-427.

- ZHANG Q J, WANG Z, CHEN H Z, ZHOU S, ZHENG W, LIU G, WEI Y S, CAI H, LIU D P & LIANG C C (2008) Endothelium-specific overexpression of class III deacetylase SIRT1 decreases atherosclerosis in apolipoprotein E-deficient mice. *Cardiovasc Res*, 80(2): 191-9.
- ZHANG W, AN J, JAWADI H, SIOW D L, LEE J F, ZHAO J, GARTUNG A, MADDIPATI K R, HONN K V, WATTENBERG B W et al. (2013) Sphingosine-1-phosphate receptor-2 mediated NF κ B activation contributes to tumor necrosis factor- α induced VCAM-1 and ICAM-1 expression in endothelial cells. *Prostaglandins Other Lipid Mediat*, 106: 62-71.
- ZHANG Z, XU J, LIU Y, WANG T, PEI J, CHENG L, HAO D, ZHAO X, CHEN H Z & LIU D P (2018) Mouse macrophage specific knockout of SIRT1 influences macrophage polarization and promotes angiotensin II-induced abdominal aortic aneurysm formation. *J Genet Genomics*, 45(1): 25-32.
- ZHAO Y, VANHOUTTE P M & LEUNG S W (2015) Vascular nitric oxide: Beyond eNOS. *J Pharmacol Sci*, 129(2): 83-94.
- ZHU L, VRANCKX R, KHAU VAN KIEN P, LALANDE A, BOISSET N, MATHIEU F, WEGMAN M, GLANCY L, GASC J M, BRUNOTTE F et al. (2006) Mutations in myosin heavy chain 11 cause a syndrome associating thoracic aortic aneurysm/aortic dissection and patent ductus arteriosus. *Nat Genet*, 38(3): 343-9.

10 Appendix

Table A1. Reaction kits, components and manufacturers used for cDNA synthesis and RT-qPCR

Table A2. Laboratory equipment used for the analyses of the aortic tissue samples

Table A3. Reagents used for the immunohistochemical Mac2 staining

Table A4. Patient related data and results from quantitative measurements

Figure A1. Isotype controls for Mac2 stained aortic tissue sections (Figure 15).

Figure A2. Macrophage staining of infrarenal aortic tissue sections, subgroup 0.

Figure A3. Macrophage staining of infrarenal aortic tissue sections, subgroup P.

Figure A4. Macrophage staining of infrarenal aortic tissue sections, subgroup AP.

Figure A5. Macrophage staining of infrarenal aortic tissue sections, subgroup D.

Table A1. Reaction kits, components and manufacturers used for cDNA synthesis and RT-qPCR.

Kit	Components	Manufacturer
Maxima First Strand cDNAse Synthesis Kit for RT-qPCR	Maxima Enzyme Mix (Maxima Reverse Transcriptase and RiboLock RNase Inhibitor) 5X reaction mix (reaction buffer, dNTPs, oligo(dT) ₁₈ and random hexamer primers nuclease-free water	Thermo Scientific
Rotor-Gene SYBR Green PCR Kit	Rotor-Gene SYBR Green PCR Master Mix, containing: - HotStarTaq [®] <i>Plus</i> DNA Polymerase - Rotor-Gene SYBR Green PCR Buffer - dNTP mix (dATP, dCTP, dGTP, dTTP) RNase-Free Water	Qiagen

Table A2. Laboratory equipment used for the analyses of the aortic tissue samples.

Device	Manufacturer
T100™ Thermal Cycler serial number: 621BR05102	BIO-RAD
Rotor Gene Q serial number: R0513113 and R0814145	Qiagen
Pipettes (various sizes)	Eppendorf
Sprout Minicentrifuge	Biozym
IKA® Vortex Genius 3	Sigma-Aldrich
Sliding microtome pfm Slide 4004 M	pfm medical
pfmWaterbath 1000	pfm medical
Incubator	Binder
Microprocessor pH Meter	HANNA instruments
microscope Biozero BZ-8100 serial number: CD900007	Keyence

Table A3. Reagents used for the immunohistochemical Mac2 staining. (Avidin-Biotin Complex method)

Reagent		Supplier
Xylene		J.T.Baker
Ethanol (99%, 96%, 70%)		ChemSolute
Aqua destillata		
Tris Buffered Saline (TBS) buffer 0,05 M, pH 7,6		
Trizma® base (Primary Standard and Buffer, > 99,9% (titration)), crystalline sodium chloride > 99,8% Aqua destillata		Sigma® Life Science Roth
Antigen Retrieval Citra Plus (Concentrated (10X) Antigen Retrieval Citra Plus Solution)		BioGenex
Hydrogen peroxide 30%		Merck KGaA
Pap Pen		Kisker Biotech GmbH & Co. KG
Avidin/Biotin Blocking Kit Vector Catalogue number: SP-2001		life technologies
Protein Block/Normal Rabbit Serum HK114-5K		BioGenex
Antibody-dilution buffer		DCS Innovative Diagnostik-Systeme
Primary Antibody:		
Purified Anti-Mouse MAC-2 Monoclonal Antibody Catalogue number: CL 8942AP LOT number: 104227A	1:1000	Cedarlane
IgG2A Isotype Control (Purified Rat Monoclonal IgG _{2A}) R&D Catalogue Number: MAB006 LOT number: CAO2414021	1:1000	R&D Systems®
Secondary Antibody:		
Biotinylated Anti-Rat IgG (H+L) Vector Catalogue number: BA-4000 LOT number: W0720	1:200	Vector Laboratories, Inc.
Vectastain® Elite® ABC Reagent Catalogue number: PK-6100		Vector Laboratories, inc.
AEC 2 Components Kit Catalogue number: AC131C100		DCS ChromoLine, DCS Innovative Diagnostik-Systeme
Hämatoxylin Mayer		Melite
Aqua-Poly/Mount		Polysciences

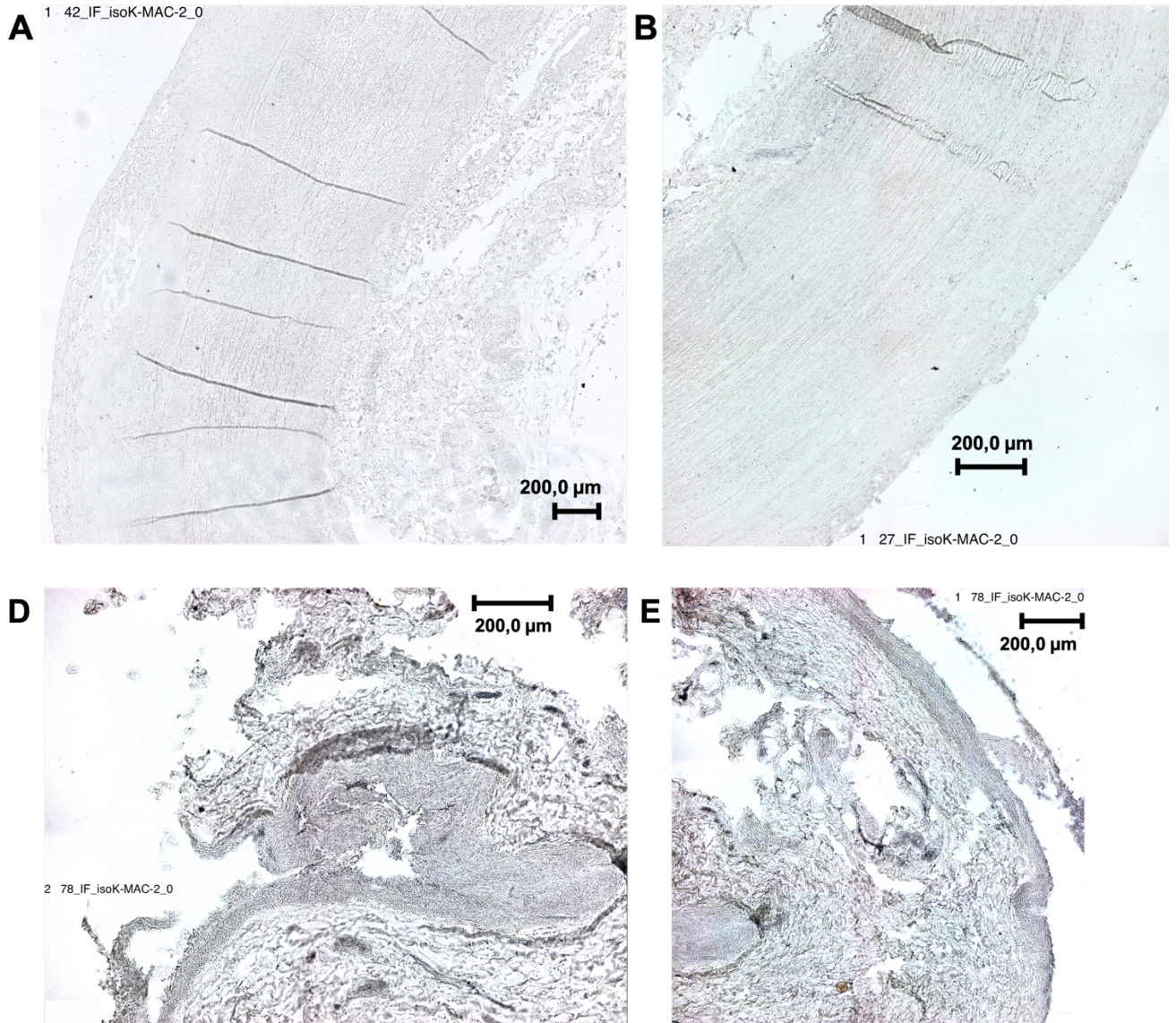
Table A4. Patient related data and results from quantitative measurements

Pat. Nr.	Alter	Sex 0=M, 1=F	Groesse (cm)	Gewicht (kg)	BMI	IF_A	IF_D	IF_P	A or D or P	log_IF_CD31	log_IF_S1	log_IF_S2	log_IF_S3	log_IF_CD68	log_IF_MYH1 1	log_IF_CD45	log_IF_NOS 3	log_IF_SIRT
1	69	1	155	61,2	25	0	0	1	1	3,81	2,78	0,71	1,60	1,24	6,32	0,99	1,18	1,72
2	49	0	183	95	28	0	1	0	1	0,28	-2,31	-3,27	-0,80	-0,94	4,29	-1,50	-2,99	-1,37
3	33	0	191	106	29	0	0	0	0	3,39	1,80	0,99	3,07	0,49	7,88	1,12	-	2,48
4	75	1	173	65,8	22	1	0	1	1	3,44	2,12	-0,73	0,62	2,36	4,41	2,30	1,59	-0,10
5	75	0	182	92	28	1	0	0	1	4,28	3,20	-0,18	1,27	1,29	5,48	0,36	2,95	0,77
6	53	0	189	99,4	28	0	0	0	0	2,43	1,66	2,97	3,25	2,71	6,70	0,92	1,18	2,13
7	79	0	172	48,1	16	1	0	1	1	4,72	3,80	-1,29	1,57	2,46	4,14	0,55	1,27	0,28
8	82	1	nd	nd	nd	0	0	0	0	0,92	-1,36	-2,19	0,31	-0,40	4,69	-2,43	-1,89	-1,30
9	65	0	180	111	34	0	1	0	1	0,94	-1,03	-0,93	1,21	0,52	6,43	-1,62	-1,76	-0,01
10	80	0	nd	nd	nd	1	0	1	1	6,49	3,90	1,10	1,29	2,75	6,38	1,68	1,80	1,75
11	67	1	169	51	18	1	0	1	1	3,07	1,86	-0,92	0,28	2,42	4,33	1,06	-0,57	0,28
12	86	1	nd	nd	nd	0	0	0	0	3,91	2,51	0,07	2,10	3,03	7,11	2,51	0,29	1,65
13	47	1	nd	nd	nd	0	0	0	0	2,70	0,62	-0,75	1,46	2,07	6,69	1,55	-0,14	1,07
14	83	1	168	109,6	39	1	0	1	1	4,89	2,50	0,93	0,89	2,21	4,06	2,09	0,44	1,16
15	67	0	174	81	27	0	1	1	1	0,63	-0,27	-0,97	1,17	0,56	5,94	-1,31	-2,85	0,74
16	73	1	nd	nd	nd	0	1	1	1	3,74	2,43	-0,92	0,56	1,27	4,03	-0,53	0,74	-0,42
17	76	0	nd	nd	nd	0	1	0	1	1,61	-0,41	-1,23	1,04	2,29	4,13	1,25	-1,84	0,07
18	75	0	187	88	25	0	0	1	1	4,41	2,66	0,35	0,93	3,10	6,44	1,52	1,31	1,20
19	72	0	184	86,2	25	1	0	1	1	1,19	-1,15	-3,64	-1,32	1,88	0,81	-0,06	-2,11	-2,28
20	64	1	165	101	37	1	0	1	1	1,93	0,58	-2,47	-0,86	3,22	3,89	-1,06	-1,43	-0,46
22	70	0	180	87	27	1	0	1	1	1,91	0,43	-1,03	0,29	2,07	2,49	-1,32	-1,21	-0,47
23	72	0	181	128,1	39	1	0	1	1	4,24	2,33	-0,58	0,24	2,01	4,61	0,78	1,35	0,75
24	43	0	nd	151	nd	0	1	0	1	4,68	2,28	1,41	1,45	1,83	6,34	1,34	1,03	2,25
25	65	0	184	102,2	30	1	0	1	1	2,61	1,38	-1,47	1,12	2,08	4,84	-0,50	-0,34	-0,52
26	40	0	199	137,8	35	0	0	0	0	4,51	1,88	-0,86	1,79	0,55	7,94	-0,38	0,39	1,00
27	65	0	184	93,1	27	0	0	0	0	2,97	1,20	-1,06	-0,34	2,65	5,31	-1,35	-0,95	-0,05
28	86	1	149	37,4	17	1	0	1	1	3,00	2,35	-1,12	0,38	2,03	3,92	-0,52	-0,36	0,09
29	58	0	nd	nd	nd	0	0	0	0	4,12	2,03	-0,76	0,76	3,37	6,44	1,71	0,85	0,75
31	79	1	160	65	25	0	0	0	0	2,74	0,77	-0,74	1,32	-0,04	5,32	-3,32	-1,57	0,54
32	75	0	168	60,1	21	0	0	0	0	3,35	1,08	-1,64	1,32	1,10	7,52	-0,26	0,25	1,09
33	73	0	176	60,5	20	0	1	0	1	2,70	0,32	-0,60	0,74	1,45	6,29	2,11	-0,56	1,13
34	71	0	180	84	26	1	0	1	1	2,60	0,49	-2,40	-1,22	0,93	4,43	-0,12	-0,33	-2,45
37	57	0	183	74	22	1	0	1	1	2,83	1,56	-0,32	0,14	3,17	5,00	nd	nd	nd
38	62	0	175	102,7	34	0	0	1	1	3,59	1,43	-0,04	0,82	0,64	4,52	0,02	0,97	1,93
39	91	1	161	71,4	28	1	0	1	1	2,49	-0,81	-1,36	-1,56	3,49	1,92	0,52	-1,52	-0,03
41	71	1	169	83,5	29	1	0	1	1	3,19	1,42	-1,51	0,25	1,91	3,23	-1,42	-1,94	-0,80
42	47	0	210	125	28	0	0	0	0	4,24	1,48	-0,92	0,73	2,28	6,81	0,87	1,80	1,34
43	57	0	nd	nd	nd	1	0	1	1	2,99	-0,10	-1,18	-2,47	3,00	4,94	-0,57	-1,33	0,50
45	64	1	160	50,1	20	0	1	1	1	3,16	0,71	-0,92	-0,34	1,57	6,24	2,60	-0,47	1,61
46	71	1	nd	nd	nd	0	0	1	1	3,62	1,13	-2,00	-0,42	2,78	5,50	-0,13	-1,19	0,21
47	68	1	174	72,6	24	1	0	1	1	3,64	1,56	-1,79	-0,34	2,26	3,73	0,23	0,16	-0,07
48	77	1	172	82	28	0	0	1	1	6,42	4,24	1,32	1,70	2,86	5,02	2,17	2,81	1,86
49	55	0	205	127,9	30	0	0	0	0	2,55	0,58	-1,25	1,28	0,95	6,93	-0,70	-0,31	1,00
50	79	1	165	73	27	1	0	1	1	4,34	1,58	-1,06	-0,25	3,12	4,26	2,81	-2,47	1,22
51	74	0	185	105	31	0	1	1	1	3,15	1,38	-2,84	0,53	1,07	5,06	-0,49	-0,68	-0,60
53	67	0	178	87,8	28	1	0	1	1	3,28	0,83	-1,84	-1,12	1,70	3,66	-0,27	0,20	0,31
54	70	0	175	90	29	1	0	1	1	4,24	2,57	0,20	0,71	1,90	6,35	0,46	1,43	0,81
55	85	0	165	63,1	23	1	0	1	1	4,12	2,05	-1,32	0,86	2,84	3,25	0,53	0,47	0,57
56	63	0	178	51,2	16	0	0	1	1	5,35	2,58	-0,36	0,52	2,37	5,06	1,78	1,54	1,37

Continued on page 81

57	86	1	160	66,3	26	1	0	1	1	4,44	0,78	-1,84	1,12	3,15	4,25	0,74	-0,02	0,50
58	59	0	187	94,2	27	1	0	1	1	4,02	1,95	-1,18	-0,18	2,08	5,19	1,19	0,69	0,05
59	56	0	165	86,3	32	0	0	0	0	0,49	-1,51	-2,12	-1,25	0,94	3,42	-2,08	-3,18	-1,63
60	64	0	180	94,5	29	1	0	1	1	3,11	2,02	-0,94	0,76	2,28	3,90	-0,35	0,38	0,79
61	80	0	177	41,5	13	1	0	1	1	4,57	3,14	0,57	-0,45	2,69	6,09	1,82	1,05	0,79
62	74	0	175	82,5	27	1	0	1	1	3,50	0,99	-1,00	-0,76	3,25	4,44	0,95	-0,64	0,15
63	53	1	174	60,2	20	0	1	0	1	1,61	1,10	-2,06	1,38	0,64	6,58	-1,13	0,84	0,68
64	64	0	175	82	27	0	0	1	1	3,88	1,28	-1,60	-0,67	3,04	4,21	2,48	1,08	0,41
65	70	1	160	52	20	0	0	0	0	3,12	2,40	-0,27	1,18	1,66	5,07	0,50	-0,51	0,31
66	43	1	158	57	23	0	1	1	1	2,86	1,66	-1,47	-0,03	1,21	3,69	1,24	0,49	0,27
67	49	1	nd	nd	nd	0	0	0	0	4,01	2,66	0,46	0,70	0,23	6,58	-0,77	1,47	1,31
68	59	0	180	83	26	1	0	1	1	5,87	3,46	-1,51	-0,64	0,42	6,31	3,55	1,85	1,13
69	47	0	186	77,6	22	0	1	1	1	1,27	-1,15	-2,32	-1,51	0,40	2,14	-0,17	-0,73	-2,04
70	76	0	173	114	38	1	0	1	1	2,63	1,21	-3,18	-0,10	0,96	4,64	-2,87	-0,20	-2,15
71	60	0	173	62	21	1	0	1	1	3,93	1,16	-1,29	-0,15	1,14	4,38	0,46	1,48	-0,24
72	88	0	170	73,9	26	0	1	1	1	3,48	1,53	-2,00	-0,14	0,61	4,86	-1,01	1,17	-0,77
73	82	1	171	89	30	0	1	1	1	4,06	2,43	-0,74	1,06	1,38	4,49	0,50	0,45	-0,30
74	76	0	178	72	23	0	0	1	1	2,57	1,03	-2,40	-0,42	1,97	5,70	-0,91	-0,95	-0,33
75	77	0	181	85,7	26	1	0	1	1	1,97	-0,14	-2,64	-1,06	0,90	2,35	-0,37	-0,94	-1,23
76	60	0	nd	nd	nd	0	0	0	0	1,15	0,15	-1,56	-0,07	2,78	5,62	-0,44	-1,63	1,23
78	71	1	174	71,3	24	0	0	1	1	4,15	1,82	-1,32	2,30	1,52	7,80	0,78	0,17	2,15
80	76	1	165	110,6	41	1	0	1	1	4,76	2,86	-0,34	0,64	1,55	5,39	-0,34	0,73	0,40
82	82	0	177	87,5	28	1	0	1	1	1,46	-1,22	-5,06	-2,94	1,15	-0,12	0,96	-1,95	-1,31
83	73	0	197	160	41	1	0	1	1	2,36	0,34	-2,94	1,55	1,92	4,23	0,75	-1,32	-0,65
84	78	1	175	77	25	1	0	1	1	5,10	2,89	-1,36	-0,32	2,01	5,45	1,75	1,33	0,83
85	86	0	nd	nd	nd	1	0	1	1	2,54	1,00	-1,89	-1,47	3,64	3,19	0,24	-1,62	-1,17
86	87	0	170	48	17	1	0	1	1	-0,67	-1,79	-3,47	-1,79	3,57	2,60	nd	nd	nd
87	55	1	nd	nd	nd	0	1	1	1	3,82	0,90	-2,47	-0,92	1,44	5,78	-1,17	0,05	0,51
88	77	1	160	48,6	19	1	0	1	1	4,11	1,53	-1,32	-0,12	1,60	4,43	1,55	0,29	0,57
89	85	1	147	68,5	32	0	0	0	0	4,77	2,17	0,29	0,64	3,25	7,29	-0,06	1,09	2,26
90	71	1	157	62,7	25	0	1	1	1	3,17	0,50	-1,40	0,79	1,26	7,24	1,46	0,65	1,73
91	86	0	173	106,8	36	1	0	1	1	2,75	0,00	-0,84	-0,10	1,43	5,09	1,58	0,02	0,74
92	56	0	173	88	29	0	1	0	1	4,58	3,58	0,82	2,50	1,28	4,89	1,05	2,77	0,85
93	72	0	189	76,8	21	1	0	1	1	3,95	1,81	-2,32	-2,18	2,45	2,86	-0,04	-0,17	-0,13
95	86	0	183	97,8	29	1	0	1	1	3,52	0,77	-1,22	-0,12	0,60	4,93	-0,13	-0,55	0,88
96	76	0	176	83	27	1	0	1	1	5,47	2,12	-0,07	0,85	3,37	3,05	1,87	1,81	1,95
97	64	0	187	90,6	26	1	0	1	1	4,21	1,91	-3,47	0,73	2,00	6,12	0,25	0,54	0,12
98	78	0	179	101,2	32	1	0	1	1	4,50	2,04	-1,94	-0,22	1,77	4,63	-1,40	0,80	0,22
99	74	0	185	80	23	1	0	1	1	2,04	-0,22	-0,92	0,03	2,23	3,41	-1,19	-2,26	0,60
100	70	0	nd	nd	nd	1	0	1	1	3,61	1,30	-1,09	-0,49	1,64	4,80	0,24	-0,46	0,78
101	85	1	nd	nd	nd	0	0	0	0	4,54	2,66	-0,12	0,91	1,47	6,69	1,67	1,07	1,73
102	77	0	188	86	24	1	0	1	1	1,67	0,32	-0,58	0,11	3,25	3,44	-0,08	-3,16	-0,16
103	48	1	165	83	30	0	1	0	1	1,26	-0,60	-2,12	0,66	1,14	5,47	-1,19	-0,54	-0,08
104	75	0	168	93,8	33	0	1	0	1	3,17	2,59	-0,32	0,82	1,31	4,21	-0,79	0,55	1,43
105	69	0	170	78,4	27	1	0	1	1	4,80	2,47	-1,56	-0,32	2,21	4,23	1,75	0,67	0,13
106	72	1	161	76	29	1	0	1	1	-2,94	-5,06	-4,32	-4,06	1,43	6,21	-1,58	-7,64	-1,47

Figure A1. Isotype controls for Mac2 stained aortic tissue sections (Figure 15). Tissue sections stained with Mac2 antibody are shown in Figure 15. For all samples, respective control stains with an isotype control antibody were prepared (see Section 3.4) and all were negative. A, B: subgroup 0, #42 (A) and #27 (B), both at 200x magnification. (No overview image was taken of the isotype control sample of #78, reflecting section C in Figure 15). D, E: subgroup P, #78, both at 200x magnification. F, G: subgroup AP, #25 (F) at 200x magnification and #102 (G) at 40x magnification. H, I: subgroup D, #24 (H) and #104 (I), both at 200x magnification.



Continued on page 83

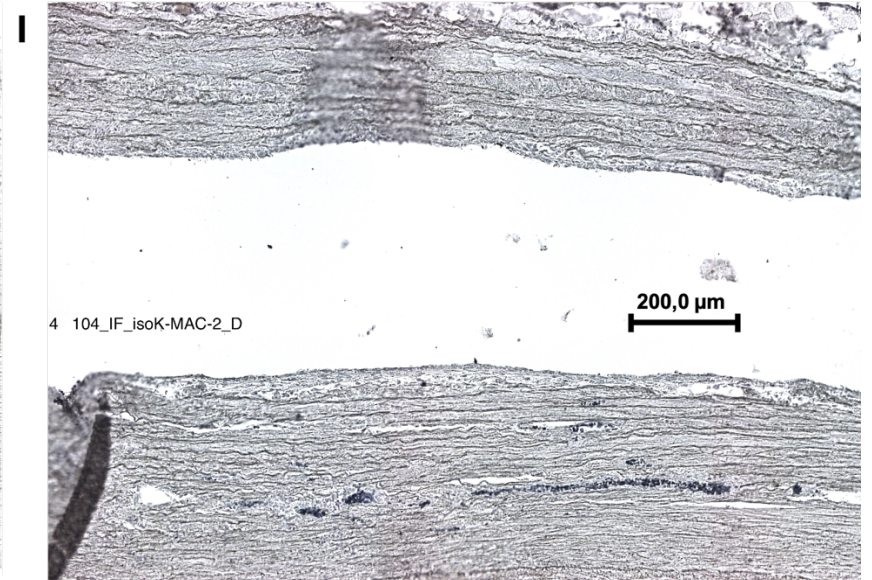
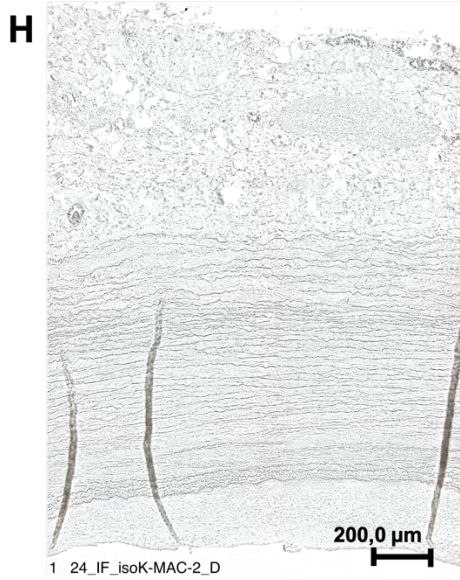
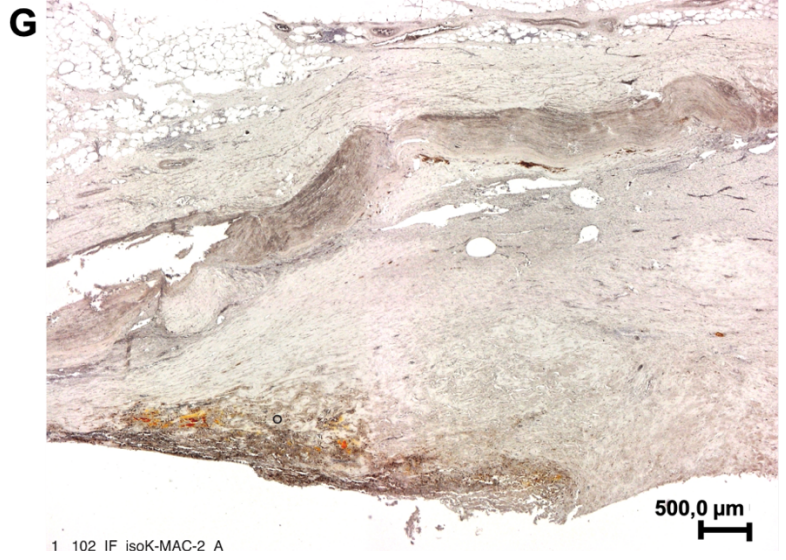
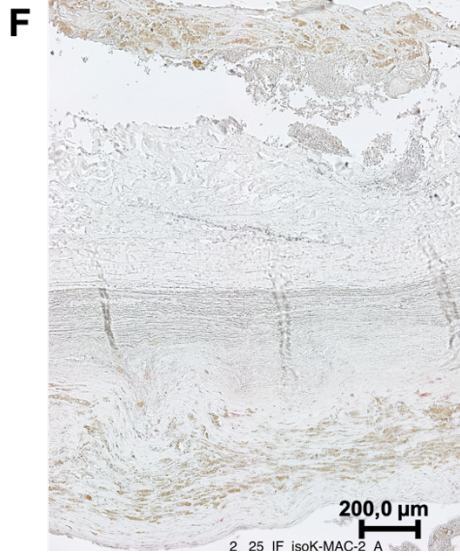
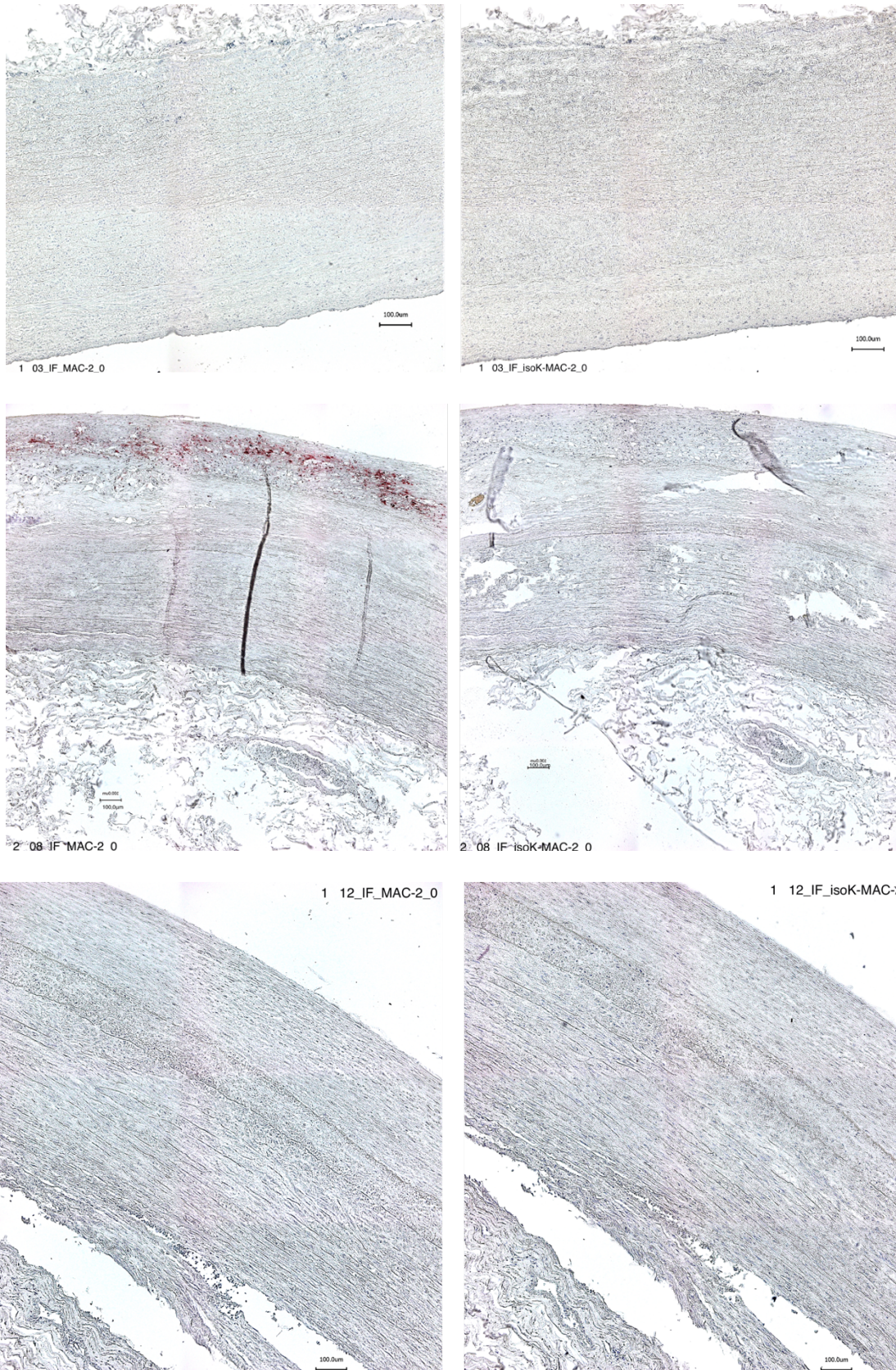
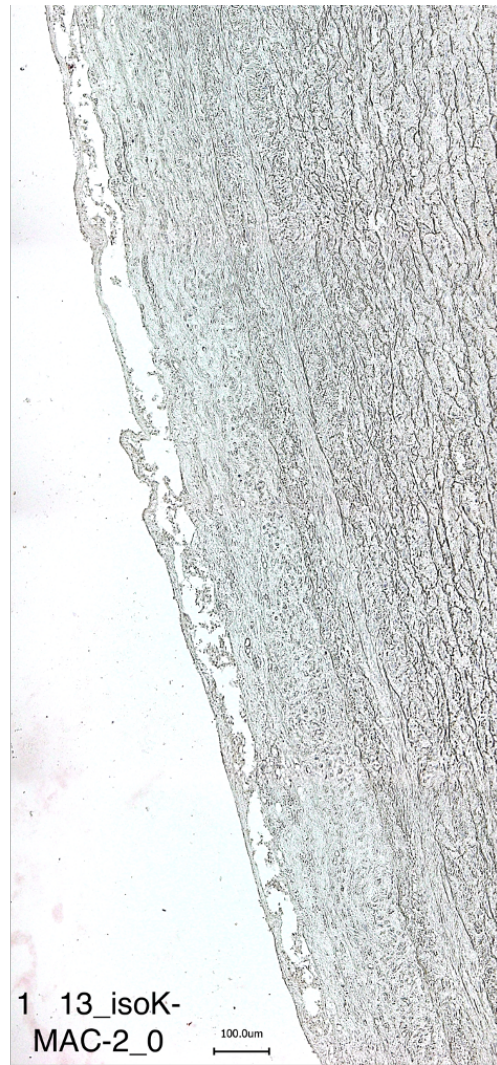
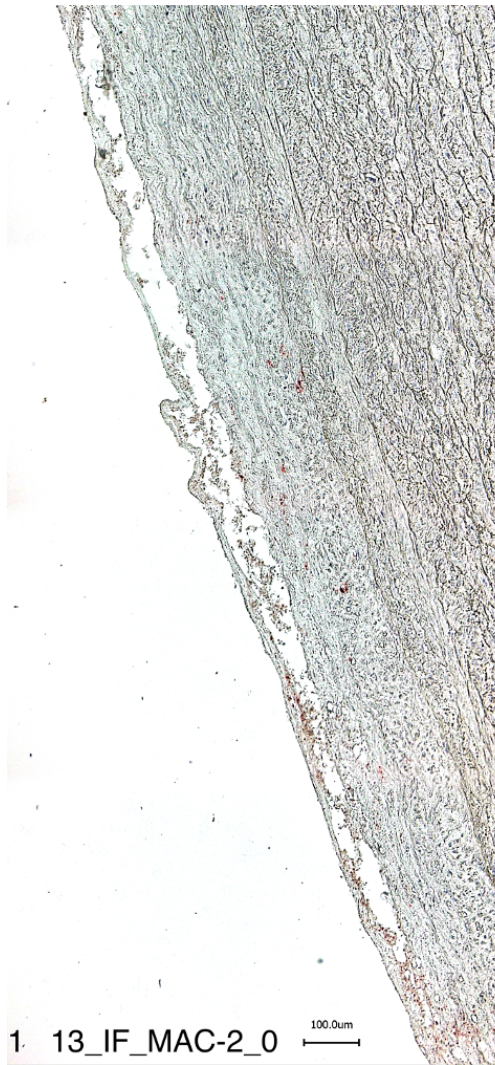
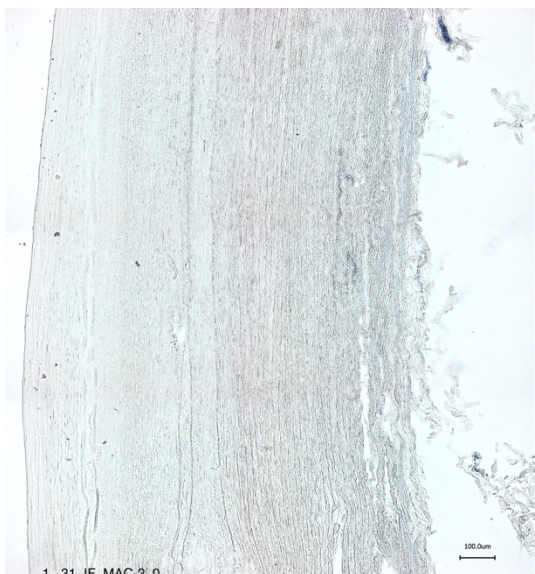


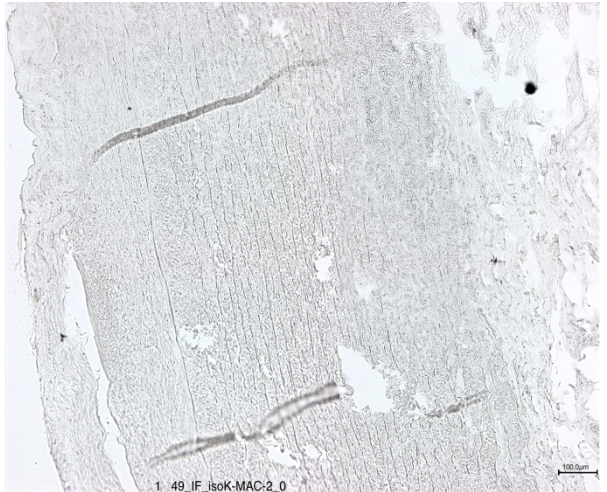
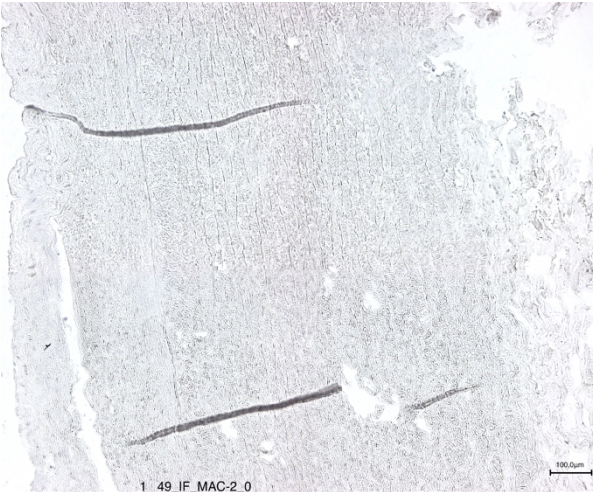
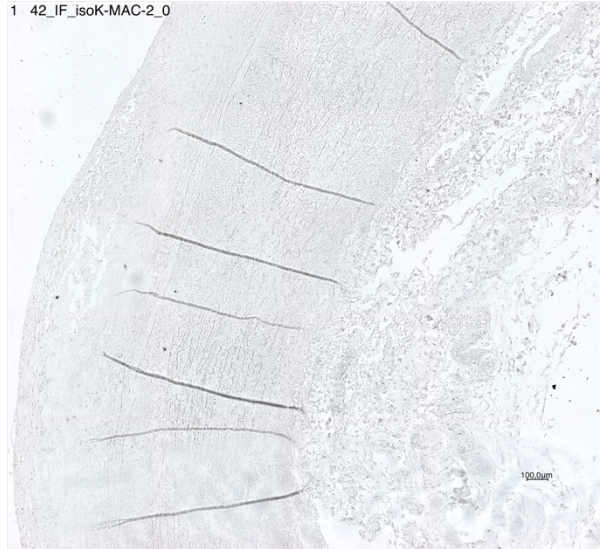
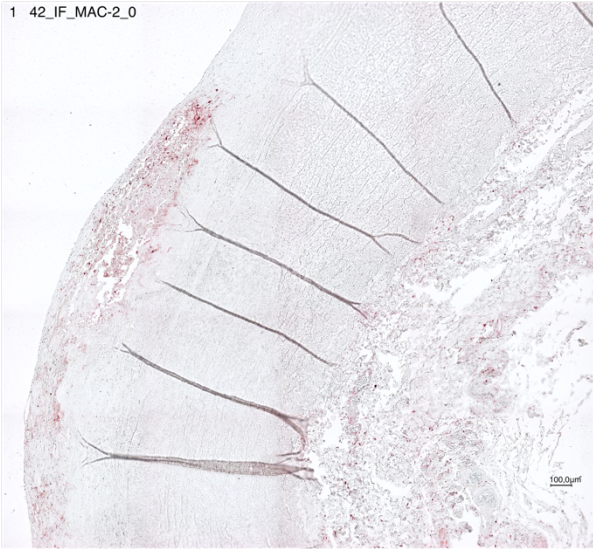
Figure A2. Macrophage staining of infrarenal aortic tissue sections, subgroup 0. Representative sections of all stained tissue samples from pathology subgroup 0 (left) and respective isotype control sections (right). All images were taken at 200x magnification.

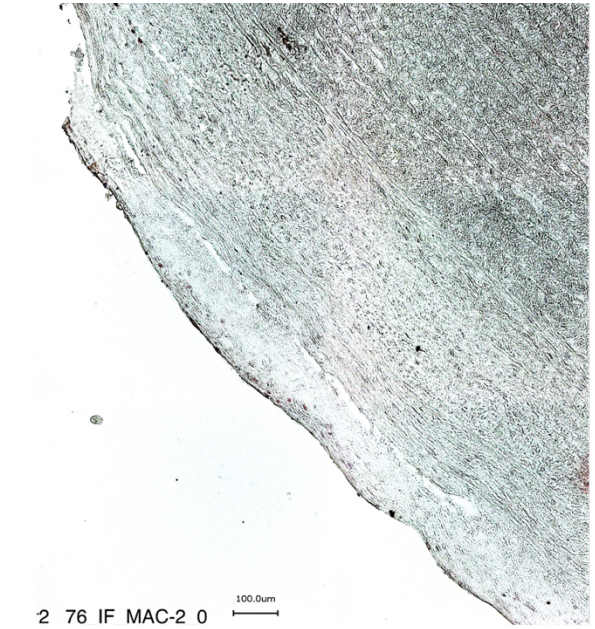
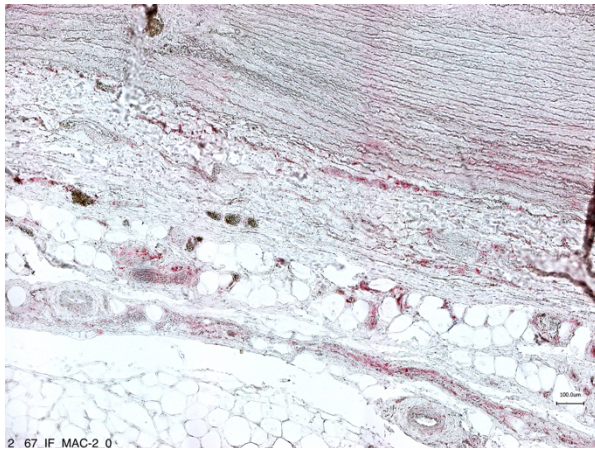
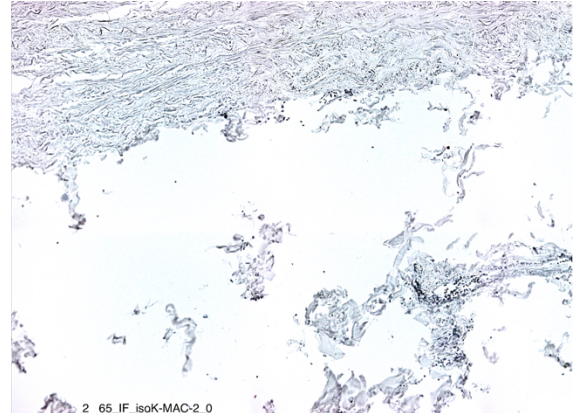
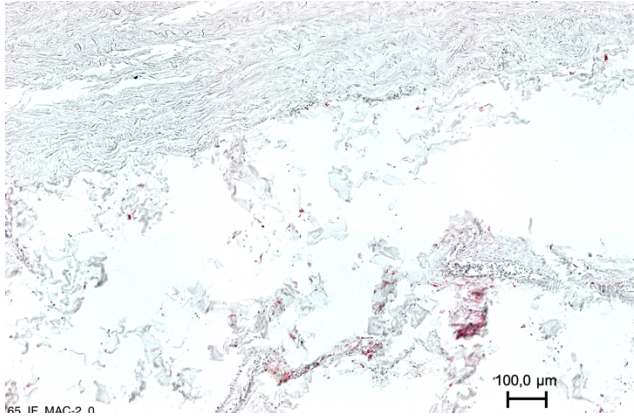


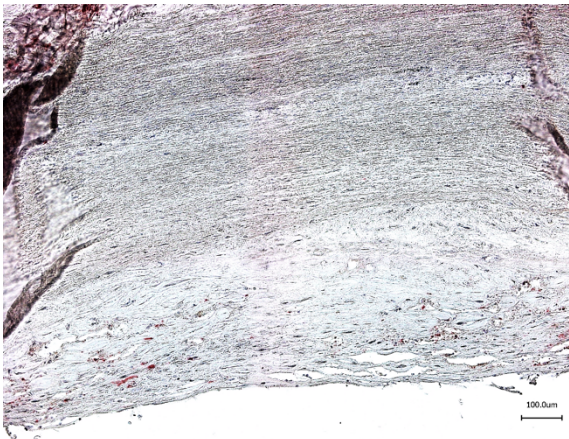
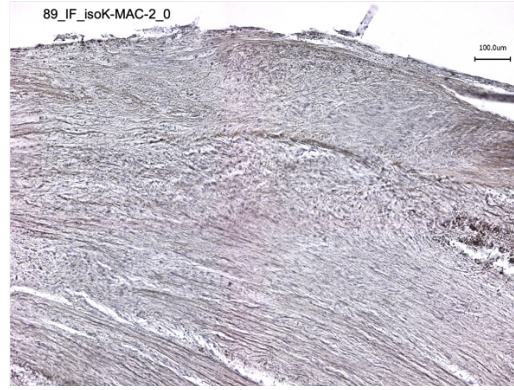
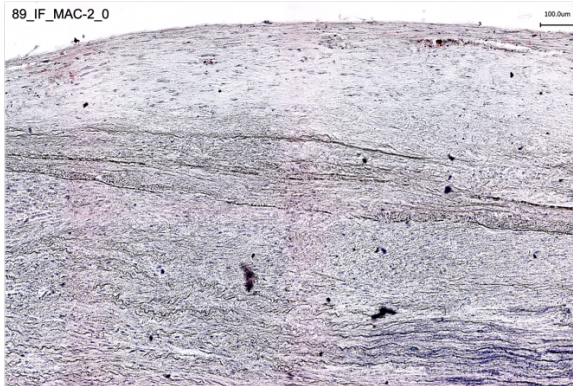
Continued on pages 85-89



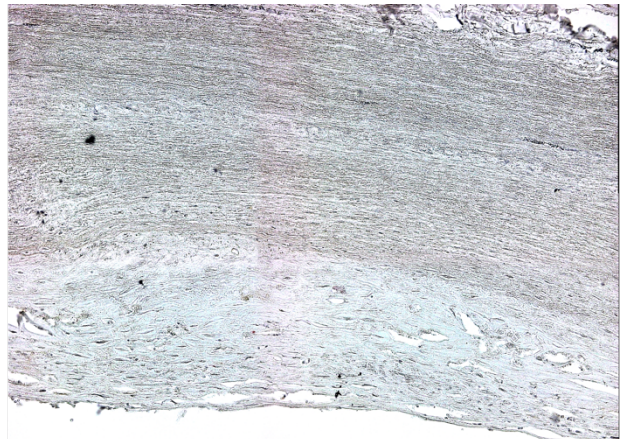








101 IF MAC-2-0



101_IF_isoK-MAC-2_0

Figure A3. Macrophage staining of infrarenal aortic tissue sections, subgroup P. Representative sections of all stained tissue samples from pathology subgroup P (left) and respective isotype control sections (right). All images were taken at 200x magnification.

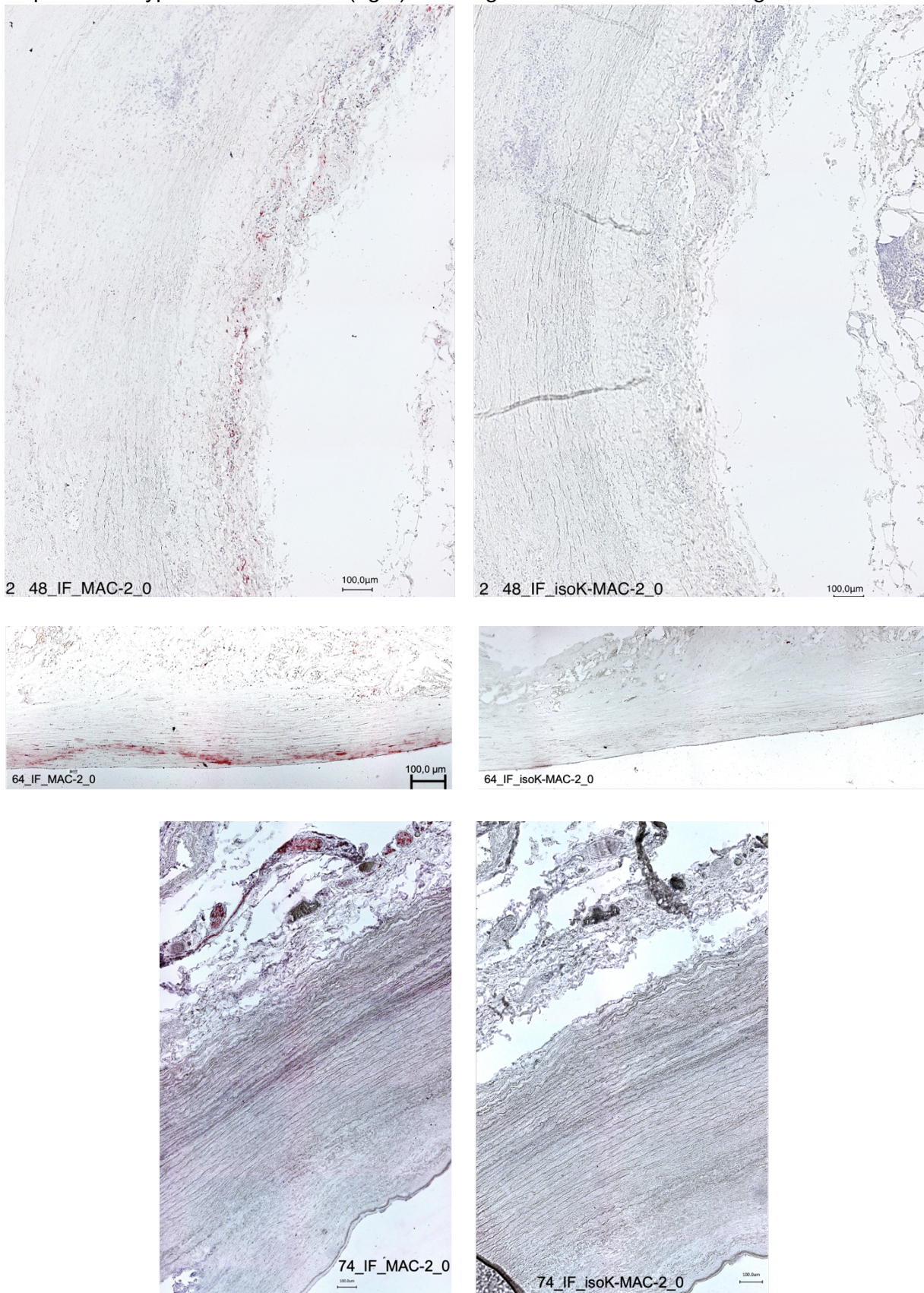
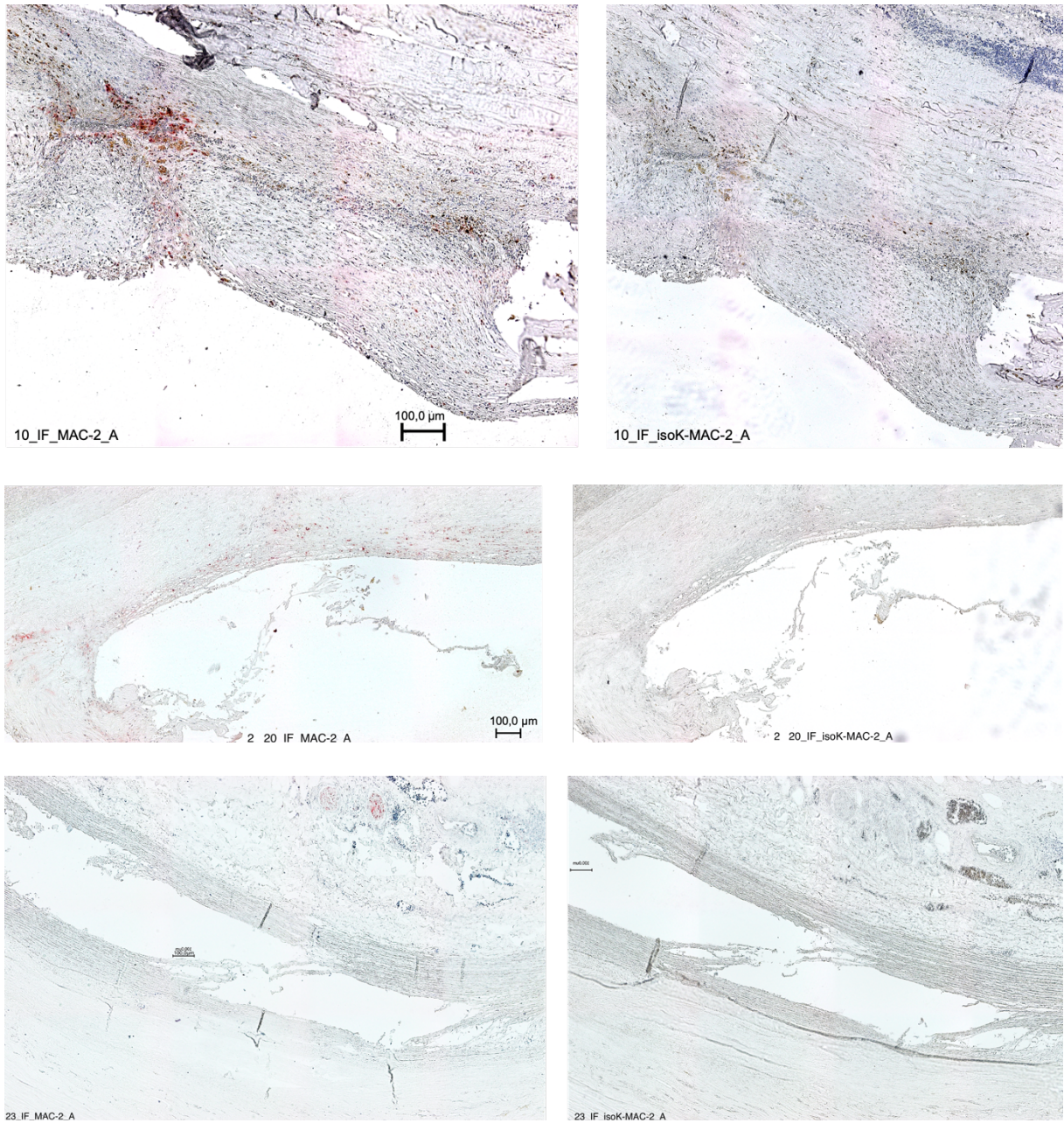
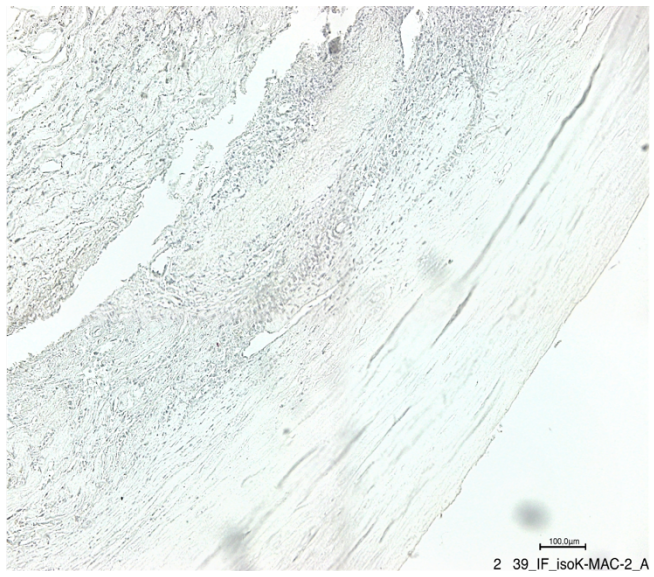
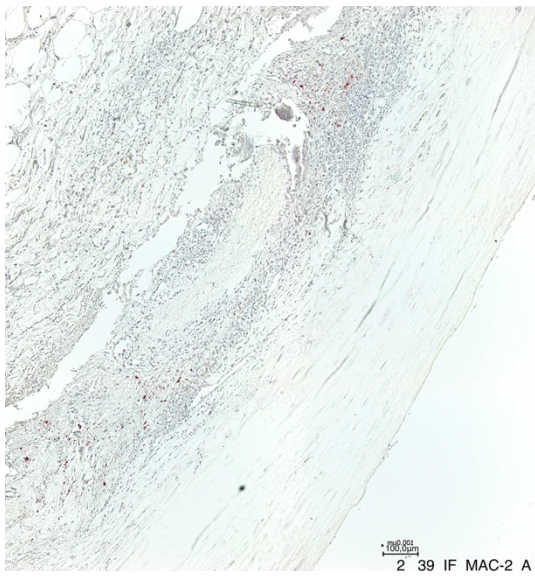
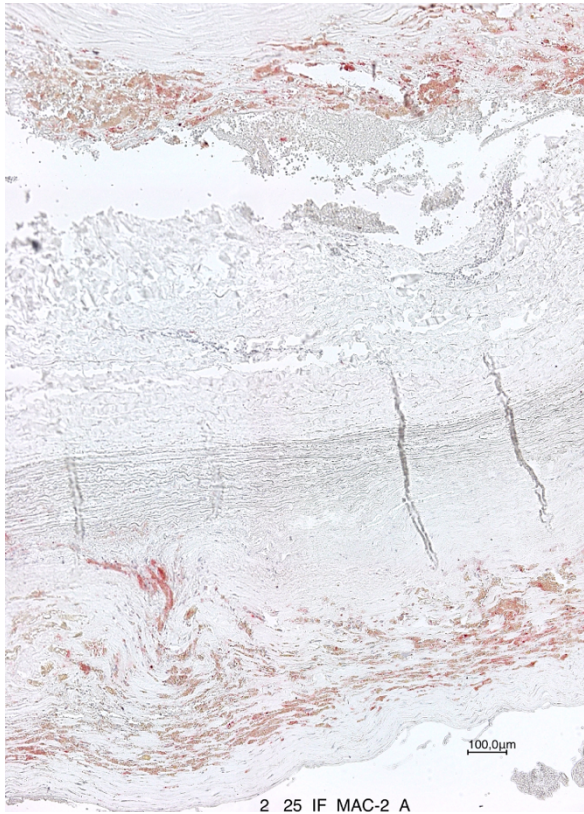
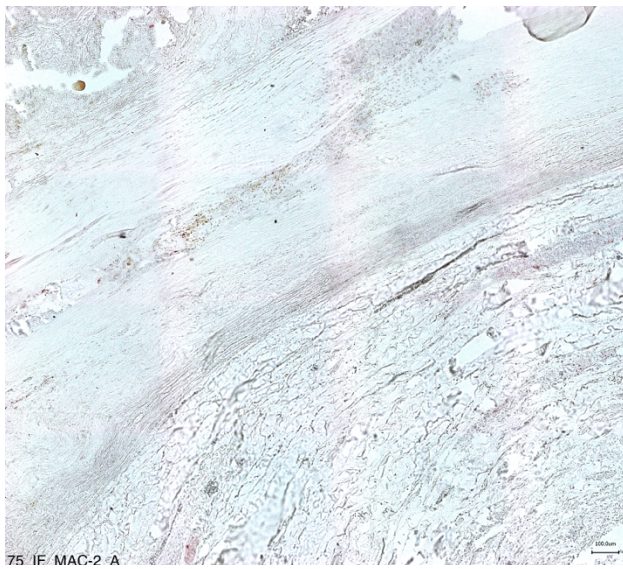
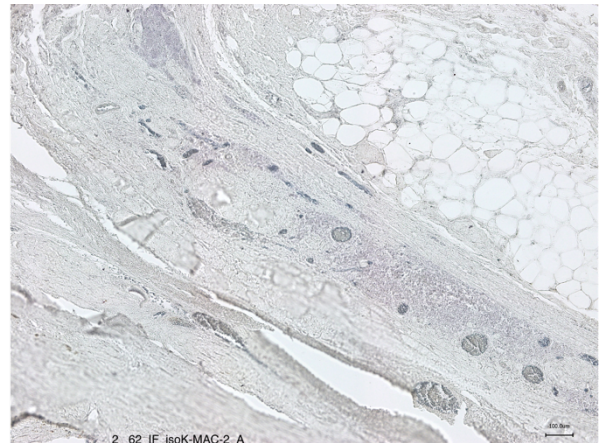
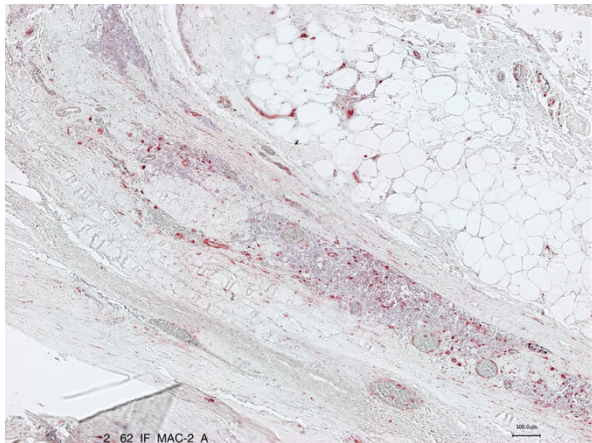
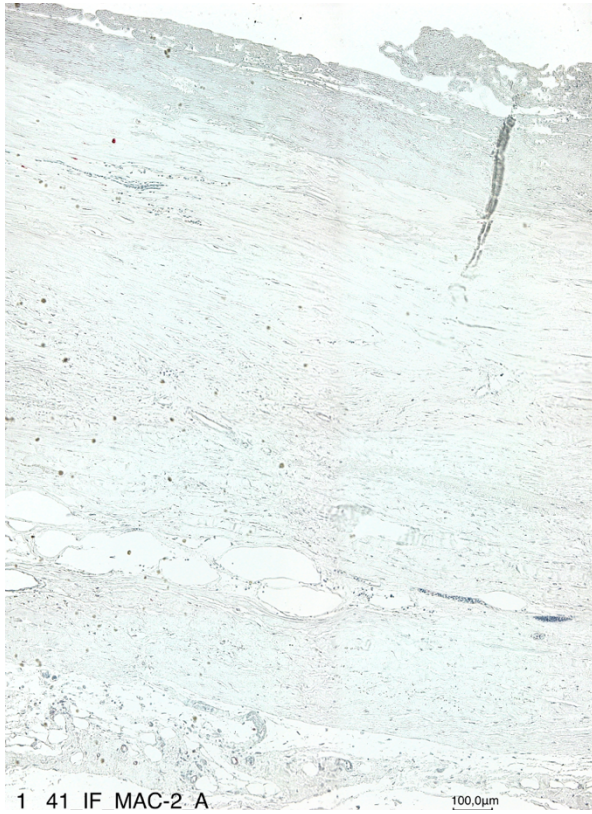


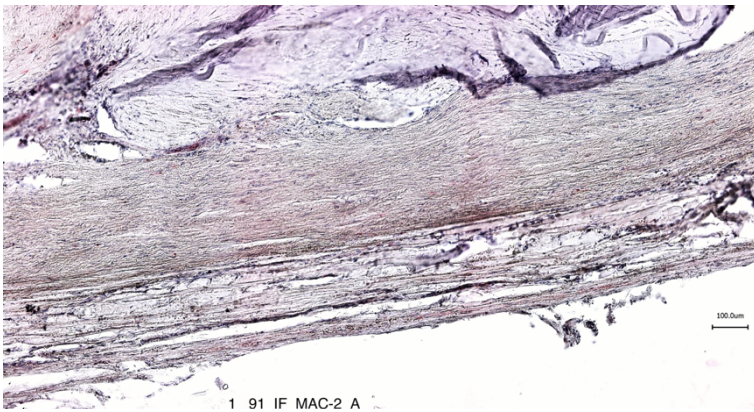
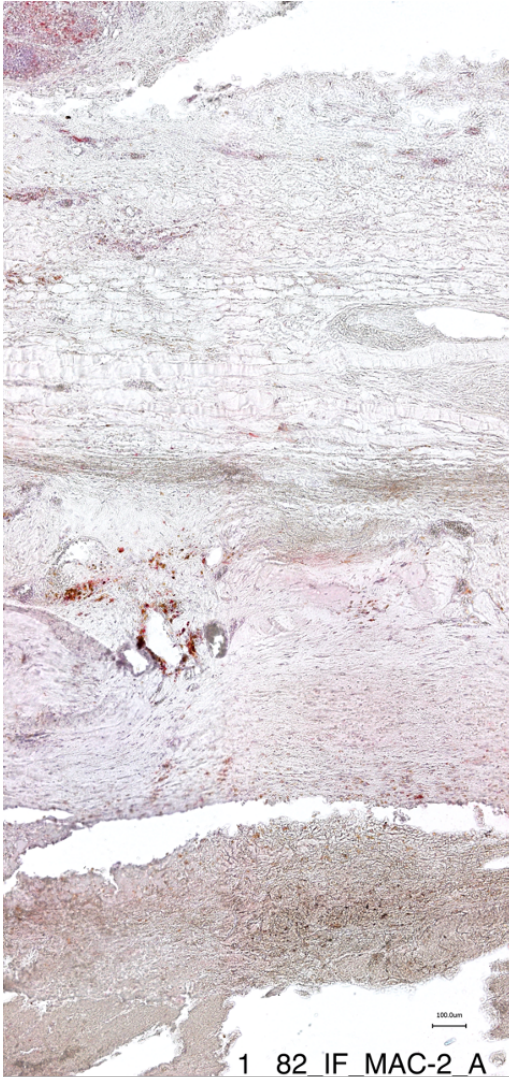
Figure A4. Macrophage staining of infrarenal aortic tissue sections, subgroup AP. Representative sections of all stained tissue samples from pathology subgroup AP (left) and respective isotype control sections (right). All images were taken at 200x magnification, except for #102: 40x magnification.



Continued on pages 92-95







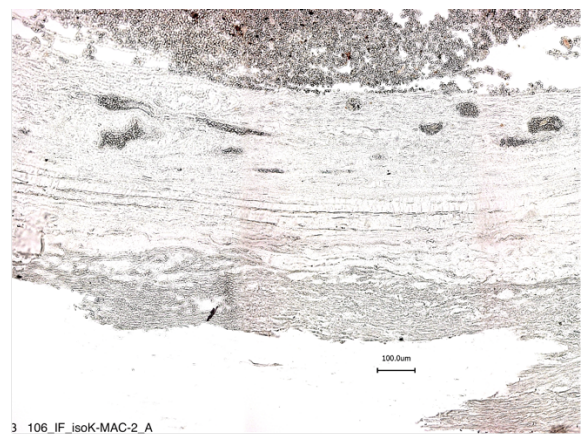
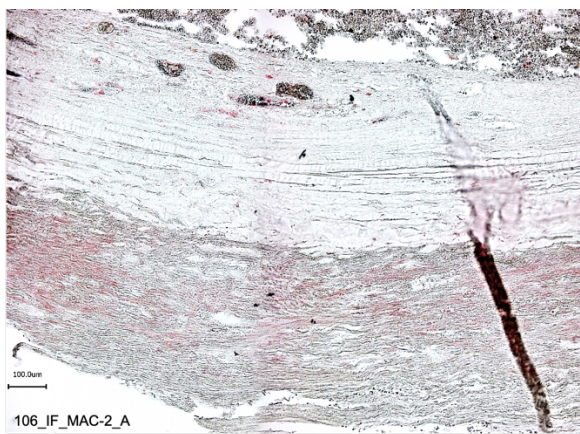
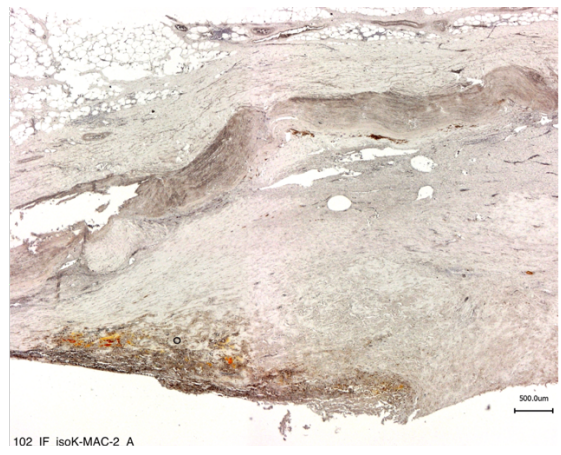
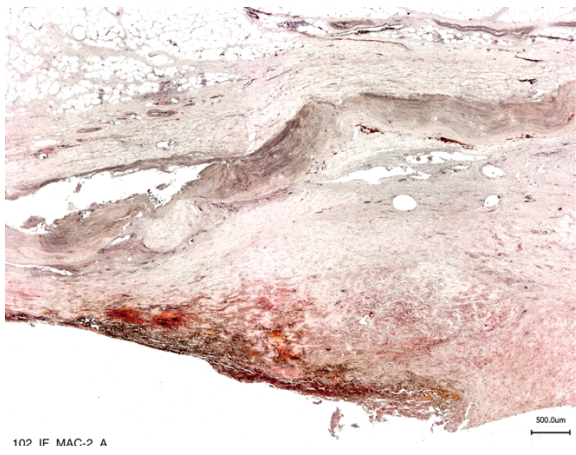
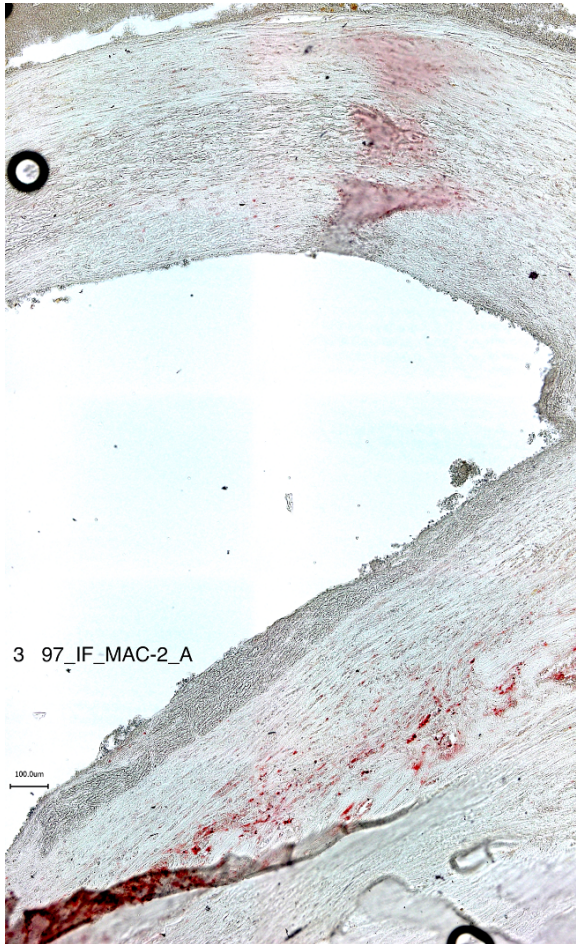
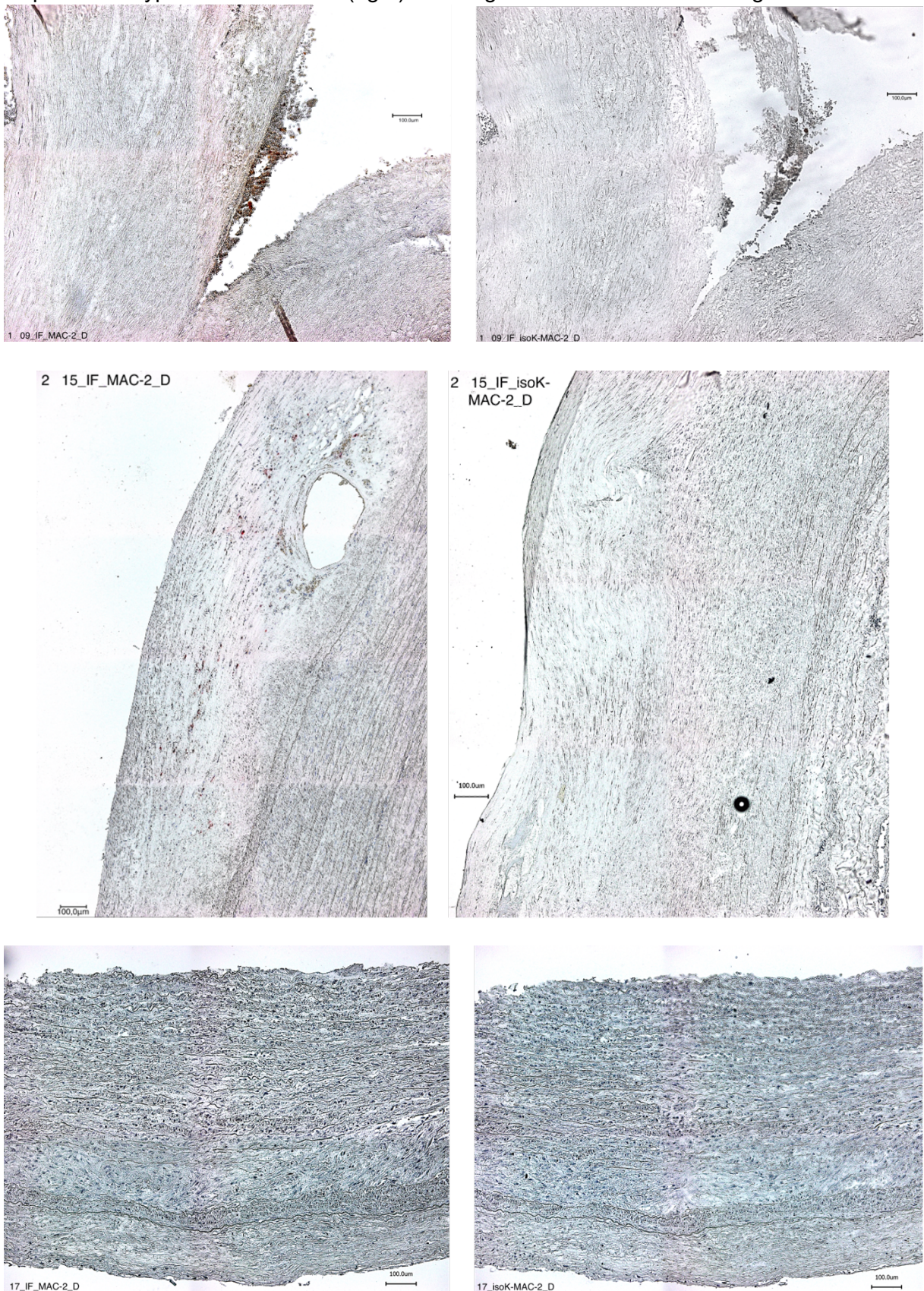
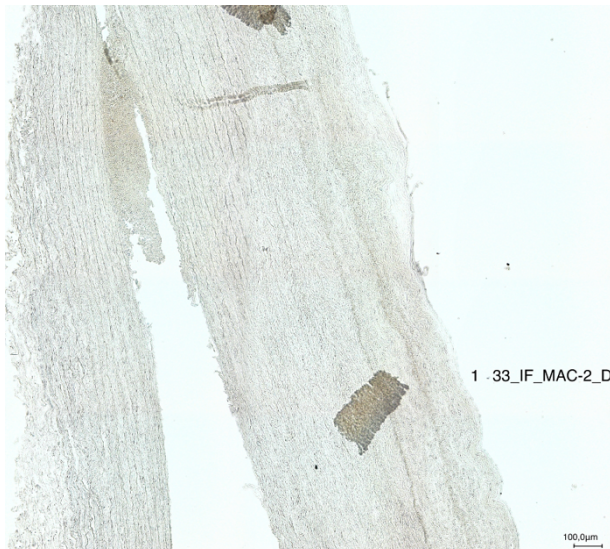
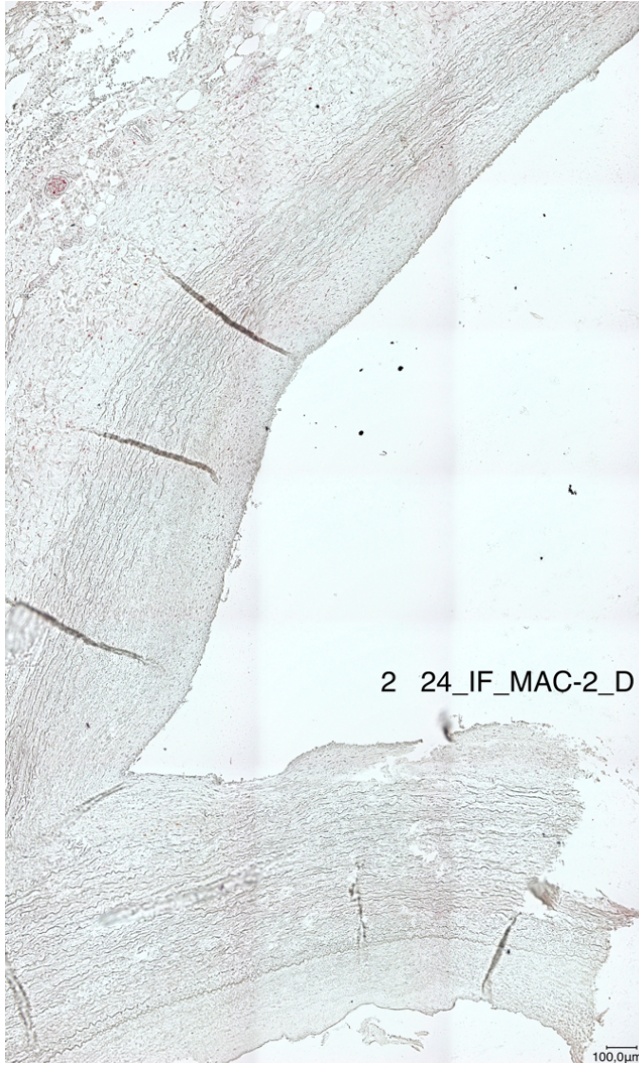
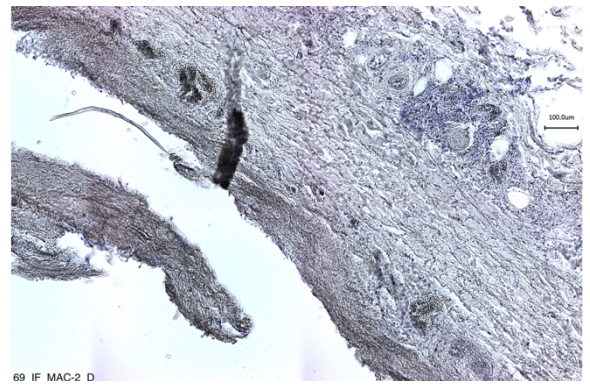
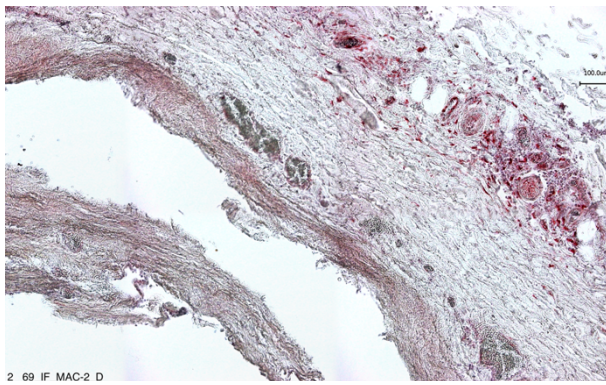
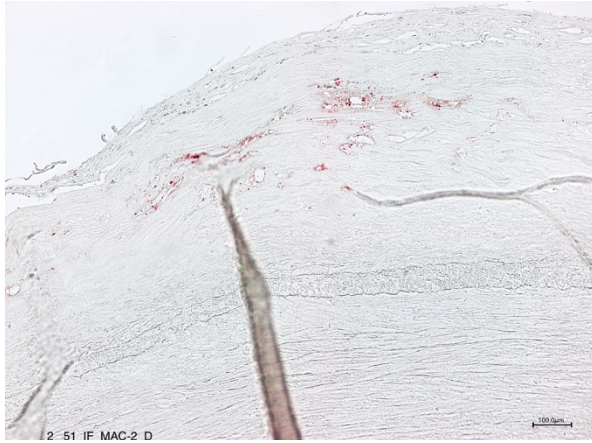


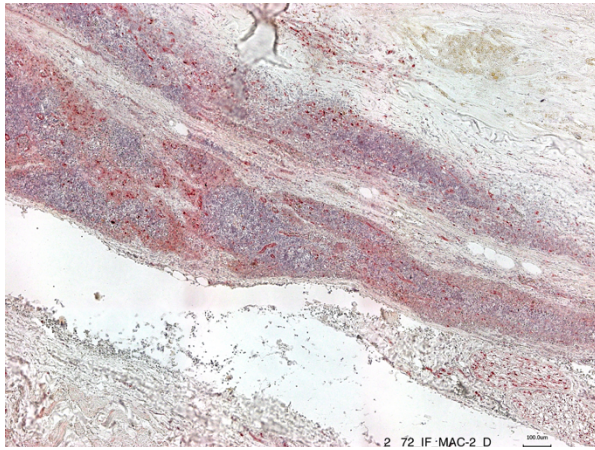
Figure A5. Macrophage staining of infrarenal aortic tissue sections, subgroup D. Representative sections of all stained tissue samples from pathology subgroup D (left) and respective isotype control sections (right). All images were taken at 200x magnification.



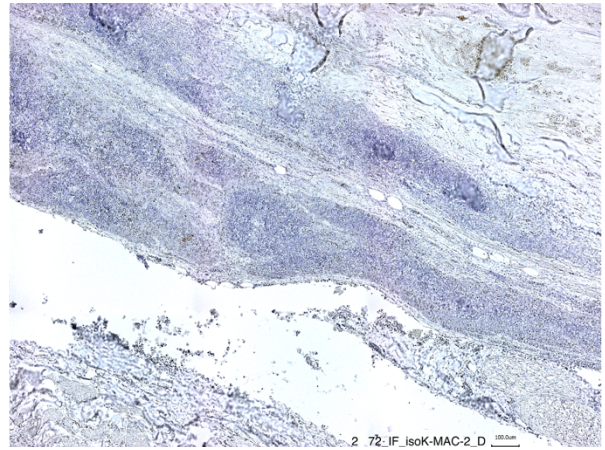
Continued on pages 97-100



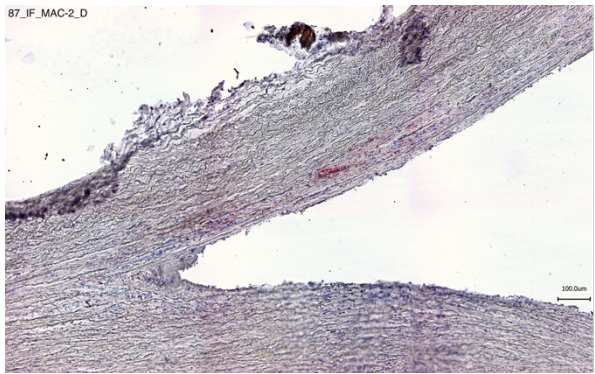




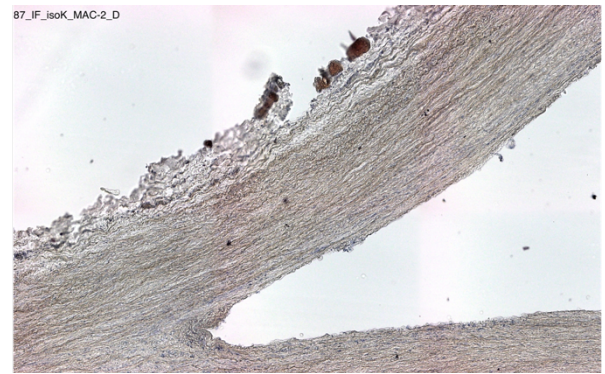
2 72 IF MAC-2 D



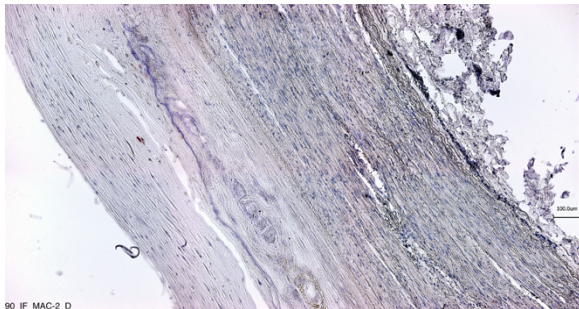
2 72 IF isoK-MAC-2 D



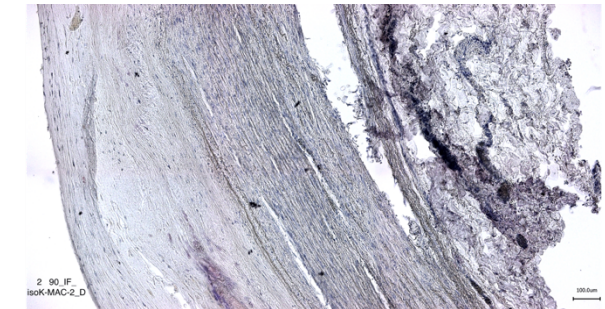
87_IF_MAC-2_D



87_IF_isoK_MAC-2_D

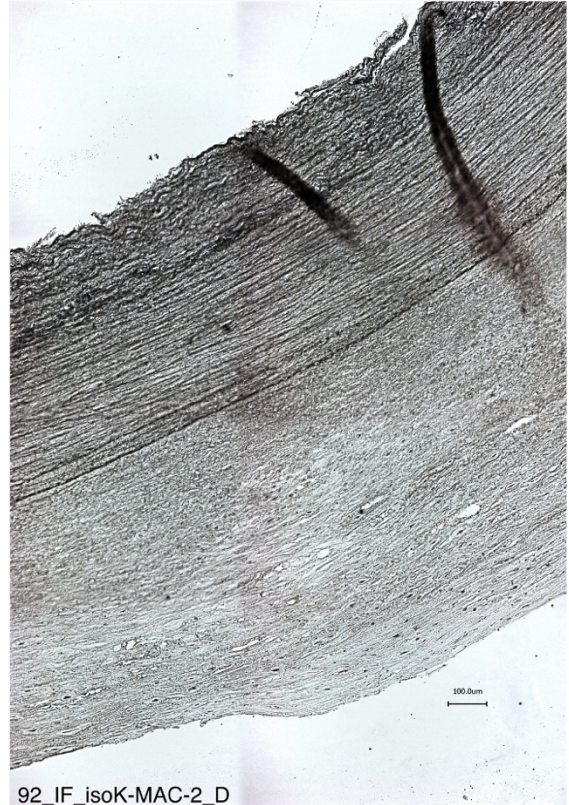
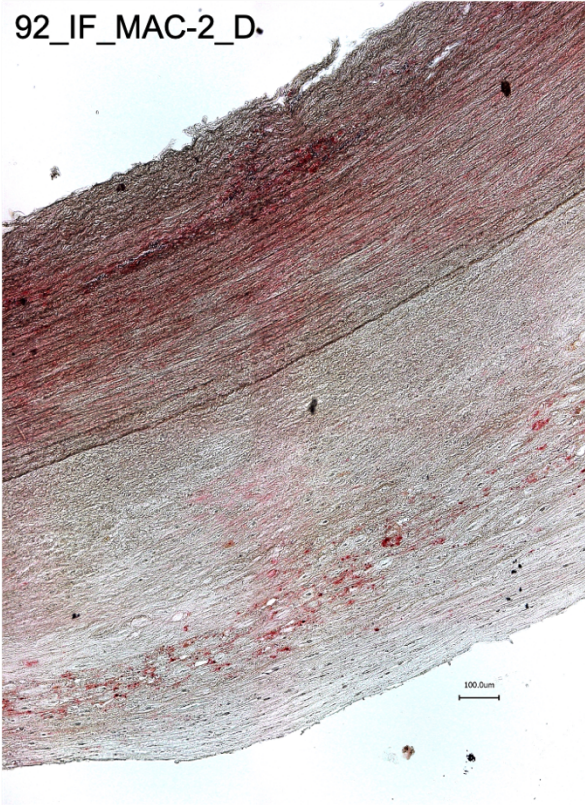


90 IF MAC-2 D

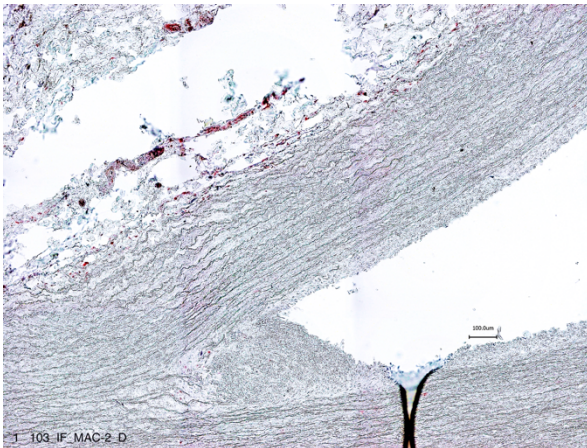


2 90 IF isoK-MAC-2_D

92_IF_MAC-2_D.



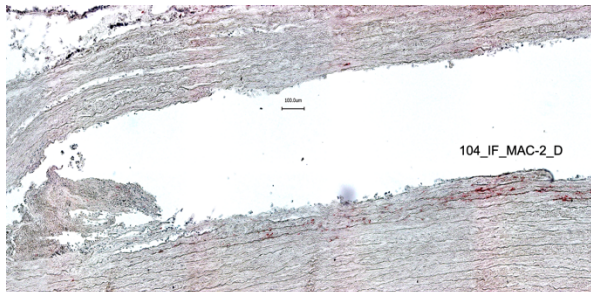
92_IF_isoK-MAC-2_D



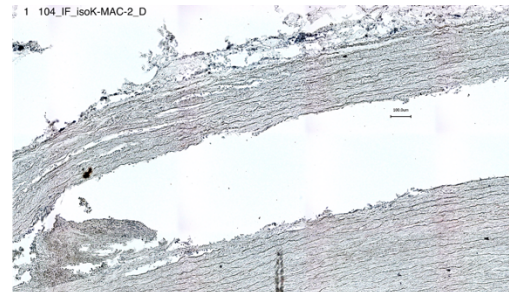
103_IF_MAC-2_D



103_IF_isoK-MAC-2_D



104_IF_MAC-2_D



104_IF_isoK-MAC-2_D

11 Acknowledgment (Danksagung)

Ich möchte mich herzlich bei all den Menschen bedanken, die mir bei der Erstellung dieser Arbeit geholfen und mich in dieser herausfordernden, aber auch sehr spannenden und lohnenden Phase meines Lebens unterstützt haben.

Ein großer Dank gilt Herrn Prof. Dr. Larena-Avellaneda für die Überlassung des Themas und die wertvollen thematischen Anregungen und Kommentare während der Ausarbeitung dieser Arbeit. Ebenso bedanken möchte ich mich bei Herrn Dr. Guenter Daum für die großartige Unterstützung in der gesamten Zeit. Ohne die Hilfe bei der statistischen Auswertung, die sehr gute wissenschaftliche Beratung und die Beantwortung all meiner Frage zu jeder Uhrzeit an wirklich jedem Wochentag wäre diese Arbeit sicher nicht zu der jetzigen Form gekommen. Vielen herzlichen Dank Ihnen beiden noch einmal für Ihre unermüdliche Unterstützung.

Bedanken möchte ich mich auch beim gesamten Team des Labors der Gefäßmedizin AG, die mich so herzlich aufgenommen und unterstützt haben. Mein Dank gilt hier besonders Frau Astrid Becker für die Unterstützung bei der histologischen Aufarbeitung der Gewebeproben und das vorsorgliche Bereithalten von Verbandsmaterial für die ein oder andere kleine Verletzung bei der Herstellung der Gewebeschnitte. Genauso bedanken möchte ich mich bei Herrn Dr. Markus Geißen für die überaus geduldige Einarbeitung in die Arbeit im Labor, insbesondere die Technik der qPCR sowie die vielen interessanten Gespräche über gemeinsame Hobbys an langen Nachmittagen im Labor.

Weiterhin bedanken möchte ich mich bei Herrn Prof. Dr. Püschel sowie den Dres. Anna und Michael Kammal (Institut für Rechtsmedizin am Universitätsklinikum Hamburg-Eppendorf) für die Sammlung und Bereitstellung der Gewebeproben.

Martje Odinga und Angelina Strauch möchte ich an dieser Stelle danken für die qPCR-Messung der S1P Rezeptoren sowie für die histologischen Färbungen eines Teils der Gewebeproben.

Ganz herzlich bedanken möchte ich mich auch bei Lea-Sophie Wegmann und Jonas Zimmermann für die gute gemeinsame Zeit im Labor. Ohne euch und die tolle gegenseitige Unterstützung wäre diese Zeit nicht dieselbe gewesen.

Ein herausragender Dank gilt meiner Familie, die mich in allen (Hoch- und Tief-) Phasen dieser Arbeit begleitet hat. Meinen Eltern möchte ich an dieser Stelle für die Unterstützung während des gesamten Studiums danken, ohne die ich auch nicht in der Lage gewesen wäre, diese Arbeit zu verfassen. Meinen beiden Geschwistern danke ich sehr für die stetige emotionale und auch wissenschaftliche Unterstützung, die mir bei der Ausarbeitung dieser Arbeit sehr geholfen hat.

Mit einem Bild für eine bleibende Erinnerung an das Thema möchte ich diese Arbeit beenden:

Diesem „Aortenaneurysma“, wenn auch in künstlerisch-abstrakter Form, bin ich im Sommer 2021 in den Straßen im Zentrum von Prag begegnet (s. Foto). Einmal mehr wurde an die Relevanz des Themas der Aortenpathologien erinnert.



12 Curriculum vitae

Louisa Michaels, *06.07.1996

Beruflicher Werdegang

seit 01/2023 Asistenzärztin in der Klinik für Augenheilkunde, Asklepios Klinik Barmbek

Ausbildung

10/2015 – Studium der Humanmedizin, Universität Hamburg
12/2022

Auslandsaufenthalte

02 – Auslandssemester an der Universität Zürich (Swiss european mobility
07/2022 programm)

Förderungen

11/2021 Förderung „Hamburgglobal“ der Universität Hamburg für das Praktische
Jahr
02 – Stipendium der Heyning-Roelli Stiftung für ein Auslandssemester in der
07/2020 Schweiz
04/2019 Reisestipendium der Deutschen Gesellschaft für Innere Medizin (DGIM)
seit 03/2017 Nominierung und Teilnahme am Mentoringprogramm für exzellente
Studierende des UK Hamburg-Eppendorf; Simon-Claussen Stiftung

Praktika

07 – 3. PJ-Tertial, Chirurgie; Kantonsspital Graubünden in Chur, Schweiz
08/2022
03 – 2. PJ-Tertial, Augenheilkunde, Asklepios Klinik Barmbek, Hamburg
06/2022
11/2021 – 1. PJ-Tertial, Innere Medizin, Spital Zweisimmen, Schweiz
02/2022
2017 – 2020 Famulaturen: Hausarztpraxis Dr. Samadzade, Dr. Kaan, Steilshoop,
Hamburg; Klinik für Neurologie, Regio Klinik Pinneberg; Zentrale
Notaufnahme, Universitätsklinikum Hamburg-Eppendorf; Intensivstation
für Brandverletzte, Universitätsspital Zürich, Schweiz; Klinik für
Allgemeinchirurgie, Israelitisches Krankenhaus, Hamburg

Hamburg, 13.03.2023

Louisa Michaels

13 Declaration on oath (Eidesstattliche Erklärung)

Ich versichere ausdrücklich, dass ich die Arbeit selbständig und ohne fremde Hilfe verfasst, andere als die von mir angegebenen Quellen und Hilfsmittel nicht benutzt und die aus den benutzten Werken wörtlich oder inhaltlich entnommenen Stellen einzeln nach Ausgabe (Auflage und Jahr des Erscheinens), Band und Seite des benutzten Werkes kenntlich gemacht habe.

Ferner versichere ich, dass ich die Dissertation bisher nicht einem Fachvertreter an einer anderen Hochschule zur Überprüfung vorgelegt oder mich anderweitig um Zulassung zur Promotion beworben habe.

Ich erkläre mich einverstanden, dass meine Dissertation vom Dekanat der Medizinischen Fakultät mit einer gängigen Software zur Erkennung von Plagiaten überprüft werden kann.

Louisa Michaels